Acid-Sensing Ion Channels (ASICs):

Ischemia Sensors in Heart and Brain

Presented by

Stephani P. Sutherland

to the

Neuroscience Graduate Program

September 17, 2001

School of Medicine
Oregon Health & Science University

CERTIFICATE OF APPROVAL

This is to certify that the Ph.D. thesis of

Stephani P. Sutherland

has been approved

[redacted]
Professor in charge of thesis

[redacted]
Member

[redacted]
Member

[redacted]

[redacted]
Member

[redacted]
Member

Table of Contents

List of Abbreviations

ASIC—acid-sensing ion channel

BK—bradykinin

DRG—dorsal root ganglia

CNS—central nervous system

ATP—adenosine tri-phosphate

OGD—oxygen and glucose deprivation

NMDA—n-methyl-D-Aspartate

AMPA--α-amino-3-hydroxy-5-methyl-4-isoxazole-propionate

TTX—tetrodotoxin

ENaC—epithelial sodium channel

VDNC—voltage-dependent sodium channel

I-V—current-voltage (as in plot or curve)

Acknowledgements:

Dr. Chris Benson played a significant role in experimental design, data collection, and analysis presented in Chapter 3: Results. In addition, Dr. Benson developed the cardiac labeling surgery for the identification of myocardial sensory neurons, as described in Chapter 2: Methods.

Technicians Vu Dang and Michelle Bobo aided in the preparation of some sensory neurons for electrophysiological studies.

The cDNA for each of the cloned ASIC channels was kindly provided by Drs. Waldmann and Lazdunski of the CNRS in Valbonne, France. The DNA was prepared for transfection by technicians in the laboratory of Dr. John Adelman.

Ben Brooks was instrumental in creating the three-dimensional images of chemicals.

Laurie Vaskalis created the cartoon rendering of the ASIC1a channel and chemicals.

Abstract:

The work presented here examines a role for acid-sensing ion channels (ASICs) as molecular sensors of ischemia in the heart and brain. I have shown that sensory neurons that innervate the heart respond to the pH of muscle ischemia with large, inward depolarizing currents. These currents are carried by the channel ASIC3, the primary molecular ischemia sensor in the heart. Another channel, ASIC1a, is expressed in CNS neurons and may act as a molecular ischemia sensor in the brain. I have found channel properties of ASIC1a that are analogous to both NMDA-type glutamate receptors and to voltage-gated sodium channels.

We developed a surgical method to label cardiac sensory neurons of rat so that they could be identified in primary dissociated tissue culture. We then determined that these neurons have an overwhelming response to extracellular protons, and characterized the acid-evoked currents using whole-cell electrophysiology. These electrophysiology studies have led me to the conclusion that protons are the primary fast chemical mediator of ischemic pain in the heart.

I aimed to find the molecular identity of the acid-sensing channel in heart. I examined the five cloned ASIC channels using whole-cell electrophysiology to determine which channel carries the current seen in rat cardiac sensory neurons. I concluded that

ASIC3 is the primary ischemia sensor in the heart. The defining properties of the two currents lie in their activation, gating, and permeability.

Next I examined the ASIC1a channel, which could act like an ischemia sensor in brain. I observed a negative slope region in the I-V curve of ASIC1a that is due to voltage-dependent intra-pore block by Mg^{2+} ions. The block by Mg^{2+} ions may allow ASIC1a to act as a coincidence detector of acidity and depolarization, much in the way that the NMDA receptor is a coincidence detector of glutamate and depolarization.

A study of permeation revealed that ASIC1a is analogous to voltage-dependent sodium channels (VDNCs). Like VDNCs, I found that ASIC1a is permeable to the organic cation guanidinium but not the smaller methyl-ammonium ion. Guanidine and some other permeant ions can form hydrogen bonds with atoms that line the channel pore and compress in size in order to slide through the channel pore's permeation pathway. This seems to indicate that, like the VDNCs, ASIC1a has a pore that is only around 3 Å wide and is lined with oxygen atoms that form hydrogen bonds with some permeant ions. Finally, I found that the guanidine toxins amiloride and tetrodotoxin block the ASIC1a channel with low affinity. An interaction between guanidine and the ASIC1a pore may form the basis for block by guanidine-containing drugs or toxins.

Chapter 1: Introduction

The work described in this thesis is a study of Acid-Sensing Ion Channels, or ASICs. These channels pass inward, depolarizing currents in response to a drop in extracellular pH. Some ASICs, expressed in sensory neurons and central neurons, are extraordinarily sensitive to protons and provide a large excitatory signal. ASIC channels are prime candidates for molecules that act as neuronal sensors of ischemia in both the heart and the brain. This chapter will include an introduction to the following: the physiology of cardiac ischemic sensation, the ASIC family of ion channels that may act as molecular ischemia sensors, and the ion channel physiology of ischemia in the CNS.

Part One—Physiology of Myocardial Ischemic Sensation

Ischemia, from the Greek "suppression of blood," is defined as a "deficiency of blood in a part, due to functional constriction or actual obstruction of a blood vessel"[1]. The condition includes hypoxia, an insufficiency in the oxygen supply relative to demand, and also includes a reduction in the nutrients carried by the plasma. When ischemia occurs chronically in the heart, it can produce pain called angina pectoris; acute ischemic pain is experienced during myocardial infarction (heart attack). While many of the earliest experiments aimed at understanding ischemia were performed in skeletal muscle, the following overview will focus on myocardial ischemia. Ischemic pain in

skeletal muscle and in myocardium are thought to be mediated by the same process, as Lewis suggested[2]. The experiments presented here shape our current understanding of the processes involved in the generation of ischemic pain.

Keele and Armstrong's review[3] provides a good overview of the following early investigations aimed at understanding the nature of ischemic pain. Occlusion of a blood vessel at rest does not produce pain; therefore, pain is dependent not only on hypoxia or arrested circulation but also on continued muscle contraction, which results in an increase in oxygen demand. MacWilliam and Webster were the first to recognize this[4] and attributed such pain to "want of oxygen and its consequences, with excessive accumulation of metabolic products, acids and other bodies." They suggested that the pain was "protective in character, tending to limitation of effort and shielding the muscle from being spurred on to further and injurious activity." Pickering and Wayne[5] showed in anemic patients that ischemic pain depends on the oxygenation state of the blood and not the flow itself; thus they postulated that the algogenic substance that accumulates in tissue spaces can be removed by reoxygenation. Thus, while ischemia consists of more than simply hypoxia, the lack of oxygen plays the major part in producing pain rather than depletion of some other substance in blood. Finally, Lewis concluded[2] that the algogenic substance arises from muscle contraction and acts directly at nerve endings in the muscle tissue.

The search has since ensued for a metabolite that (1) is produced in contracting muscle (perhaps only in hypoxic conditions), (2) is stable enough to accumulate during ischemia, and (3) the effects of which would be alleviated by reoxygenation. Lewis termed the substance 'factor P', and stressed that factor P may be present before and after the sensation of pain, but that only during the ischemic condition does it accumulate to a level sufficient to produce pain[2]. While potassium ions were considered a possible mediator early on, the evidence does not point to a major specific role of K^+ in mediating ischemic pain. Three more likely candidates considered in this section are adenosine, lactic acid, and bradykinin. Since this discussion will focus on myocardial ischemia, it will be helpful at this time to review the sensory innervation of the heart.

Sensory anatomy of heart attack and angina

Since the time of these early studies, it has been recognized that a potential mediator of ischemic pain must stimulate the afferent pathway from the muscle to the CNS. The anatomy of cardiac innervation was largely determined through clinical experience[6]. Three populations of afferent neurons innervate the heart, as illustrated in Figure 1[7]. Two populations of sensory neurons innervate the cardiac muscle (myocardium) itself; they are called vagal afferents and sympathetic afferents. The name of these neurons is descriptive solely of their anatomical location, and does not imply that

they are sympathetic neurons. Both populations are afferent sensory neurons. Vagal afferent axons follow the vagus nerve to their cell bodies located in the nodose ganglia. Sympathetic afferent axons follow the sympathetic nerve to their cell bodies in the upper thoracic dorsal root ganglia (C_8-T_3). Sympathetic afferents may be the primary mediators of myocardial pain because sympathectomy relieves pain in most patients suffering from chronic angina[8]. Moreover, Brown et al.[9] found that coronary occlusion in cats causes pain that is accompanied by afferent nerve activity in the sympathetic nerve tract. However, the vagal afferents should not be discounted as a source of ischemic sensation from the heart. In a comprehensive review of experimental literature, Meller and Gebhart[10] present an overview of cardiac afferent innervation. Sympathectomy is ineffective in relieving angina in some patients, and transection of vagal fibers has been found to relieve cardiac pain in some cases. Meller and Gebhart propose spatial differences in cardiac innervation by sympathetic and vagal afferents. Perhaps patients suffering from angina in an area innervated by vagal afferents would be relieved of pain by a vagotomy but not with a sympathectomy. There certainly is evidence that vagal afferents transduce some form of cardiac pain, but the vast majority of literature on cardiac pain has studied the sympathetic afferents. Therefore the following discussion will only address pain mediated by cardiac sympathetic afferents. Neurons that innervate the pericardial membrane, which encapsulates the heart, have axons that follow the

phrenic nerve to their cell bodies in the upper cervical dorsal root ganglia (C_3-C_5). There is no evidence that these pericardial nerve endings sense cardiac ischemia.

It is generally accepted that pain is the only conscious sensation arising from the heart, and that myocardial ischemia is the source of cardiac pain. Cervero[11] has compiled an extensive review of literature examining the modalities of cardiac afferents and their possible functions. Cardiac sympathetic afferents consist of myelinated and unmyelinated fibers. The myelinated fibers display both mechanosensitive and chemosensitive behavior, and the unmyelinated fibers are predominantly chemosensitive but may display various degrees of mechanosensitivity. Uchida et al.[12] found that all A-delta and C fibers responded to coronary occlusion and displayed chemosensitivity regardless of mechanosensitivity. The mechanosensitive sympathetic afferent neurons fire rhythmically—but only once per cardiac cycle under normal conditions, so they are not well suited to provide information about the cycle. However, these neurons respond robustly to coronary occlusion and to application of lactic acid or bradykinin[13] with a firing pattern that is dictated by the cardiac cycle. This suggests that these mechanosensitive sympathetic afferent neurons may provide information about the cycle *under ischemic conditions* by integrating chemical and mechanical signals. In contrast, the unmyelinated, exclusively-chemosensitive neurons fired with an irregular burst pattern. Despite the fact that a significant portion of sympathetic afferents is

mechanosensitive, the entire population appears able to sense ischemic conditions, and might all transmit pain sensation.

Both the mechanically and chemically sensitive neurons may be important to elicit the sympathetic reflex response that arises with coronary occlusion or myocardial ischemia. Malliani et al.[14] found that the sympathetic, rather than the vagal, afferents are instrumental in exciting the sympathetic efferent neurons, resulting in a cardio-cardiac sympathetic reflex arc. This curious reflex causes the heart to contract more forcefully at a time when it is already oxygen-deficient. Clearly counterproductive, this reflex can cause an increase in myocardial injury during heart attack or chronic ischemia[15]. Thus it appears that the cardiac sympathetic afferents respond to myocardial ischemia with two consequences: the sensation of pain, and the sympathetic reflex response. Both of these functions are probably mediated by some of the following chemicals produced during ischemia.

Chemical Mediators of Myocardial Ischemic Pain

Adenosine: Adenosine has been considered a candidate for a chemical mediator of ischemic pain for many years, but the evidence for and against a major role of adenosine are in conflict. Intra-coronary administration of adenosine to patients with angina caused chest discomfort that was similar to their typical anginal painThemes et al. found that

cardiac sympathetic afferent firing in response to a coronary occlusion was inhibited by intra venous administration of the adenosine receptor antagonist aminophylline, and the firing was augmented by dipyradimole, an adenosine uptake inhibitor. Gnecchi-Ruscone et al.[16] found that adenosine caused sympathetic afferent firing in a dose-dependent manner that was blocked by administration of aminophylline; however, afferent firing in response to coronary occlusion was not reduced by aminophylline, indicating that adenosine is not the sole mediator of cardiac pain. These studies support a role for adenosine in cardiac sensation.

Other studies, however, do not. In a recent study by Pan et al.[17], intracardial injection or epicardial application of adenosine failed to cause cardiac afferents to fire. Application of the A1 receptor agonist N6-cycloadenopentasine did not cause firing, and dipyradimole did not potentiate the response of ischemically sensitive afferents to 5 min of myocardial ischemia. Further, aminophylline did not attenuate firing during ischemia. Therefore, the authors concluded that adenosine does not play a substantial role in activation of cardiac sympathetic afferents during myocardial ischemia. Abe et al.[18] found that only one of 12 fibers tested was sensitive to epicardial application of adenosine, and this fiber did not fire in response to coronary occlusion. Others have shown that adenosine failed to cause a sympathetic reflex response when applied

epicardially[19] and failed to activate afferents in skeletal muscle[20]. The part played by adenosine in cardiac sensation remains unclear due to these conflicting results.

Bradykinin: Bradykinin (BK) has also been shown to play a role in activating afferent neurons in the heart. Baker et al.[13] found with single unit recordings of cardiac afferent neurons that both mechanically and chemically sensitive neurons responded to intra-pericardial application of BK. They examined many mechanosensitive neurons (140) and found that BK either directly stimulated the nerve endings or sensitized them to the mechanical stimulus of the beating heart. The small number (18) of purely chemosensitive neurons they tested all showed a robust response to BK. Abe et al.[18] found that 13 of 16 mechanosensitive sympathetic afferents responded to epicardial application of BK. Stebbins and Longhurst[21] examined the role of BK in eliciting the reflex cardiovascular response to contracting skeletal muscle. They showed with pharmacological manipulation of bradykinin metabolism that BK contributes to stimulation of this reflex response. Likewise, Veelken[19] found that epicardial application of BK induced a sympatho-excitatory response through B2 receptors, which probably reside on cardiac afferent neurons. Thus it is clear that BK activates cardiac sympathetic afferents, plays a role in eliciting a sympathetic response to contracting muscle, and may evoke the sensation of pain.

Lactic acid: Lindahl[22] suggested that protons are the sole mediator of nociception. This was an overestimate of the role of acid, but it was an early indicator of its importance in the nociceptive system. Ischemic tissue acidification results from generation of lactic acid. Lactate and ATP are both products of anaerobic glycolysis, and breakdown of ATP produces protons[23]. Lactate and protons produced during myocardial ischemia rise first in tissue and later in blood[24]. This suggests that the acid metabolites accumulated during ischemia are washed into the bloodstream by reperfusion. Lactic acid solutions stimulate sympathetic cardiac afferents, and prior application of H^+ buffer blocks afferent firing in response to coronary occlusion[25,12]. Uchida found that while the chemosensitive afferent firing was markedly inhibited by buffer during occlusion, the mechanosensitive afferents were only slightly (0-25%) inhibited. This suggests that lactic acid may not be the critical stimulus for all types of cardiac afferents during ischemia. Benson et al.[7] found that 93% of labeled, dissociated cardiac sympathetic afferents responded to a drop in pH with very large depolarizing currents, while BK and adenosine evoked very small currents in a much smaller fraction of the cells (see Chapter 3: Results).

Interestingly, the effects of pH seen in cardiac afferents are somehow modulated by lactate. Pan[25] showed that cardiac afferents were stimulated better by lactic acid than

by an acidic phosphate buffer solution at the same pH. Furthermore hypercapnia, which decreased epicardial pH to the same level as lactic acid, had no effect on afferent firing. Thimm[26] found that perfusion of the rat hindleg with lactic acid caused changes in heart rate that increased with lactate concentration. Hong[27] also found that while injection of lactic acid to the right atrium caused a decrease in arterial blood pH and caused pulmonary C fibers to fire, injection of HCl at the same pH had no effect on blood pH or afferent firing. Formic acid (with an identical pKa to lactic acid) caused a similar fall in blood pH but the afferent response was not as robust. Although the lactate ion does not directly cause firing of sensory afferents, it may potentiate the response to protons.

These experiments are consistent with the hypothesis that a decrease in pH due to production of lactic acid during anaerobic metabolism is the primary mechanism for activation of cardiac sympathetic afferents. Lactic acid is produced during ischemia, but is the level of acidosis reached in ischemic tissue sufficient to stimulate sensory nerve endings? While early measurements of pH in ischemic tissue were attempted, they were not accurate prior to 1978[28]. Technological advances since then allow much faster and more accurate measurements of tissue pH. Cobbe[29] used a pH-sensitive needle electrode in the epicardium to measure changes in pH during myocardial ischemia. The accumulation of protons caused pH to fall by 0.15 units after 5 min of ischemia, and by 0.66 units after 15 minutes. Recently Pan et al.[25] measured epicardial pH using the

needle electrode during myocardial ischemia and found that tissue pH fell from 7.35 to 6.98 within five minutes, and this decrease was prevented by neutral phosphate buffer in the pericardial space. Further, they made single unit recordings from cardiac sympathetic C-fiber afferents and found that the afferent firing matched the fall in tissue pH and was also diminished by buffering.

Proton-Sensitive Currents of Sensory Neurons

Krishtal and Pidoplichko[30] were the first to propose a molecular sensor of pH at sensory neuron terminals. They found that isolated cultured sensory neurons of the rat responded to a rapid decrease in pH from 7.4 to 6.9 and lower with an inward, depolarizing current carried by sodium. They showed that 74% of neurons smaller than 26 microns were proton-sensitive, while 75% of neurons larger than 26 microns were proton-insensitive[31], suggesting that this small-diameter, nociceptor-enriched population of sensory neurons is specialized to sense protons. They described three currents that desensitized at different rates.

The slowly activating, non-inactivating type of current has been the cause of much debate over sensory neuron proton-gated currents. Bevan[32] has contended that the slowly or non-inactivating current is present only in cells that display a current in response to capsaicin, and that this slow acid current is carried by the same ion channels

that are opened by capsaicin. In contrast, Zeilhofer et al.[33] found that while the slow, non-inactivating acid current and the capsaicin-sensitive current were both carried somewhat by Ca^{2+} ions, the proportional contribution of Ca^{2+} to each current was significantly different, indicating two populations of channels. However, they did find that a drop in extracellular protons augmented the responses to capsaicin. Others have found currents in sensory neurons that could be activated by either capsaicin or protons without complete overlap in cell distribution[34,35]. These reports indicate that sensory neurons express a diverse population of channels, some of which respond to either capsaicin or to protons, and some that can respond to either ligand.

The recently cloned vanilloid receptor VR-1, also referred to as the capsaicin receptor, can integrate multiple stimuli[36]. VR-1 is opened by noxious heat and is augmented by protons. The channel can be opened in the absence of capsaicin by an external pH of 5.9 or lower at room temperature[37]. These channels may exist in sub-populations of nociceptors specialized to detect noxious heat.

The investigations of dissociated neurons discussed thus far have been undertaken in sensory neurons, many in a nociceptive-enriched population. However the specific sensory modality or site of innervation of these neurons was not known. To examine cardiac sensory neurons and their responses to chemical mediators of ischemia, Benson et al.[7] devised a method to label the sensory neurons innervating the myocardium *in vivo* for

later identification *in vitro*. Surprisingly, these cardiac afferent neurons are remarkably insensitive to capsaicin as a population, and those that did respond to capsaicin had very small currents (<200 pA). Conversely, 93% responded to pH 5.0 with large currents (average 8.6 nA, see Chapter 3: Results). This suggests that VR-1 is not the major proton sensor in cardiac afferent neurons. The acid-sensitive current in sympathetic afferents resembles the fastest of the three kinetic currents described by Krishtal, is activated by pH 7.0 ($pH_{1/2}$ =6.7), and is blocked by amiloride, an ASIC antagonist[7].

Cardiac afferents display a biphasic current. In addition to the large, transient current evoked at pH 7 and below, there is a smaller sustained current evoked at very low pH levels (<5.0). This current is the same as that described by Bevan and Yeats[38]. Its sustained nature seems important because cardiac pain is sustained. However, the extreme pH required for activation of this current is not achieved even after 60 minutes of total myocardial ischemia[29], which would be a fatal insult. Thus, there are two parts of the ischemia-sensing current, neither of which is obviously suited to signal persistent pain. One possibility is that the sustained component is activated by less extreme pH levels *in vivo* than seen with electrophysiology. The discrepancy may be due to experimental conditions that differ during measurements of cardiac physiology and cellular electrophysiology: cellular experiments are performed at room temperature and in the absence of cardiac metabolites (other than low pH). Alternatively, the transient

current might generate persistent firing because it does not fully desensitize at the pH achieved during myocardial ischemia[7].

Part Two—Cloned Acid-Sensing Ion Channels (ASICs)

In recent years, a group of channels has been cloned called ASICs, or acid-sensing ionic channels[39]. These channels belong to a diverse family that includes epithelial sodium channels (ENaCs) and the degenerin channels (DEG). Members of this family share a membrane topology consisting of two transmembrane domains, short intracellular N- and C-termini, and a large extracellular loop. They all preferentially pass Na^+ ions, are blocked by amiloride, and are insensitive to voltage. The family displays great diversity as well: some channels are constituitively open (ENaC), others are gated by ligands including protons (ASIC) or peptides (FMRF-amide gated channel, FaNaC), and still others become active after a mutation and may be mechanically sensitive (DEG). These channels are found in a variety of species; they include mammals as well as *Drosophila*, the snail *H. aspersa*, and the nematode *C. elegans*[40]. Members of this family may form channels made of four subunits (tetramers)[41-43], although other evidence argues for different numbers of subunits[44]. Incidentally, while the capsaicin-sensitive channel VR-1 is sensitive to protons[36], ASICs are insensitive to capsaicin. ASICs and

vanilloid receptors are members of entirely different families with distinct properties and membrane topologies.

The chronology of the cloning of the proton-gated channels has resulted in some discrepancy in the nomenclature. Most of the proton-gated channels have been discovered by Lazdunski's group, the first of which is now referred to as ASIC1a[45]. This channel is activated by a rapid decrease in pH to 6.9 or lower. The current displays single exponential activation and desensitization kinetics. A splice variant, called ASIC1b, has been cloned that displays similar kinetics to ASIC1a, but is much less sensitive to protons. Further, the channels differ in permeability to Ca^{2+} and inhibition by extracellular Ca^{2+} ions[46]. While ASIC1a is expressed throughout the central nervous system and the dorsal root ganglia, ASIC1b is absent from CNS neurons and is expressed in a subset of DRG neurons.

Before ASIC1, the mammalian homologue to the degenerin channels was cloned and named MDEG[47]. Shortly after ASIC1a was cloned, MDEG1 was found to be gated by protons, and a splice variant, MDEG2, was cloned[48]. These MDEG channels are now referred to in the ASIC family as ASIC2a and ASIC2b. ASIC2a differs from ASIC1 in that it has slower kinetics and opens at a much lower pH, with a half-maximal activation at pH=4.35. ASIC2b does not form a functional channel when expressed as a homomer, but it can associate with other ASIC subunits to change their permeation properties.

ASIC2a and ASIC2b are expressed in the same areas of CNS, but, of the two, only ASIC2b is present in sensory neurons[48].

ASIC3 May Be the Cardiac Ischemia Sensor

ASIC3 may be the most important cloned proton-gated channel in terms of sensory physiology. ASIC3 mRNA is abundant in DRG, so this channel was initially called DRASIC[45]. ASIC3 is absent from brain and all other areas examined, suggesting that this channel is specialized to detect sensory signals. Like the acid currents reported in some sensory neurons[7,38], this current displays biphasic kinetics: a fast transient component that is very sensitive to protons ($pH_{1/2}$=6.5), followed by a smaller sustained component that is far less sensitive ($pH_{1/2}$=3.5)[49]. Unlike the sensory neuron currents, in which the sustained component is a non-selective cation conductance, both the transient and sustained components of ASIC3 are Na^+-selective.

How could the ASIC3 channel achieve the differential selectivity that is seen in neurons but not in the heterologous system? One possibility is that the channel undergoes some post-translational modification in neurons, such as phosphorylation. Another way that ASIC3 could account for the properties seen in native neurons is by heteromerization with another ASIC channel subunit. Although ASIC2b does not form a functional channel as a homomer, it can alter the properties of other ASIC channels when co-

expressed as heteromers. In fact, ASIC3 and ASIC2b heteromers display the kinetic and selectivity characteristics seen in sensory neurons[48].

Characterization of the various members of the ASIC family in native neurons has been made difficult by the absence of a good pharmacological tool that differentiates between the channels. Like the ENaCs, ASICs are sensitive to the diuretic drug amiloride, but it does not distinguish between the ASIC channels well.

It is evident that members of the new ASIC family play an important part in sensory physiology. The diversity of currents seen in sensory neurons[7,38,31] are almost certainly carried by ASIC channels, a family that will perhaps continue to grow. Cardiac afferent neurons are particularly well suited to use an ASIC channel, an exquisitely sensitive proton sensor, as a way to detect myocardial ischemia and elicit cardiac pain. This study of ASICs will use functional characteristics to create a "fingerprint" for each of the ASIC channels, which is then compared to the characteristics of the acid-evoked currents in cardiac sensory neurons.

Part Three—Physiology of Ischemia in the Central Nervous System

In muscle, as we saw in the previous sections, ischemia results in oxygen deprivation and often pain, and under extreme conditions can result in cell death. In the

CNS, the damage caused by ischemia is more severe and fast-acting, often resulting in massive neuronal death. Glutamate-induced excitotoxicity was once hailed as the primary mediator of neuronal death, but recently the focus has shifted to examine other additional neurotoxic components of ischemia[50,51]. A prominent feature of anaerobic cellular metabolism is extracellular acidification, which contributes to the neuronal damage that occurs during stroke[52-54]. Despite recent studies that have begun to elucidate the roles of acid, the specific molecules that elicit the neurotoxic effects of acidosis are unknown. A good candidate for such a molecule is an acid-sensing ion channel (ASIC); this is a family of ion channels that pass inward current in response to extracellular acidification[40]. Several ASICs are expressed in the CNS, and ASIC1a is active in the pH range relevant to ischemia and may display distinct properties that would enable it to convey the neurotoxic effects of ischemia[45].

Ischemia is a complex event, resulting in a cascade of events that ultimately causes massive neuronal death. Hypoxia, hypoglycemia and acidosis are prominent features that occur due to loss of perfusion[50,55]. Energy depletion leads to failure of ATPase pumps and breakdown of ionic gradients. As a result, cells become depolarized and release excitatory amino acids, which then activate the glutamate receptor-coupled ion channels[51]. During anaerobic metabolism, extracellular pH falls to around pH 6.5; in some conditions, the pH can fall even lower[56]. Rapid acidification is thought to be

simultaneous with release of excitatory amino acids[57]. Cell death during ischemia is selective for neurons, while glia for the most part survive. Thus, neurons must express some molecule that renders them vulnerable to ischemic conditions. Experiments aimed at examining these molecules have mainly been performed *in vitro*, and mimic ischemia. Such paradigms include exposure of cultured neurons to various ischemic conditions, such as oxygen and glucose deprivation (OGD), acidosis, glutamate, or ligands that activate specific glutamate receptors such as NMDA or AMPA.

Of the conditions that accompany ischemia, glutamate release has been the focus of most *in vitro* research. Glutamate release causes activation of NMDA, AMPA, and kainate-type glutamate receptors. Neuronal Ca^{2+} loading through the Ca^{2+}-permeant NMDA receptor channel has been the most widely studied cause of excitotoxic cell death[51,58,59]. In culture, a short exposure to NMDA or glutamate can cause almost total neuronal death[60,61]. NMDA antagonists protect neurons from glutamate exposure and from oxygen and glucose deprivation (OGD)[62]. Despite this evidence and success in animal studies, clinical trials of NMDA-type glutamate receptor antagonists have been disappointing[51]. While NMDA-mediated toxicity is certainly important, it is no longer considered the sole mediator of ischemic cell death.

AMPA channels are also known to mediate ischemic neuronal death[63]. Unlike the rapid Ca^{2+}-mediated excitotoxic death that results from NMDA exposure, AMPA-

mediated death requires a much longer excitotoxic exposure. AMPA channels are thought to mediate the acute cell swelling that occurs with OGD or glutamate exposure[60,64,61]. AMPA channels are far less permeant to Ca^{2+} than are NMDA channels, and cause neuronal death primarily by increasing Na^+ influx[65,63]. Excessive Na^+ influx can cause osmotic stress and indirect Ca^{2+} entry through activation of voltage-dependent channels and reversal of the Na^+-dependent pumps.

Acidosis and Cerebral Ischemia

What could explain the failure of glutamate receptor antagonists to protect against neurotoxicity *in vivo*? The failure of neuroprotective drugs can be partially blamed on poor clinical trial design, but this question has led to the examination of other possible mechanisms of ischemic neurotoxicity including acidosis. The studies that pointed to the NMDA receptor as the lethal molecule shared an important experimental detail: they were done at pH 7.4. Later studies—done at lower pH—revealed a surprising and paradoxical neuroprotection by acid[57,62,66]. Dual roles have now been indicated for acid: protons can be both neuroprotective and neurotoxic. When ischemic conditions (glutamate or OGD) are accompanied by low pH, early NMDA-mediated death is decreased while the later, non-NMDA mediated death is potentiated[62,67]. The protective effect of acid arises from block of the NMDA channel by extracellular protons[68,69]. Cell

death *in vivo* can actually increase during reperfusion; the removal of extracellular protons may allow NMDA channels to exert their neurotoxic effects[52]. Perhaps acidosis protects neurons from massive NMDA-receptor-mediated excitotoxicity early on, but contributes to other mechanisms of cell death over time. While the neuroprotective effects of acid are now understood, the mechanism of acid-mediated neurotoxicity is less clear.

A large body of work has shown that acid contributes to ischemic neurotoxicity[70,57,56]. Dissociated neurons, however, can survive long exposures to pH 6.5[52,53]. Rather than directly mediating toxicity, acid may play a potentiating role. McDonald et al. found that lowered pH speeds and increases non-NMDA-mediated death in culture[71]. The authors concluded that protons specifically potentiate AMPA-mediated neurotoxicity. But how this could occur is unclear, especially in light of the fact that the AMPA channel, like the NMDA channel, is inhibited by protons (although to a lesser extent)[72]. Another interpretation of their data might be that depolarization concurrent with low pH is key to the toxic effects of acidosis. Low pH (6.6) alone is sufficient to cause widespread neuronal death in hippocampal slices[73]. Perhaps in this setting of intact cellular architecture, input from other neurons provides depolarization or some other signal that allows acid to mediate its neurotoxic effects.

Two types of neuronal death occur during ischemia: *necrosis*, associated with ion influx, swelling, and rupture of the plasma membrane; and *apoptosis*, a programmed cell death that requires new gene transcription[70,74,50]. While acidosis has been found to cause both types of cell death in hippocampal slices, the topic of this introduction is necrotic death. Na^+ influx during ischemia is a major contributing factor to cell death due to simple osmosis[75]. When Na^+ ions enter the cell, they are followed by Cl^- ions and water, which leads to swelling and can eventually cause the membrane to rupture. Another lethal effect of Na^+ influx during acidosis is more complex: when the cell is presented with an acid load, the Na^+/H^+ exchanger becomes more active, extruding protons and bringing in more Na^+ ions. This increased intracellular concentration of Na^+ depletes the driving force and reverses the Na^+/ Ca^{2+} exchanger, preventing Ca^{2+} extrusion. These pumps contribute to the massive derangement of ion homeostasis that can lead to cell death over time[76,77,54].

What sort of molecule could mediate the neurotoxic effects of acid? One possibility is an ion channel gated by extracellular protons. ASICs (acid-sensing ion channels) are a prime candidate. ASICs belong to a diverse superfamily of channels that includes the epithelial sodium channels (ENaCs)[40]. ASICs are cation channels that pass predominantly sodium and are gated by extracellular protons. The ASIC family now consists of five cloned subunits. One of these, ASIC1a, displays a negative slope region

in its I-V curve[45]. This suggests that it could act as a coincidence detector. One possibility is that the simultaneous presentation of acid with depolarization—as during ischemia—allows for increased activation of ASIC, contributing to vulnerability.

Several ASIC subunits (1a, 2a and 2b) are expressed in the CNS, notably at high levels in hippocampus and cortex, where ischemic neuronal damage is extensive. ASIC2b does not form a functional channel as a homomer, but can assemble with other subunits to form novel channels. The possible combinations of ASIC subunits in CNS are 1a, 2a, 1a+2a, and 2a+2b. With a $K_{0.5}$ around pH 6.4, ASIC1a is opened in the pH range relevant to ischemia. ASIC1a seems to be primed to act as a coincidence detector, primarily because of its negative slope region and its high sensitivity to protons. The other ASIC channels formed in the CNS, however, are less sensitive to protons, and are not in fact activated until pH goes much lower. Nevertheless, they too may express the ability to act as a coincidence detector in certain conditions. *In situ* data suggests that the three subunits are expressed in the same brain regions. Electrophysiological data has revealed some heterogeneity in acid current in central neurons. Expression of an ASIC with a negative slope region in the physiologically relevant pH range may render a neuron more vulnerable to ischemic neurotoxicity. Other ASICs may have the capability to act as coincidence detectors, however they are not activated in the pH range relevant to ischemia[78,48]. Perhaps they play a role in circumstances of extremely low pH, such as

incomplete ischemia or hyperglycemic stroke, during which more glucose is available as a proton source.

Coincidence Detection by Ion Channels

The term coincidence detector describes a property of an ion channel whereby it passes more current when two conditions that affect the channel are coincident, or occur at the same time. The NMDA-type glutamate receptor is an example of a coincidence detector: it can only pass current when it senses both extracellular glutamate and depolarization. This "coincidence detection" occurs because the NMDA channel is blocked by external Mg^{2+} ions at the rest potential, and this block is relieved by depolarization[79,80]. Thus, when cells are depolarized in the presence of glutamate, the NMDA channel is opened and unblocked, allowing the channel to pass Ca^{2+} current and thereby exert its toxic effects during CNS ischemia.

The current-voltage (I-V) curve of a coincidence detector channel displays a biophysical property called a "negative slope region". This I-V plot results from the channel passing more inward current at depolarized potentials than at rest. If the blocking ion, such as Mg^{2+} in the case of NMDA receptors, can permeate the channel, they might be forced through the pore when the voltage becomes extremely low. This results in an N-shaped I-V curve, as in the NMDA receptor[79,80].

ASIC1a might also act as a coincidence detector much like the NMDA receptor—ironically, in the same CNS condition. The two signals that ASIC1a would detect would be coincident depolarization and extracellular protons—conditions that occur simultaneously during CNS ischemia. ASIC1a displays a negative slope region in its I-V curve[45], perhaps suggestive of voltage-dependent block by a divalent cation such as Mg^{2+}.

A negative slope region is often evidence of voltage-dependent block by some ion (other than the principal permeant ion)[81,82]. The blocking ion may gain voltage dependence by binding at a site within the pore of the channel, which lies some distance into the electrical field across the membrane; the membrane potential then influences the binding affinity of the site for the blocking ion. When the blocking ion occupies the channel, the normal conductive ion cannot pass through; therefore, any current must pass through unblocked channels. At positive potentials, the blocking ion (if positively charged) is repelled from the channel site and the block is relieved, allowing more channels to pass current. This work will examine the possibility of voltage-dependent block of ASIC1a by Mg^{2+}.

Part Four—Significance

A family of acid-sensing ion channels (ASICs) has been identified, cloned and characterized in recent years. The work presented here examines a role for ASICs as molecular sensors of ischemia in the heart and brain. The physiology of cardiac sensation calls for a chemical mediator of pain with requirements that are fulfilled by protons, in the form of lactic acid. Sensory neurons that innervate the heart respond to the pH of muscle ischemia with large, inward depolarizing currents. I will show that these currents are primarily carried by the channel ASIC3, a molecular ischemia sensor in the heart.

In the CNS, ischemia can have disastrous consequences resulting in massive neuronal death. Monumental research efforts have led to a detailed, but incomplete, understanding of the ion channel physiology of CNS ischemia. ASIC1a is expressed in CNS neurons and may act as a molecular ischemia sensor in the brain as well as in heart. I have found channel properties of ASIC1a that are analogous to both NMDA-type glutamate receptors (voltage-dependent block by Mg^{2+}), and to voltage-gated sodium channels (selectivity properties of the pore).

Chapter 2: Methods

Part One—Cell Culture

Labeling and Culture of Cardiac Sensory Neurons From the DRG

Surgical Preparation for Labeling: Sprague-Dawley rats (200-300g) were anesthetized by intramuscular injection of 1 ml/kg rat cocktail (55 mg/ml ketamine; 5.5 mg/ml xylazine; 1.1 mg/ml acepromazine). The animal was intubated and respiration maintained with a rodent ventilator (Harvard model 683). The heart and thymus were exposed through a left lateral thoracotomy at the fifth intercostal space. The thymus, with the anterior superior portion of the pericardium adherent to its under-surface, was gently retracted cephalad to better delineate the pericardium and pericardial space. Twenty-five μl of a suspension of 17 mg/ml of DiI (1,1'-di-octtadecyl-3,3',3'-tetramethyl indocarbocyanine perchlorate; Molecular Probes, Eugene, OR) in saline solution was injected into the pericardial space. The rat pericardial membrane is thin and contains microscopic pores;[83] thus, a suspension rather than solution of the lipophilic DiI was used to decrease the potential of leakage of dye from the pericardial space. After injection, the ribs were approximated, the thoracic cavity evacuated, and the incision closed in layers. The animals were cared for in accordance to the current *Guide for the*

Care and Use of Laboratory Animals (DHHS/USPHS); and the Institutional Animal Care and Use Committee of Oregon Health Sciences University.

Tissue Culture and Identification of Labeled Cardiac Sensory Neurons: During the two to four week post-operative period, DiI was carried through retrograde transport back to the cell bodies of the cardiac sensory neurons. The rats were then sacrificed and the right and left dorsal root (C_8-T_3) and nodose ganglia were collected. The ganglia were dissociated and cultured as previously described, except that the Percoll spin was omitted[84]. In brief, the ganglia underwent enzymatic dissociation successively in papain, and collagenase/dispase solutions; this was followed by trituration in Hanks solution. The cells were then plated on polylysine- and laminin-coated plastic in F12 media plus nerve growth factor (NGF, 50 ng/ml) at 37°C in 5% CO_2. After several hours, the media was changed to L15 plus NGF, and the cells were maintained at 22°C in air. cardiac sensory neurons were identified by fluorescence microscopy (see Fig 2C,D). From the animals that underwent the pericardial space injection preparation, three populations of sensory neurons were obtained for study: 1) labeled neurons from the DRG (cardiac DRG neurons); 2) unlabeled neurons from the DRG (unlabeled DRG neurons); and 3) labeled neurons from the nodose ganglia (cardiac nodose neurons).

Labeling Control Experiments: To check for dye leakage from the pericardium and to explore the effects of labeling at different injection sites, we performed several controls. First, after a pericardial space injection, the heart and lungs were sectioned at the time of sacrifice and viewed under a fluorescence microscope. While the heart consistently displayed confluent fluorescence over the epicardium, the surface of the lungs contained only an occasional isolated crystal of dye. Next, to test if dye leakage from the pericardial space would cause significant contamination, we intentionally injected dye in the following sites in separate animals: the left pleural space, the left ventricular chamber, or the right ventricular chamber. As expected, sectioning of the lungs after injecting into the right ventricular chamber revealed confluent pulmonary vascular embolization of the dye. Next, in an effort to label sensory nerve terminals deeper within the myocardium, we stabilized the heart with sutures and made several intramural injections into the left ventricular myocardium.

The pericardial space injection resulted in a significantly greater number of labeled neurons in the DRG than the various control injection site experiments. Thus, despite the potential for dye leakage from the pericardial space, it would cause little contamination because relatively few cells were labeled with intentional injection into the pleural space. Because of the low number of neurons labeled by the intramural injections, we abandoned this experimental preparation. The number of nodose ganglia neurons

labeled by the pericardial space injection was not quantified; however there appeared to be a higher fraction of labeled cells in the nodose ganglia (~10%) than in the DRG (~1%) cultures.

Culture of Mechanosensory Neurons from the Mesencephalic Nucleus

Mechanosensor neurons were prepared from the mesencephalic nucleus of the trigeminal nerve (MeN5) as previously described[84]. Below is a description of the methods for isolating and culturing these neurons. Most recordings from MeN5 neurons were made the day after dissociation and none were made after 3 days; we saw no evident change in currents in this time.

Solutions: The following solutions are used in the preparation of dissociated glial cells, which serve as a substrate for the cultured sensory neurons. Complete Glial Media: Minimum Essential Media (MEM) without L-glutamine, with Earle's Salts (Gibco); 0.1% Mito-plus serum extender (Collaborative Research); 10% heat inactivated fetal calf serum (Gibco); 1.5% high glucose MEM (made up of 25 g glucose per 100 ml MEM). Store at 5% CO_2. Inhibitor solution: Complete glial media with 0.25% trypsin inhibitor (Sigma) and 0.25% bovine serum albumin (Sigma). Trypsin solution: 0.05% trypsin (Gibco) in

phosphate-buffered solution (PBS). Papain solution: 20 U/ml papain (Worthington) in CMF Hank's solution. Filter sterilize all solutions.

Glial preparation: We found that MeN5 cells survive far better on glia than on any other surface. Both hippocampal and cortical tissue have worked for generation of glia; others are likely to work as well. Sacrifice 3-10 day old Sprague-Dawley rat pups by decapitation. Unroof the skull, remove meninges, and dissect 5x6 mm blocks of hippocampal or cortical tissue with a scalpel; chop into small pieces. Transfer pieces to 3 ml papain solution in a 15 ml polystyrene conical tube and incubate at 37°C for one hour. Allow the chunks to settle out of solution, then aspirate fluid and add inhibitor solution. Let the pieces settle again, and aspirate.

Add 2 ml complete glial media and triturate once with a polished glass Pasteur pipette. Remove turbulent media to a second conical tube, then add another 2 ml media to the tissue chunks. Triturate and let pieces settle, again removing the cell-containing media to the second tube. Repeat once more with 4 ml media. In a final volume of 10 ml media, place cells into a 250 ml Primaria tissue culture flask (Falcon). Make a complete media change within 24 hours, then feed every 2-3 days.

Glial Passage: Remove all media from flask, then rinse the flask twice with 5 ml 37° C Versene (Gibco). Add 2 ml trypsin solution and swirl around flask. Close tightly and incubate at 37° C for about 5 min., until cells have lifted from the surface of the flask and are floating freely in the media. Add 2-3 ml Versene and triturate cells using a 5 ml plastic pipette, approximately 20 times. Remove all media to a 15 ml polystyrene conical tube. Rinse flask with another 1 ml of Versene and add to the tube. Centrifuge at 1200 RPM for 3 min.

Aspirate fluid and resuspend cells in 2 ml complete glial media. Triturate gently with media-coated glass pipette. Check cell density on a 35 mm Primaria TC plate (Falcon) to determine seeding volume. Cells should cover 40-60% of the plate's surface, including cells still suspended in the liquid. Seed the cells onto the desired number of plates each containing 2 ml glial media, then return the remaining cells to the flask containing 8-10 ml glial media. Glia will grow confluent again and may be passaged repeatedly. Make a complete media change within 24 hours of splitting, then feed every 2-3 days. Allow 2-3 days after splitting for glia to form a totally confluent monolayer before seeding neurons.

Culture of Mesencephalic Sensory Neurons: The sensory neurons of the MeN5 have not been grown in culture before; regardless, the preparation follows standard tissue

culture procedure, making use of a glial monolayer for adhesion and micro-dissection of brainstem slices for cell isolation. Microdissection is necessary to separate MeN5 neurons from the motor nucleus of the 5th nerve because motorneurons can be as large as the sensory neurons and can be mistaken for sensory neurons. The challenge of the preparation is to successfully harvest and maintain the small number of sensory neurons in the MeN5; a typical yield is 40-100 cells.

Solutions: For dissociation: use Ca^{2+}/Mg^{2+}-free Hanks (CMF Hanks) balanced salts solution (Gibco #14180-020) buffered with 5mM Na^{+}-Hepes. For storing cells in incubator: Ham's F12 media (Gibco #11415-023) with 5mM Na^{+}-Hepes buffer; 5 mM glucose; 10% heat inactivated fetal calf serum (Gibco); 1% Pen/Strep (10,000 U/ml Penicillin and 10,000 µg/ml Streptomycin, Gibco). Kreb's: 126 mM NaCl, 2.5 mM KCl, 1.2 mM $MgCl_2$-$6H_2O$, 2.4 mM $CaCl_2$-$2H_2O$, 1.2 mM NaH_2PO_4, 21.4 mM $NaHCO_3$, 11.1 mM glucose; filter sterilize.

Blocking and slicing: Unlike acute slice procedures, equipment and solutions must be sterile. Sacrifice the rat without causing damage to the hindbrain. Remove the brain and complete brainstem and place in ice cold Kreb's solution equilibrated with 95% O_2/ 5% CO_2. For blocking, place the brain on a piece of filter paper with the ventral side

up. Using a fresh razor blade, cut off the spinal cord just caudal to the cerebellum. Remove the forebrain with a cut 2-3 mm rostral to the pons. Then flip the brain 90° onto its caudal surface, and trim away the 2 mm of cortex on either side, and the dorsal cortex, leaving approximately a 5 mm^3 cube of tissue. Using a razor blade to aid you, gently slide the end of a spatula under the cube and appropriately orient the cube onto the vibratome stage for coronal slices (i.e. with the dorsal surface against the block and the rostral surface facing up). Make the first slice at the rostral end of the pons, and progress at 300 μm slices. Keep the 3-5 slices in which the aqueduct opens into the fourth ventricle. Place these slices in Kreb's at 35°C and bubble with 95% O_2/5% CO_2 for 30-60 min.

Micro-dissection: Examine slices in a glass petri dish under a dissecting scope to determine which contain MeN5. The MeN5 is grayish and round, lateral to the locus coeruleus, just central to the white fiber tracts of the brachium conjunctivum, above the ventricle and lateral to the central gray. Immobilize the slice with a short piece of wire; score and cut out the MeN5 with a 26 gauge hypodermic needle. Avoid the motor nucleus of the trigeminal nerve, which is 1-2 mm ventral of the MeN5 in the most caudal slices.

Dissociation and culture: Place chunks of MeN5 tissue in 3 ml papain solution at 37°C for 5 min. Aspirate fluid, add 2-4 ml F12 media and swirl the tissue chunks to wash. Aspirate again and add 1 ml complete F12. Using a media-coated glass pipette, triturate tissue extremely gently, until chunks are diminished. The sensory neurons are far more hardy than other neurons present, but extensive mechanical dissociation causes cell death. Divide the cells among four plates of glia and incubate at 37°C, 5%CO_2, in F12 medium supplemented with the growth factors NT3 and GDNF at a concentration of 50 nM. The large size of MeN5 sensory neurons easily distinguishes them from other neurons in the preparation. Moreover, the sensory neurons are more hardy than others, so they are often the only neurons present after dissociation.

Culture and Heterologous Transfection of COS7 Cells

I used a line of COS-7 cells to study ASIC channels in the heterologous system. All ASIC clones were kindly provided by Drs. R. Waldmann and M. Lazdunski. The COS7 cell line I used had less than 100 pA of acid-evoked current at pH 5, and no transient acid-evoked current. Our sequence analysis of the ASIC1b clone used in this study differs from the GenBank ASIC-β sequence (accession no. AJ006519) at one residue: a threonine instead of a serine at position 82. The COS-7 cells were cultured in

DMEM media with 10% heat-inactivated fetal calf serum (Gibco) and 1% Pen/Strep (Gibco). Cells were transfected using Lipofectin reagent (GibcoBRL #18292) or the electroporation method with DNA for various ASICs and for the CD4 receptor in the pcDNA3 vector (Invitrogen). All recordings were made 24-72 hours later; transfected cells were identified with CD4-coated microbeads (Dynal #111.05).

Cell culture: COS 7 cells (ATCC) were maintained for use in a heterologous expression system. Cells were grown on 10 cm tissue culture plates (Falcon) in Dulbeco's Modified Eagle Medium (DMEM, Gibco) with 10% heat-inactivated Fetal Bovine Serum (FBS, Sigma) and 1% Pen/Strep, kept at 37° C. Cells are split, or passaged, when they reach a level of 40-80% confluence, according to the following method:

Rinse plate with 2 mL Versene (Gibco) to remove divalent ions. Remove, and then add 2-3 mL Trypsin (Gibco) to the plate. Place in 37° C incubator for 10-15 min. When cells have detached from the plate, add 2-3 mL DMEM to the plate. Triturate using a 5 mL pipette against the bottom of the plate. Add 100-500 µl of this cell mixture to a new tissue culture plate containing 10 mL media.

Lipid-based transfection: After splitting cells from tissue culture plate, add 20-100 µl cells to five 35-mm tissue culture plates, each containing 2 ml media. Allow cells

to settle for 5-24 hrs. For transfection, mix in a 10-ml snap-top tube: 4 ml Optimem transfection buffer (Gibco); 30 µl Lipofectin transfection agent (Calbiochem); 1 µg CD4 cDNA; 30 µg channel cDNA. Shake up the tube several times over 10 min. Meanwhile, rinse the 5 plates of cells for transfection with Optimem buffer. Then drop 800 µl of transfection mix over each plate. Allow to sit in incubator for four hours, with a gentle shaking about half way through. Suck off all liquid from plates, and replace with warm DMEM media. Cells may be used for electrophysiology 24-72 hours later.

Electroporation transfection: Place 6-7 1-cm glass coverslips in a 35 mm t.c. dish. They may be coated with an adherence protein, but this is only necessary for pulling excised patches. Split cells as above through incubation step. Meanwhile, place the following on ice in a bucket: HBS solution (see recipe below); 1 15-ml polystyrene centrifuge tube; 1 electroporation cuvette (Invitrogen #65-0032).

When cells have lifted from the surface of the tissue culture dish, add 3 ml cold HBS. Triturate slightly to break up clumps of cells. Remove entire volume (5 ml) to the chilled centrifuge tube. Spin cells down at speed level 1.5 (approx. 1500 rev./ min.) for 3 min. Carefully suck off supernatant, leaving the cell pellet in the tube. Then add 1 ml cold HBS and triturate thoroughly. Using a hemocytometer (10 µl cells under glass), check the cell density; there should be approx. 7-12 cells per square. Cells are more likely

to be usable for two days of recording if a slightly lower density is used. If density is too high, add a small volume of HBS to the cells. If density is really too low, spin down cells again and add a smaller volume of HBS. If cell density on the culture plate was low, you may want to only add 0.8 ml cells initially. If density is appropriate, continue with transfection.

Add 200 µl cells to the electroporation cuvette, and then add 0.5 µg CD-4 cDNA and 5-20 µg channel cDNA (according to the channel density you want to achieve). Make sure cDNA is added by watching for the bubble at the end of the micropipette. Flick the cuvette lightly to mix, and place on ice. Set the electroporator to 380 V and 0.075 µF capacitance. Wipe off the sides of the cuvette to remove any condensation, then place it in the electroporator with the notch facing toward the back, so that it clicks into place. Hold down both buttons at once until you hear the tone indicating that electroporation is complete (several seconds). Remove the cuvette and place back on ice. Let the cuvette rest on ice for five to ten minutes.

If you wish to maintain the line of cells in culture, place 10 ml media in each of two 10 cm culture dishes. Drop 100-200 µl untransfected cells from centrifuge tube into each t.c. dish. Gently shake back and forth (don't swirl) to disperse. (This can be done earlier.) Place 2 ml media on the 35 mm t.c. dish with the glass coverslips in it. Using a P200, drop the transfected cells from the cuvette onto the glass coverslips and gently

shake to disperse. Place all dishes in incubator. Cells can be used for electrophysiology the next morning, for one or two days.

To make HBS, combine the following: NaCl, 8.18 g; HEPES buffer (Sigma), 5.95 g; Na_2CO_3, 0.2 g; pH to 7.4 with NaOH. Bring to volume of one liter.

Part Two—Electrophysiology and Data Analysis

Experiments presented in Results Chapter 3: Whole cell currents were recorded with an EPC-9 amplifier (HEKA Elektronik, Lambrecht, Germany). For most experiments, pipettes of 2-4 MΩ resistance were filled with KCl internal solution (mmol/L): KCl 100, EGTA 10, HEPES 40, $MgCl_2$ 5, Na_2ATP 2, Na_3GTP 0.3, adjusted to pH 7.4 with KOH, unless otherwise stated. For the monovalent permeability experiments, NaCl replaced KCl in the internal solution and pH was adjusted with NaOH; high internal Na^+ eliminated contamination by large, outward K^+ currents. For the Ca^{2+} permeability experiments, internal solution was N-methyl glucamine (NMG) 90 (titrated with HCl), NaCl 10, EGTA 10, HEPES 40, $MgCl_2$ 5, Na_2ATP 2, Na_3GTP 0.3, pH adjusted with TMA-OH. Our strategy was to measure relative Na^+ and Ca^{2+} permeability by using similar Na^+ and Ca^{2+} activities inside and outside the cell, respectively. Standard extracellular solutions contained (mmol/L): NaCl 130, KCl 5, $CaCl_2$ 2, $MgCl_2$ 1, HEPES

10, MES 10; pH adjusted with TMA-OH. TMA-Cl was added to the various pH solutions to equalize the concentration of TMA. For the monovalent permeability experiments, the extracellular solutions were (mmol/L): NaCl (or KCl or $NaMeSO_4$ or CsCl) 130, $CaCl_2$ 2, $MgCl_2$ 1, HEPES 10, MES 10; pH was adjusted with NaOH or KOH or CsOH. For the Ca^{2+} permeability experiments, external solutions were (mmol/L): NMG 120 (titrated with HCl), HEPES 10, MES 10, and $CaCl_2$ 10 or 30. For experiments on Ca^{2+} block, external solutions were: NaCl 130, HEPES 10, MES 10, and $CaCl_2$ 1, 2 or 10. The series resistance ranged from 3-7 MΩ, and it was compensated by ~50%.

All dose-response curves were made by random-order application of various concentrations at 30 sec intervals. Solutions were applied through an array of 1 or 10 μl pipes positioned ~50 μm from the cell under 40 cm of water pressure. Rapid solution exchanges were controlled via computer-driven solenoid valves, and were accomplished within 5 msec as measured by an osmotically induced change in current (see Fig 5A). Cells were held at -70 mV unless otherwise stated. Experiments were performed at room temperature (~22°C). We studied most cells after one to two days in culture, however some experiments were done on cells cultured up to 7 days. We saw no obvious difference in the responses of cells cultured for longer times.

The equation $I(H^+)=1/[1+(K_{0.5}/[H^+])^n]$, where pH at half maximal response is -log $K_{0.5}$, was best-fit to the dose-response data using the program NFIT (Univ. Texas Medical

Branch, Galveston, TX), a least squares algorithm. PulseFit (HEKA Elektronik) was used to determine the time constants of current activation and desensitization, fit to a single exponential. Igor software (WaveMetrics, Inc., Lake Oswego, OR) was used to curve-fit the time of recovery from desensitization. Permeability ratios were calculated from reversal potentials using the Goldman-Hodgkin-Katz equation[81]. P_{Na}:P_K was calculated from the change in reversal potential when K^+ replaced Na^+ in the external solution: $\Delta E_{rev}=(RT/F)\ln(P_{Na+}[Na^+]_o/P_{K+}[K^+]_o)$. P_{Na}:P_{Ca} was calculated from the reversal potential with Ca^{2+} and Na^+ as the only current carriers inside and outside the cell, respectively, using: $E_{rev}=(RT/2F)\ln(4P_{Ca2+}[Ca^{2+}]_o/P_{Na+}[Na^+]_i)$. Data are reported as the mean ±SEM. Statistical analysis was made by an unpaired *t* test. A value of $P<.01$ was considered statistically significant.

All experiments presented in Results: Chapter 4 used the whole cell patch clamp method except for measurements of activation rate, which used the outside-out patch method. Recordings were made with an EPC-9 amplifier (HEKA Elektronik). Extracellular solutions were changed within 5 msec, in patch recordings, or 20 msec, in whole cell recordings, using a computer-driven solenoid valve system[7]. Recordings were made at –70 mV unless otherwise stated. Micropipettes were pulled from borosilicate glass (Garner Glass, Claremont, CA # 7052) to 1-5 MΩ resistance.

Standard internal solution contained (mM): 100 KCl, 10 EGTA, 40 HEPES, 5 $MgCl_2$, 2 Na_2ATP, and 0.3 Na_3GTP, adjusted to pH 7.4 with KOH. Standard external solution contained (mM): 130 NaCl, 5 KCl, 1 $MgCl_2$, 2 $CaCl_2$, 10 HEPES, 10 MES, pH adjusted to 8.0, 7.4, 7.0, 6.8, 6.5, 6.0, 5.5, 5.0, or 4.0 with tetramethyl ammonium (TMA)-OH, and osmolarity adjusted with TMA-Cl. In the Ca^{2+} block experiments, standard solution was used except that both control (pH 8) and test (pH 6) solutions contained 0.5, 1, 2, or 10 mM $CaCl_2$. In the Cs^+ selectivity experiments, CsCl replaced NaCl in both control (pH 7.4) and test (pH 5) solutions.

For Ca^{2+} permeability experiments, internal solution contained (mM): 90 *N*-methyl glucamine (NMG), 10 NaCl, 2 Na_2ATP, 0.3 Na_3GTP, 10 EGTA, 5 $MgCl_2$, 40 HEPES, pH adjusted to 7.4 with HCl. External solution contained (mM): 120 NMG, 10 HEPES, 10 MES, and 10 $CaCl_2$, adjusted to pH 7.4 or 6.0 with HCl. Voltage steps were made to –40, 0, 40 and 80 mV for 7 seconds, during which a 4-second pulse of pH 6.0 was applied. P_{Na}/P_{Ca} was determined from the reversal potential using $E_{rev}=(RT/2F)\ \ln\{4P_{Ca}[Ca^{2+}]_o / P_{Na}[Na^+]_i\}$. P_{Na}/P_K was determined in standard solutions (control pH=7.4, test pH=5.0) from the reversal potential using $E_{rev}= (RT/F)\ \ln\{(P_{Na}[Na^+]_o+P_K[K^+]_o) / (P_{Na}[Na^+]_i+P_K[K^+]_i)\}$. Time courses were fit with single exponentials using HEKA PulseFit software. Activation curves were fit with the Hill equation: Fraction open $= [H^+]^n / ([H^+]^n + K_{0.5}{}^n)$ using NFIT (University of Texas, Galveston) where $K_{0.5}$ is the proton concentration that causes half the channels to open. All data is reported as the average ± SEM.

The following experiments, presented in Chapter 5: Results, were performed on cultured COS7 cells transiently transfected with ASIC cDNA using the electroporation method. Cells were studied in the whole-cell patch clamp configuration, with the cell lifted off the surface of the dish. Recordings were made with an EPC-9 amplifier (HEKA Elektronik, Lambrecht, Germany). Extracellular solutions were changed within 5 msec using a computer-driven solenoid valve system. Recordings were made at –70 mV unless otherwise stated. Micropipettes were pulled from borosilicate glass (Garner Glass, Claremont, CA # 7052) to 1-5 MΩ resistance.

Solutions: Standard internal solution contained (mM): KCl, 130; EGTA, 10; HEPES, 40; MgCl2, 2; pH to 7.4 with KOH. Standard external solution contained (mM): NaCl, 140; KCl, 5; CaCl2, 2; HEPES and or MES buffer, 10; MgCl2, 0 or 10; pH to 8.0 (control) or 6.0 (test) with NMG^+. For amiloride experiments, standard solution contained 0 or 10 MgCl2 and 0, 1, 3, 10, 30, 100 or 200 μM amiloride (N-Amidino-3.5-diamino-6-chloro-pyrazinecarboxamide). For tetrodotoxin experiments, standard solution contained 0 MgCl2 and 10 μM TTX (tetrodotoxin in citrate buffer). For permeability experiments, solution contained (mM): CaCl2, 2; HEPES, 10; MES, 10; and NaCl, 130 *or* methyl-amine, 130 (Methyl-amine hydrochloride) *or* guanidine, 130 (Aminomethanamidine hydrochloride). TTX, amiloride, guanidine and methyl-amine were all obtained from Sigma (St. Louis, MO).

Ramps: Current-voltage plots were made by measuring currents as follows: pH 6.0 solution applied for 300 msec at –70 mV, potential held at +20 mV for 10 msec, then voltage ramped from +20 to –180 mV over 800 msec (Fig 1 and 2) or from +20 to –160 mV over 1 second. The voltage was then returned to –70 mV, and the solution returned to pH 8.0. Control ramps were measured at pH 8.0; this data was then digitally subtracted from each test ramp before plotting. For permeability experiments, the shift in reversal potential was determined from ramps collected in NaCl vs. guanidine or methyl-amine solution. This shift was used to determine the permeability ratios according to the following equation: $\Delta E_{rev} = E_{rev,B} - E_{rev,A} = (RT/zF) \ln (P_B[B]_{out} / P_A[A]_{out}$, where A represents Na^+ and B represents guanidinium$^+$ or methyl-ammonium$^+$[8,1].

Currents measured at various voltages were made by changing the holding potential (-60 to –180 mV) for 100 msec before changing the solution from pH 8 to 6.0 for 400 msec, then returning to pH 8 for 100 msec, and then back to –70 mV (voltage change not shown in traces; Figure 1B, 2B). To derive the $K_{1/2}$ values plotted in Figure 1C and 2C, the current amplitude was measured at each membrane voltage with and without Mg^+ or amiloride. The ratios of these amplitudes were then used to determine the apparent $K_{1/2}$ for each voltage according to the equation: $I_{10Mg}/I_{0Mg} = [0\ M\ Mg] + K(E) / [0.01M\ Mg] + K(E)$, (Figure 1) where E is the holding potential for each current ratio. (In Figure 15, 10 mM Mg is replaced by 10 μM amiloride.) These $K_{1/2}$ values were then

plotted on a log scale vs. their corresponding voltage potential. These equations are used as in Woodhull[82]. This data was then fit with the equation: $y = K(0) \exp(z \delta F E/R T)$, where z is the valence of the blocking ion, δ is the relative distance within the pore of the blocking site, F is Faraday's constant, E is the relevant holding potential (or x), R is the gas constant, and T is temperature. (For Mg, z=2; for amiloride, z=1.) Thus, the slope of this line determines delta. All plotted data points represent mean ± SEM.

Chapter 3: Results—Acid-Evoked Currents of Cardiac Sensory Neurons

Introduction: Although much is understood about the effect of the autonomic nervous system's input to the heart, the cardiac sensory--or afferent--system and its role in physiologic and pathologic conditions are less well understood. Historically, the major impetus for research on the cardiac sensory system has been to find the source of cardiac pain, or angina. During the first half of this century, the neuro-anatomical pathways of the cardiac sensory system were defined by clinical reports of surgical attempts to relieve angina, and by experimental studies[6,8]. These studies revealed that the cardiac sensory neurons follow the sympathetic and vagal nerve tracts en route to the central nervous system (Figure 1). The cell bodies of those sensory axons following the sympathetic tracts are found in the upper thoracic DRG; those following the vagal tracts are located in the nodose ganglia. The sensory innervation of the fibrous and serous parietal pericardium, separate from that of the heart and epicardium, follows the phrenic nerves to the cervical DRG (C_3-C_5)[85].

It has long been understood that cardiac pain is associated with myocardial ischemia, which causes oxygen supply/demand insufficiency[2]. In various whole animal preparations, occlusion of a coronary artery activates the cardiac afferent nerve fibers in

Figure 1. Illustration of the cardiac and pericardial sensory pathways. Cardiac sensory signals travel from terminals throughout the heart through both the sympathetic and the vagal nerve tracts en route to the central nervous system. Axons of some cardiac sensory neurons exit the heart via the sympathetic cardiac nerves and course through sympathetic ganglia (middle (MCG) and inferior cervical, and upper thoracic) en route to their cell bodies, located in the lower cervical and upper thoracic dorsal root ganglia (DRG). Axons of other cardiac sensory neurons travel within the vagal nerve to their cell bodies in the nodose ganglia. Afferent neurons from the pericardium follow the phrenic nerves to their cell bodies in the DRG of the upper cervical region (C_3-C_5).

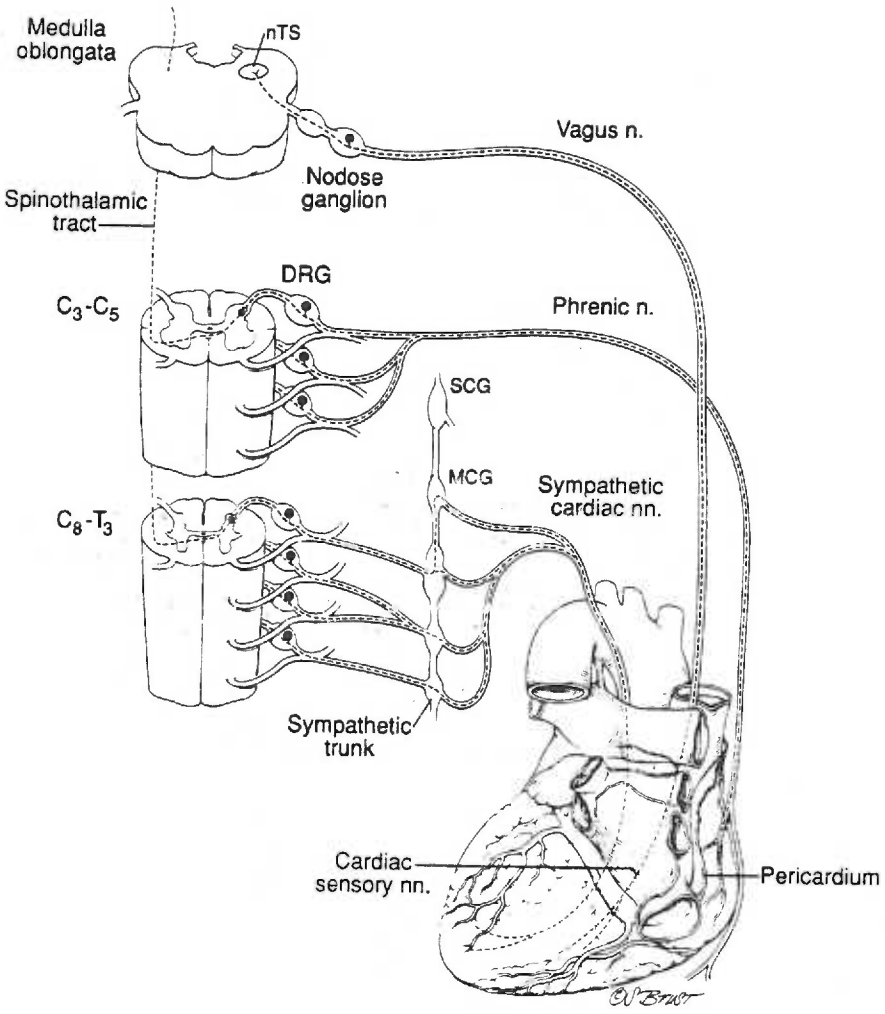
Medulla oblongata
nTS
Vagus n.
Nodose ganglion
Spinothalamic tract
DRG
C_3-C_5
Phrenic n.
SCG
MCG
Sympathetic cardiac nn.
C_8-T_3
Sympathetic trunk
Cardiac sensory nn.
Pericardium

the sympathetic[86,87,9] and vagal tracts[88,89]. Various substances released during myocardial ischemia have been implicated as chemical mediators of myocardial ischemic sensation. Several of these substances have been shown to activate cardiac sensory neurons: ATP[86,88], 5HT[90], BK[91,13], and adenosine[86,88]. In turn, stimulation of sensory fibers elicits specific sympathetic-[14] and vagal-mediated reflexes[92]. Still, the precise stimuli that are sensed during myocardial ischemia are incompletely understood (see Meller and Gebhart[10] for review).

A likely contributor is acid. The heart is an organ of high metabolic activity and is susceptible to drops in pH during ischemia or hypoxia. It has been demonstrated that pH is lowered intracellularly[93] and extracellularly[29,94] in ischemic heart models, and clinically in patients with coronary artery disease[95]. In dogs, lowered pH stimulates afferent cardiac sympathetic nerve fibers[12]. In another organ system, rat skin, acid plays a dominant role in exciting sensory neurons when compared to other potential chemical mediators of inflammation[96].

Acid evokes depolarizing currents in sensory neurons studied in primary dissociated culture[38,97,98,30], and a variety of different components are distinguished by kinetic criteria[31]. Most components activate somewhere between pH 7 and pH 6 and desensitize in response to a maintained stimulus. These desensitizing currents all have the unusual property of selectively passing Na^+ over K^+ about as effectively as voltage-gated

Figure 2. Fluorescent labeling of cardiac sensory neurons. A, Corresponding phase and B, fluorescence micrograph of an apical slice of myocardium three weeks after surgically injecting fluorescent dye into the pericardial space. C, Phase and D, fluorescence micrograph of two cardiac sensory neurons in primary dissociated culture of DRG neurons. E, Phase and F, fluorescence micrograph of a myocardial slice after an intramural injection of dye. Scale bars: 0.5 mm for A,B, E and F, and 0.25 mm for D.

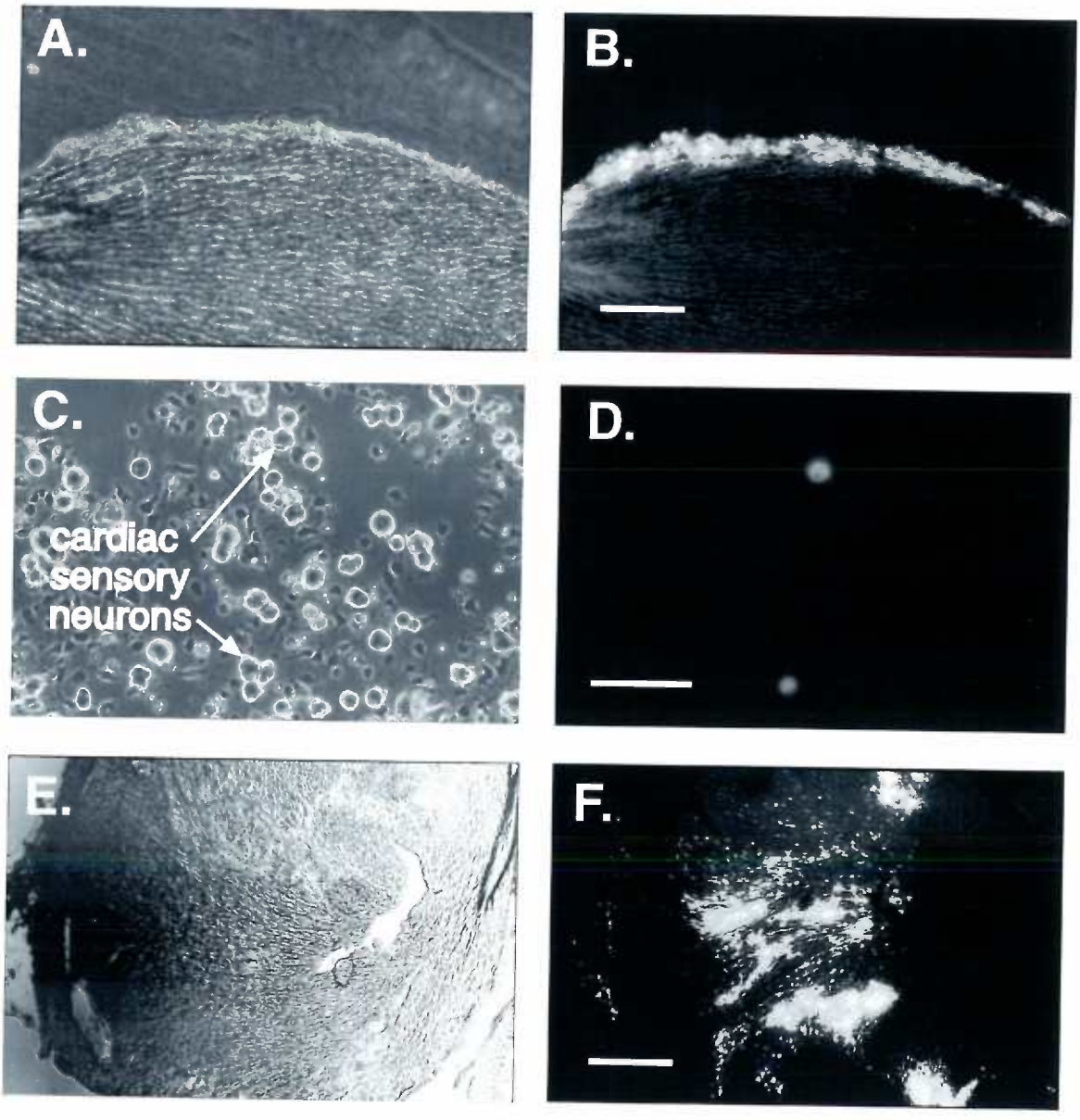
A.
B.
C.
cardiac
sensory
neurons
D.
E.
F.

Na^+ channels. In addition to the desensitizing, Na^+-selective currents in DRG neurons, there is a sustained, non-selective current that is evoked by pH below 6.0[38]. The channels underlying these currents are believed to be the recently cloned acid-sensing ion channels (ASICs), which are members of the amiloride-sensitive Na^+ channel/ degenerin family of cation channels[40].

These acid-evoked currents may play a role in mediating the pain of cardiac and skeletal muscle ischemia, and perhaps also of inflammation. It is difficult to explore this possibility in culture because the sensory modality and the site of innervation of individual neurons are not known. The first goal of the present study was to fluorescently label cardiac sensory neurons in the rat so they can later be distinguished from other sensory neurons in dissociated culture; we accomplished this using a retrogradely transported dye placed in the pericardial space (Figure 2). We found that acid evoked extraordinarily large currents in the cardiac DRG neurons compared to other, unlabeled DRG neurons. The very high expression of these currents in cells thought to be specialized for sensing ischemia suggests an important role of acid in mediating cardiac pain.

Response of Cardiac Sensory Neurons to Chemical Stimuli

We studied the response of cardiac sensory neurons to potential chemical mediators of ischemia by applying them to dissociated neurons and measuring the current responses to each chemical. The following chemicals were dissolved in an external solution of pH 7.4: ATP 30 μmol/L;[99] 5HT 30 μmol/L;[100] capsaicin 1 μmol/L;[36] ACh 200 μmol/L;[101] BK 500 nmol/L;[102] or adenosine 200 μmol/L[103]. The concentrations chosen for each compound produced maximal responses in our experiments and in the references cited.

The largest measured currents (8.58 ±1.44 nA) were consistently evoked (93%) by acid applied to cardiac DRG neurons, as seen in Figure 3. A smaller percentage of unlabeled DRG neurons (54%) and cardiac nodose neurons (74%) responded to acid, and the cells that responded displayed significantly smaller currents (3.48 ±1.10 nA in unlabeled DRG neurons and 1.15 ±0.23 nA in cardiac nodose neurons, $P<.01$ vs. pH-evoked current in cardiac DRG neurons)(Fig. 3B,C). These differences between cell populations refer to the amplitude of transient acid-evoked current (see below); the sustained component evoked by very low pH was seen in virtually every neuron and did not distinguish different cell populations.

Another consistent and large response (4.87 ±0.59 nA) was evoked by ATP in cardiac nodose neurons. The current was slow-activating and only partially desensitized

Figure 3. Cardiac sensory neurons respond to a variety of chemical activators. A, Representative currents evoked by application of various chemicals to cardiac DRG neurons. Note the different scale bars and application times. Each of the test solutions were applied to cells, in random order, for a minimum of 3 seconds; a longer application was made if needed to see the peak current amplitude. Control solution was flowed onto the cells for 30 seconds between chemical applications. B, The percentage of cardiac DRG neurons, unlabeled DRG neurons, and cardiac nodose neurons that responded to various chemicals: pH 5.0, ATP 30 μmol/L, 5HT 30 μmol/L, capsaicin (Cap) 1 μmol/L, ACh 200 μmol/L, BK 500 nmol/L, and adenosine (Aden) 200 μmol/L. A positive response was defined as an evoked current >50pA. For pH response, the number of cardiac DRG neurons studied = 29; unlabeled DRG neurons = 22; cardiac nodose neurons = 19. Not all of the cells studied were tested for all chemicals; each bar represents at least 12 cells. C, Mean current amplitudes of the responding neurons. Error bars = SEM. *$P < .01$ vs. pH-evoked current in cardiac DRG neurons.

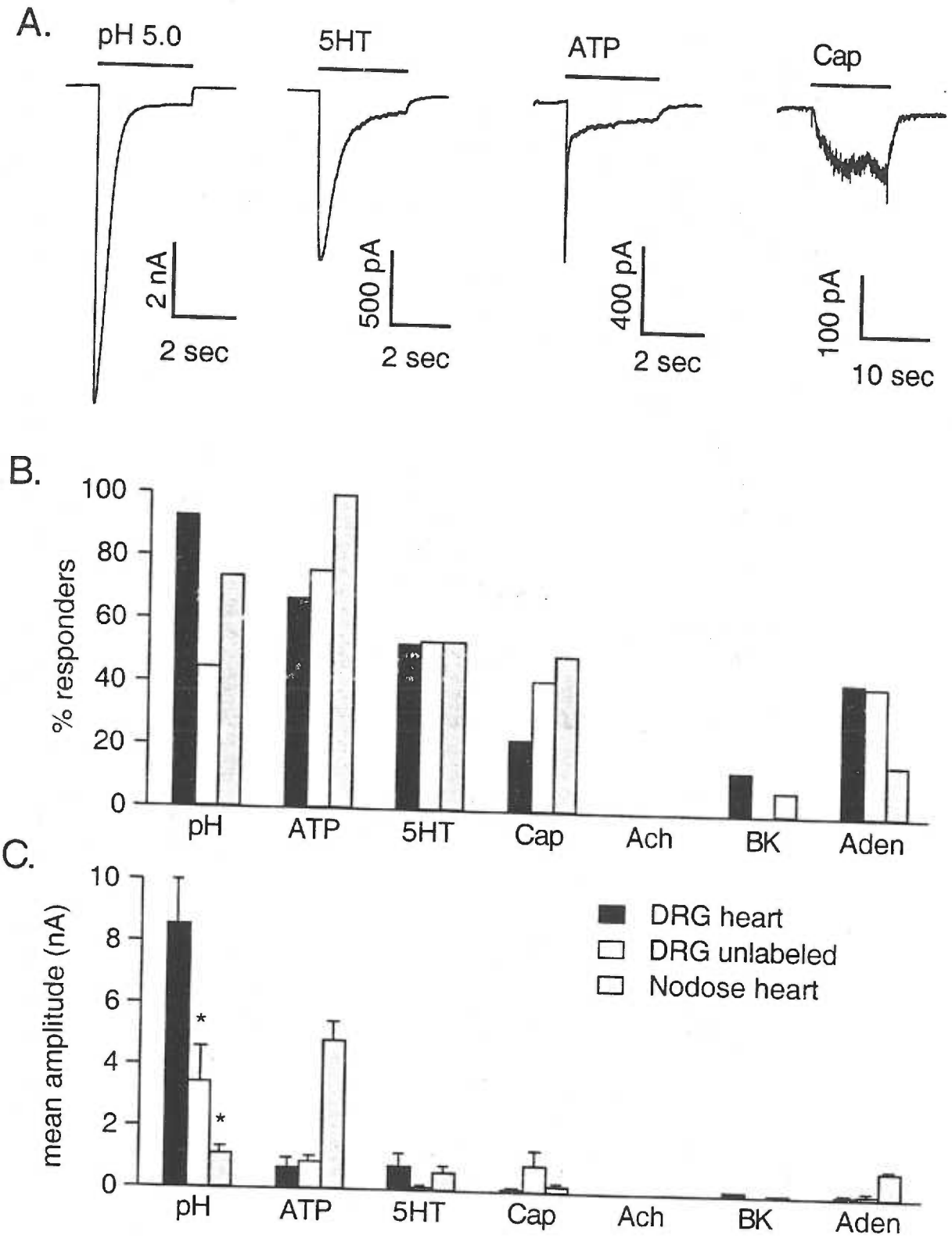
A.
pH 5.0
5HT
ATP
Cap
2 nA
2 sec
500 pA
2 sec
400 pA
2 sec
100 pA
10 sec
B.
% responders
100
80
60
40
20
0
pH
ATP
5HT
Cap
Ach
BK
Aden
C.
mean amplitude (nA)
10
8
6
4
2
0
*
*
DRG heart
DRG unlabeled
Nodose heart
pH
ATP
5HT
Cap
Ach
BK
Aden

(data not shown), which is indicative of the heteromeric combination of P2X2 and P2X3 receptor subtypes previously described in nodose neurons[104]. In contrast, the ATP-evoked currents in cardiac DRG neurons and unlabeled DRG neurons were substantially smaller and consisted primarily of a fast-activating and -desensitizing current (see Fig. 3A), which suggests the P2X3 receptor subtype[105]. Cardiac sensory neurons sometimes responded to the other chemicals indicated in Figure 3; however they did so inconsistently, and the amplitude of evoked currents in the responders was much smaller than with either pH or ATP (Fig. 3B,C).

Biophysical and Pharmacological Properties of Acid-Evoked Currents in Cardiac Dorsal Root Ganglion Neurons

The exceptionally large amplitude and prevalence of the transient acid-evoked current in cardiac DRG neurons suggests its significance in sensing cardiac ischemia. Therefore, we characterized its biophysical and pharmacological properties to see how these compared to the variety of acid-evoked currents seen in sensory neurons[38,97,98,30]. In short, we found no properties unexpected from those described in the literature.

A drop in pH to 7.0 reproducibly evoked a transient, rapidly activating and desensitizing current in cardiac DRG neurons (Figure 4). This transient current was half-activated by a pH step to 6.6 and half-desensitized by preincubation at pH 7.2 (Fig. 4C).

Figure 4. Activation and desensitization of acid-evoked currents in cardiac DRG neurons. A, Typical currents evoked by applying various pH to a cardiac DRG neuron. Note the transient, fast-activating and -desensitizing current that is evoked by relatively low proton concentrations. At higher proton concentrations a non-desensitizing, sustained current is evoked. Resting pH = 8.0 at -70 mV. B, Superimposed currents evoked by pH 5.0 from varying resting pH. The resting pH was applied for at least 3 seconds. C, Dose-response data for acid-evoked transient (closed circles, n=6) and sustained (triangles, n=6) currents. The open circles are data obtained using the desensitization protocol in B (n=7). The transient responses are normalized to the peak current obtained from application of pH 5.0 from a resting pH of 8.0. The sustained responses are normalized to the saturation level of the curve fit. Curves are best fits of the Hill equation, $I(H^+)=1/[1+(K_{0.5}/[H^+])^n]$ (activation), or $I(H^+)=1/[1+([H^+]/K_{0.5})^n]$ (desensitization). Half-activation values were pH 6.6 (transient) and pH 3.7 (sustained); half-desensitization was pH 7.2. Hill coefficient (n) =2.5 (transient activation), =1.2 (sustained activation), and =2.6 (transient desensitization). The boxed inset magnifies the region where the transient activation and desensitization curves overlap. Points represent means ±SEM.

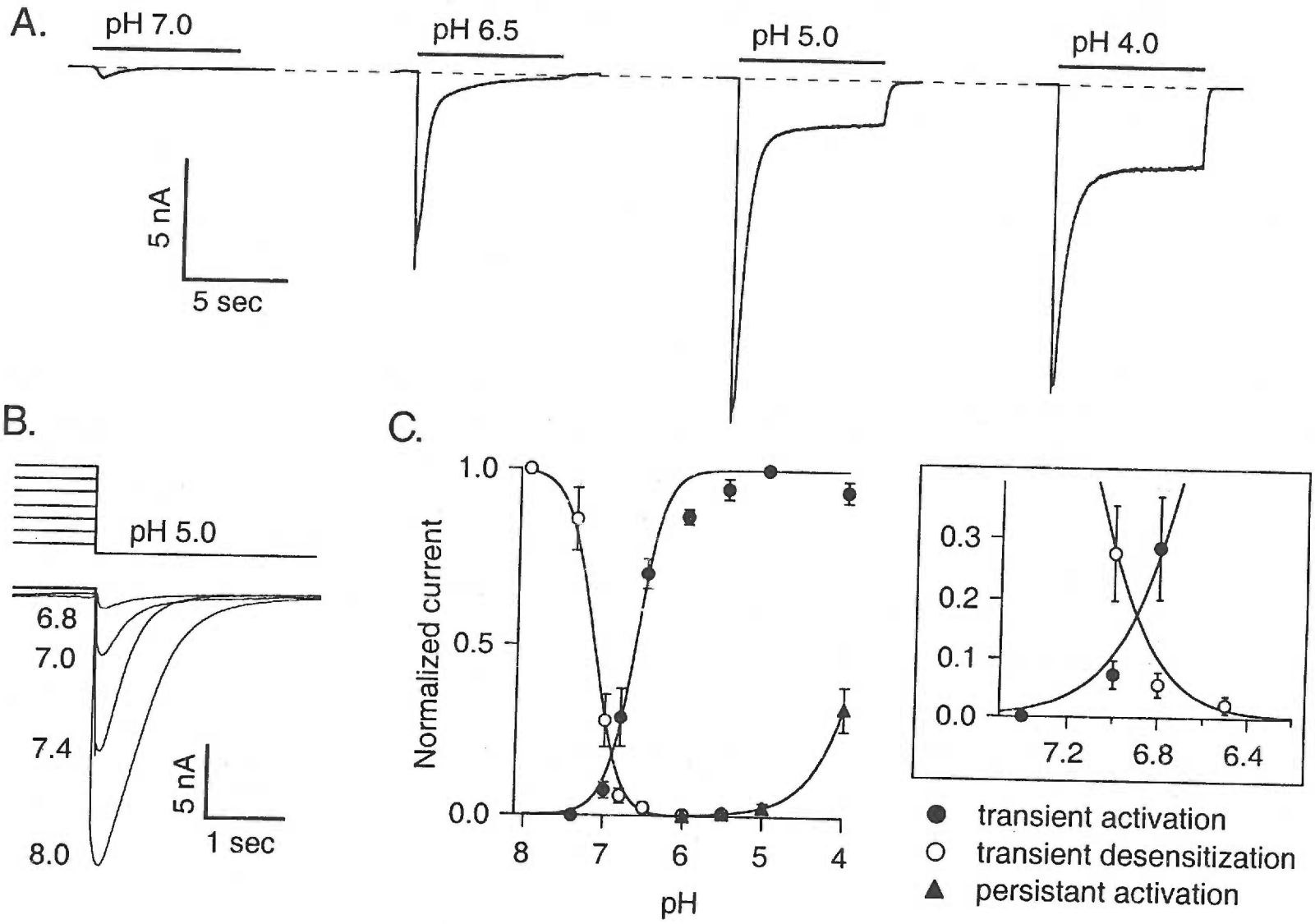
A.
pH 7.0
pH 6.5
pH 5.0
pH 4.0
5 nA
5 sec
B.
pH 5.0
6.8
7.0
7.4
8.0
5 nA
1 sec
C.
Normalized current
1.0
0.5
0.0
8
7
6
5
4
pH
0.3
0.2
0.1
0.0
7.2
6.8
6.4
transient activation
transient desensitization
persistant activation

The Hill coefficient of the activation curve was 2.5. A smaller, non-desensitizing current was evoked by more extreme decreases in pH (≤6). The activation curve for this current is fitted with a $pH_{0.5}$ =3.7. The combination of transient and sustained components at low pH has previously been seen in unlabeled rat sensory neurons[38,31].

Varying the pH before a test stimulus of pH 5 revealed that a significant fraction of the transient current is desensitized at a resting pH of 7.4 (Fig 4B). This is consistent with the previous demonstration that acid-evoked channels need not open to desensitize[97]. The steady-state desensitization and activation curves show clear overlap in the vicinity of pH 7 (Fig. 4C and inset), suggesting that the channel can generate a standing current at pH 7.

A closer look at the time constants of activation and desensitization of the transient currents in cardiac DRG neurons revealed multiple transient components (Figure 5), as noted by Krishtal and Podoplichko[31]. Most cells exhibited a rapidly activating and desensitizing current, but some had a current that was 10-fold slower. The fast and slow transient currents were not exclusive; a few neurons displayed both currents, which was evident as biphasic activation and/or desensitization. These cells were not included in the analysis of time constants. The rate of recovery from desensitization differed for the fast and slow transient currents in cardiac DRG neurons

Figure 5. Kinetics of acid-evoked transient currents in cardiac DRG neurons. A, A typical transient current evoked by pH 6.8. The trace on the right is a shorter pH application to the same cell, displayed on a faster time scale to demonstrate the fast activation. The top right trace shows the measured time course of pH application (see methods). B, In a small sub-population of cardiac DRG neurons, acid evoked a different transient current with slower activation and desensitization. The left and right scale bars correspond to left and right traces for both A and B. C, Activation, desensitization, and recovery from desensitization are each faster in the fast transient (closed circles) than the slow transient (open circles) current. Time constants for activation and desensitization at various pH are from exponential fits to the rising and falling phase of currents as in A and B. Recovery times are at pH 7.4. The horizontal axis indicates the interval at pH 7.4 spent between two pulses to pH 6.8. The first pulse completely desensitized the current and the second tests the extent of recovery. The vertical axis is the relative amplitude of currents evoked by the second and first pulses. Time constants of the exponential fits are 0.44s and 6.8s for the fast and slow currents, respectively.

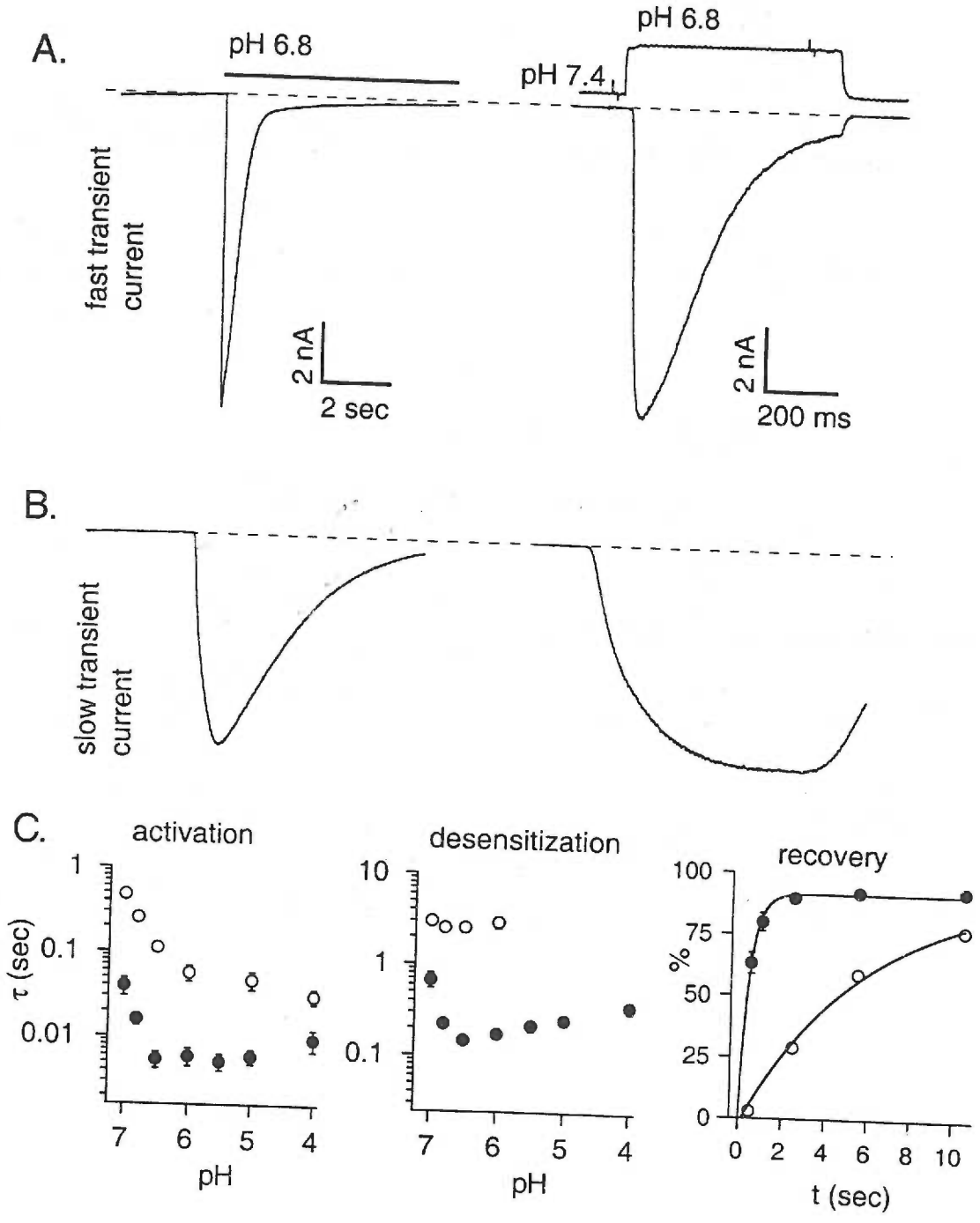
A.
pH 6.8
pH 7.4
pH 6.8
fast transient current
2 nA
2 sec
2 nA
200 ms
B.
slow transient current
C.
activation
τ (sec)
1
0.1
0.01
7
6
5
4
pH
desensitization
10
1
0.1
7
6
5
4
pH
recovery
100
75
50
25
0
%
0
2
4
6
8
10
t (sec)

(Fig. 5C). In a control solution of pH 7.4, the fast transient current recovered with a τ =0.44 seconds and the slow transient current recovered with a τ =6.8 seconds

The fast transient current is Na^+-selective but Ca^{2+}-permeable (Figure 6). With the usual internal (high K^+) and external (high Na^+) solutions, the reversal potential was in the vicinity of +50 mV (data not shown). To quantify the evident preference for Na^+ over K^+, we measured reversal potentials with Na^+ as the internal ion (see methods). The reversal potential shifted -50 ±1.2 mV when K^+ replaced Na^+, corresponding to a P_{Na}/P_K of 6.8.

Current-voltage relationships measured in 10 mM extracellular Ca^{2+} with 15 mM intracellular Na^+ displayed an average reversal potential of –47.2 ±1.2 mV (n=7), corresponding to a P_{Na}/P_{Ca} of 105 (Fig 6C). In all cells, current amplitude increased when $[Ca^{2+}]$ was increased from 10 to 30 mM (n=7; amplitude increase varied from 28% to 725%, data not shown). Thus, as previously shown[106], the current can be carried by Ca^{2+}. To determine whether the acid-evoked currents are blocked by millimolar extracellular Ca^{2+}, as seen in some native[97,98] and cloned[45] channels, we measured Na^+ currents elicited by pH 6.0 in 1, 2 and 10 mM Ca^{2+}. There was no change in amplitude (n=5; data not shown); therefore the current is not blocked by millimolar Ca^{2+} concentrations.

The fast transient and sustained current components differ in two respects: ion selectivity and pharmacology (Figure 7). Both components are cation-selective because

Figure 6. Fast transient acid-evoked currents in cardiac DRG neurons are Na^+ selective. A, Transient currents evoked by applying pH 5.0 during steps to various membrane potentials in an extracellular solution of NaCl (left) or KCl (right). Internal solution was NaCl. B, Current vs. voltage curves from the data in A. Data points are the difference between currents at pH 7.4 and pH 5.0. The mean shift in reversal potential was -50 ±1.2 mV (n=3); thus, P_{Na}/P_k =6.8. C, Currents evoked by pH 6.0 at the indicated potentials in 10 Ca^{2+} external and 15 Na^+ internal. The mean reversal potential was –47.2 ± 2.3 mV (n=7); thus, P_{Na}/P_{Ca} =105.

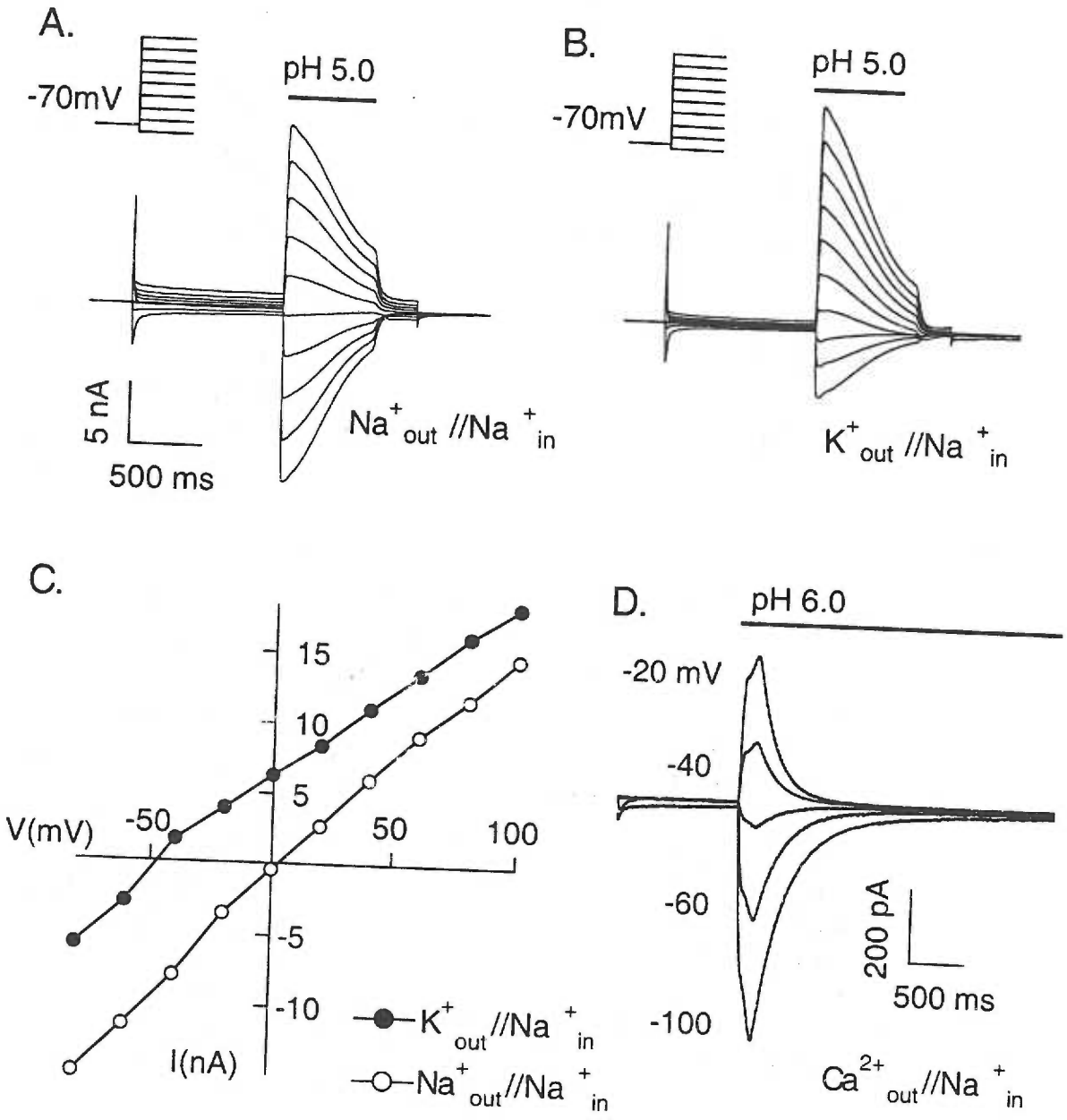
A.
-70mV
pH 5.0
5 nA
500 ms
Na+out //Na+in
B.
-70mV
pH 5.0
K+out //Na+in
C.
15
10
5
V(mV)
-50
50
100
-5
-10
I(nA)
K+out //Na+in
Na+out //Na+in
D.
pH 6.0
-20 mV
-40
-60
-100
200 pA
500 ms
Ca2+out //Na+in

they were unchanged when extracellular Cl^- was replaced with the impermeant anion $MeSO_4^-$. Replacement of extracellular Na^+ with Cs^+ revealed that the transient current does not readily pass Cs^+, whereas the sustained current does. Thus, as previously described in unlabeled DRG neurons[38], the transient current is selective for Na^+, whereas the sustained current is a non-selective cationic current.

Amiloride, a K^+ -sparing diuretic which has been shown to block proton-activated currents in mouse neuroblastoma cells[107], blocked the fast transient current (IC_{50} =9.2 μM) but not the sustained current (Fig. 7B). This difference is consistent with one of the ASICs[49]. The slow transient current was similarly inhibited by amiloride (data not shown). The amiloride derivative ethylisopropylamiloride (EIPA) inhibited the fast transient current with an IC_{50} =37.6 μM (data not shown). These blocking concentrations are about 100-fold greater than those needed to block the epithelial amiloride-sensitive Na^+ channel[108], and are high enough to block unrelated ion channels[107].

Discussion of results:

There are four key findings in this study. (1) We describe a method to distinguish cardiac sensory neurons from neurons of other sensory modalities in primary dissociated tissue culture. (2) Compared to other sensory neurons, cardiac DRG neurons have extremely large currents evoked when pH drops to 7.0 or below. (3) cardiac nodose

Figure 7. Fast transient and sustained acid-evoked currents in cardiac DRG neurons differ in ion selectivity and in amiloride sensitivity. A, Superimposed acid-evoked currents in NaCl and $NaMeSO_4$ (left). Both the transient and sustained acid-evoked currents were unchanged when extracellular Cl^- was replaced with the impermeable anion $MeSO_4^-$. Thus, neither current is carried by anions. Right, Currents evoked in extracellular solutions containing either NaCl or CsCl. The transient current is more permeable to Na^+ than Cs^+, whereas the sustained current is more permeable to Cs^+ than Na^+. B, Left, currents evoked by pH 5.0 and by pH 5.0 plus 100 μM amiloride (*). The transient current was significantly reduced by amiloride, while the sustained current was unchanged. Right, dose-response curve for amiloride on current evoked by a pH change from 7.4 to 6.8. $IC_{50} = 9.2\mu M$ (n = 5).

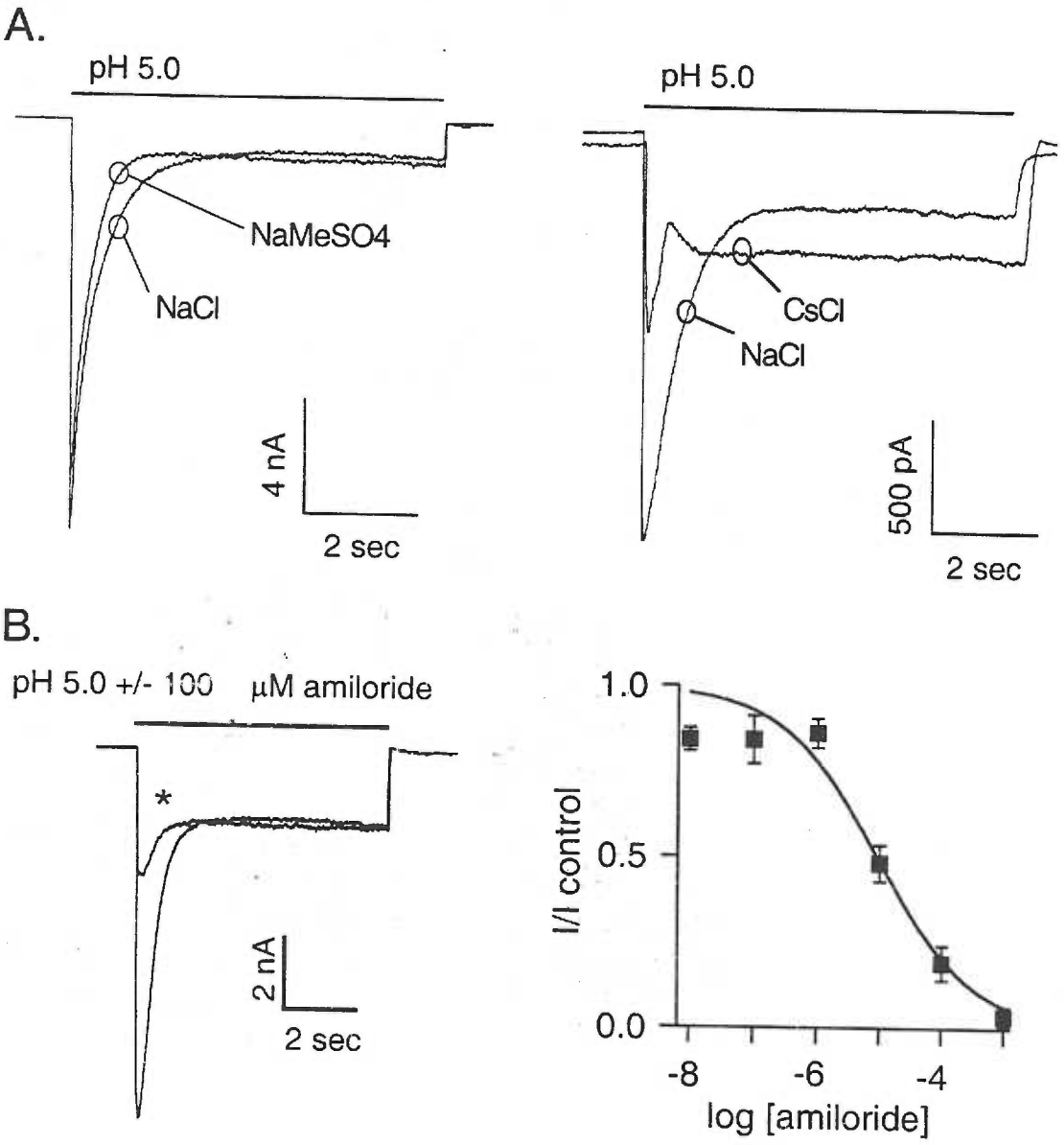
A.
pH 5.0
NaMeSO4
NaCl
4 nA
2 sec
pH 5.0
CsCl
NaCl
500 pA
2 sec
B.
pH 5.0 +/- 100 μM amiloride
*
2 nA
2 sec
1.0
0.5
0.0
I/I control
-8
-6
-4
log [amiloride]

neurons have smaller acid-evoked currents, but larger ATP-evoked currents than cardiac DRG neurons. (4) Other than its large amplitude, the acid-evoked current in cardiac sensory neurons has no biophysical or pharmacological properties that are not predicted by previous studies of acid-evoked currents in sensory neurons. The large amplitude indicates the importance of acid in mediating pain due to cardiac ischemia, but certainly does not imply that other potential mediators are unimportant. A complete discussion of the literature and implications of these results can be found in Chapter 6: Discussion.

Chapter 4: Results—ASIC3 Is the Primary Cardiac Acid Sensor

Introduction: In the previous chapter, I showed that one population of sensory neurons that innervates the heart responds to acidity by generating extraordinarily large Na^+ currents[7]. These neurons, called sympathetic cardiac afferents, have cell bodies in the upper thoracic dorsal root ganglia (C_8-T_3) and axons that follow sympathetic nerve trunks to innervate the epicardium, the outer layer of the heart[109]. Sympathetic afferents are distinct from parasympathetic cardiac afferents, which also innervate the heart but have cell bodies in the nodose ganglia and axons that follow the vagus nerve. Because surgical dissection of sympathetic cardiac afferents relieves angina, they are considered the mediators of cardiac pain (but see Mellar and Gebhart for evidence that parasympathetic afferents also contribute to pain[10]). In addition to evoking pain, these neurons trigger a sympathetic reflex response to cardiac ischemia that is counterproductive because it causes stronger and faster contraction at a time when the heart is getting insufficient oxygen[15,110,111]. Thus, suppression of sympathetic cardiac afferents might relieve both pain and a damaging reflex that accompanies it.

We showed that both sympathetic and parasympathetic cardiac afferents have acid-evoked currents, but the currents have dramatically (about 10-fold) greater amplitude in the sympathetics[7]. The currents are blocked by amiloride and pass Na^+ better than K^+. This identifies

them as being carried by acid-sensing ion channels (ASICs) and distinguishes them from another type of proton-gated channel, vanilloid receptors. Krishtal's group first identified ASICs as several kinetically distinct, Na^+-selective, Ca^{2+}-permeant currents in sensory neurons that are evoked by lowered pH and are blocked by amiloride[106,112,31,30]. Lazdunski's group found that the currents are carried by a proton-sensitive sub-family of channels within the larger family of epithelial Na^+ channels and degenerins of C. elegans[45]. At present, the ASIC family has five members in rat: ASIC1a[113,45]; ASIC1b[46]; ASIC2a[113,48,114,47]; ASIC2b[48]; and ASIC3[49] (nomenclature as in Waldmann et al., 1998[40]). The proteins are small (~500 AA) with two putative transmembrane domains, and several subunits are required to form functional channels.

Sensory ganglia are richly endowed with ASIC mRNAs. The mRNA for four of the 5 family members (all but ASIC2a) are detected in sensory ganglia[39] and two (1b and 3, also called ASICβ and DRASIC, respectively) are only in sensory ganglia[46,49]. We sought to find which, if any, of these clones forms the ion channel responsible for the large acid-gated currents in sympathetic cardiac afferents. There is no pharmacological agent that distinguishes the different ASICs. Therefore, we measured 8 different functional properties of the native cardiac afferent channel and compared these to each cloned ASIC expressed in COS7 cells. ASIC3 matched the native currents in all parameters, many of which excluded the other ASIC subtypes.

Extreme Size and Sensitivity of Acid-Gated Currents in Cardiac Afferents

We fluorescently labeled cardiac afferents in rats by placing a lipid soluble dye (DiI) in the pericardial space (methods previously described in Benson et al.[7]). The dye intercalates into membranes of nerve endings in the epicardium, gets endocytosed, and the resulting fluorescent vesicles are transported to the neurons' cell bodies. Upper thoracic dorsal root ganglia are dissected and dissociated about 4 weeks after dye placement and the sympathetic cardiac afferents are distinguished from other kinds of sensory neurons by fluorescence. In order to highlight the unique properties of the cardiac afferents, they are compared in Figure 8 to non-nociceptive, low-threshold mechanosensors—sensors of either fine touch or muscle length—that are isolated from the mesencephalic nucleus of the trigeminal tract (see methods).

The pH of solutions flowing onto individual dissociated neurons was changed from 8.0 to the indicated value (Fig. 8A) for 600 msec (20 msec delay time for solution exchange). The currents activated by these pH changes were dramatically larger in cardiac afferents than in mechanosensors (note the 8-fold difference in the vertical scales), and cardiac afferents responded at a 3-fold lower proton concentration. Normalized peak currents are plotted against the activating pH and fit with the Hill equation (Fig. 8B). Half-activation of the cardiac afferent channel occurs at about pH 6.6, and it clearly opens at pH 7, a value reached within the first few minutes of severe

Figure 8. Cardiac afferents have larger and more sensitive acid-evoked currents than do non-nociceptive mechanosensors. (A) Currents evoked from a cardiac afferent and a mechano-sensing afferent by pulses to the indicated pH from pH 8. Vertical scales: 8 nA (top), 1 nA (bottom). Horizontal scale: 500 msec. (B) Average (±SEM) fractional current vs. pH. Solid lines are fits of the Hill equation for cardiac afferents (filled circles, n=14, normalized to current evoked by pH 5) and mechanosensors (squares, n=7, normalized to current evoked by pH 4). COS7 cells expressing ASIC3 show an identical dose-response curve to that of cardiac afferents (open circles, $pH_{0.5}$=6.6, n=11, normalized to current evoked by pH 5, curve fit not shown). (C) Average amplitude of currents evoked by pH 5 in cardiac afferents (12.8 nA) is over 3 times larger than in mechanosensors (4.04 nA). Data is from the same cells used in (B).

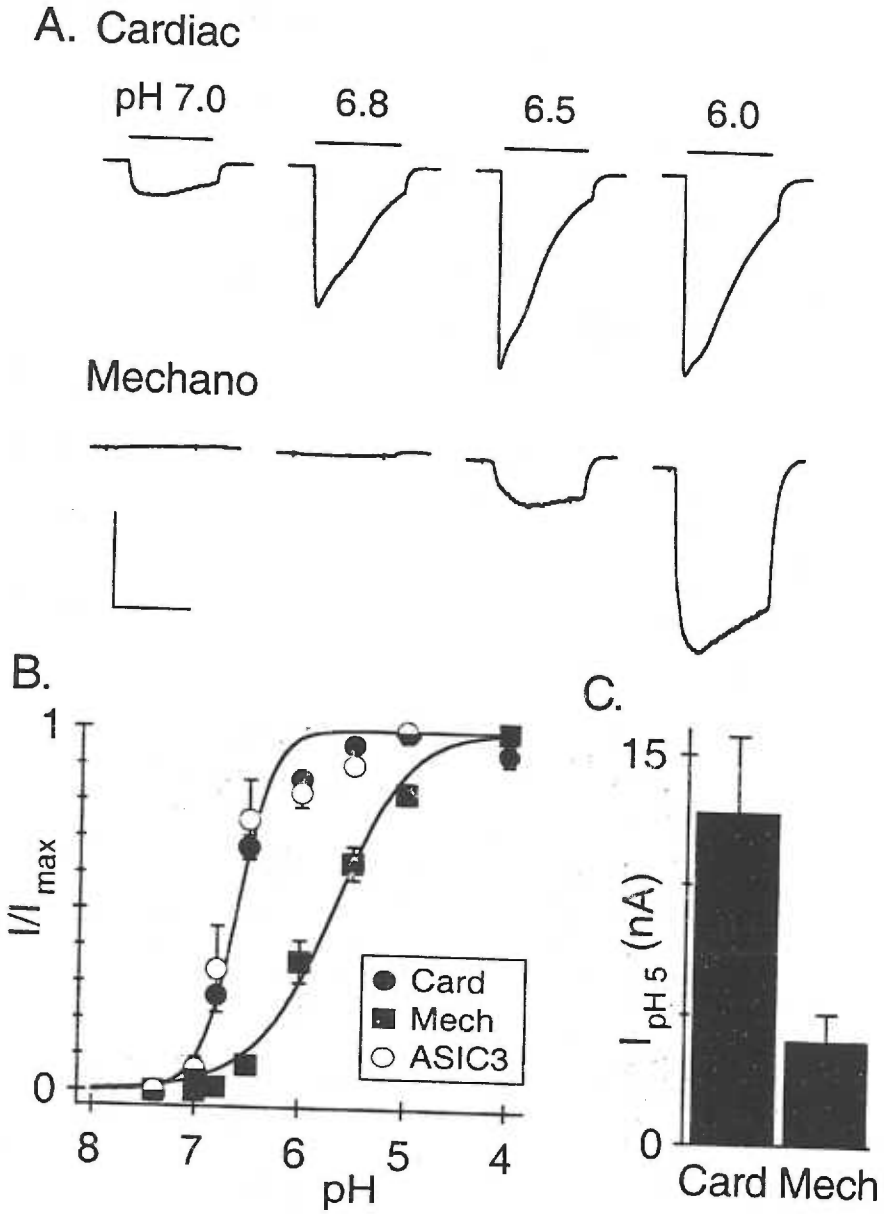
A. Cardiac
pH 7.0
6.8
6.5
6.0
Mechano
B.
1
0
I/I max
8
7
6
5
4
pH
Card
Mech
ASIC3
C.
15
0
I pH 5 (nA)
Card Mech

cardiac ischemia[25,95,29]. The average maximal acid-sensing current in the cardiac afferents was 13 nA, over three times larger than in the mechanosensors (Fig 8C). Acid-evoked currents in cardiac afferents routinely reach well over 20 nA, certainly the largest depolarizing current in rat sensory neurons and among the largest in the rat nervous system. Because the current has extreme amplitude in neurons specialized to detect cardiac ischemia and has the correct proton sensitivity to detect the pH changes that occur, it likely is the sensor that triggers acid-evoked cardiac pain.

Only ASIC3 Mimics the Acid-Evoked Current in Cardiac Afferents

In considering whether a known ASIC clone might generate the current in cardiac afferents, we ruled out two subtypes (ASIC2a and 2b) on the basis of published data: ASIC2b does not form a functional channel as a homomer[48]; and mRNA for ASIC2a is reported absent from sensory ganglia[39]. We further confirmed that ASIC2a channels require unphysiological acidity (pH 5) to open. Therefore, we asked if the characteristics of the native channel in cardiac afferents could be matched when ASIC1a, 1b, or 3 is expressed in COS7 cells alone or in combination with ASIC2b. The results show that ASIC3 is the primary acid-sensing ion channel expressed in cardiac sensory neurons. The properties of ASIC3 are effectively identical to those of the current seen in the native neurons, as detailed in Table 1.

Table 1.

Functional Property	Cardiac	ASIC3	ASIC1a	ASIC1b
$pH_{0.5}$ Activation	6.6	6.7	6.4	5.9[46]
$pH_{0.5}$ Desensitization	7.2[7]	7.1	7.3	
τ Act. (msec, at pH 6)	<5	<5	13.7 ± 3.5*	
τ Densens. (sec, at pH 6)	0.35 ± .04	0.32 ± .07	3.5 ± .39*	1.7 ± .27*
τ Recovery (sec, at pH 7.4)	0.61	0.58	13	5.9
% Block by 10 mM Ca^{2+}	44 ± 7.3	34 ± 9.2	82 ± 4.9*	83 ± 2.5*
I_{30Ca}/I_{10Ca}	3.1 ± .77	2.5 ± .42	0.99 ± .16*	
P_{Na}/P_K	6.8[7]	4.5	5.5	2.6[46]
IC_{50} Amiloride (μM)	37	63[45]	10[45]	21[46]

Table 1. ASIC3 matches the native cardiac afferent channel in all functional properties, whereas the other ASIC subtypes do not. Asterisks are means that differ from the cardiac afferent with greater than 99% certainty (two-tailed t-test, n=3-6). Values without standard errors are derived from curve fits (n=3-12). I_{30Ca}/I_{10Ca} is the ratio of peak amplitudes when Ca^{2+}, at either 30 mM or 10 mM, is the only permeant ion. Numbers obtained from the literature are referenced; we confirmed similar results from our clones. Activation rates were measured in outside-out patches; all others were made using the whole-cell configuration. The different IC_{50} values for amiloride likely reflect use of

Figure 9. ASIC3 responds to protons in the neutral range. (A) Currents evoked from COS7 cells expressing either ASIC3 or ASIC1a by steps to pH 7, 6.9, and 6.8. Vertical scale bar represents 10% of current evoked by pH 5 (2 nA ASIC3; 46 pA ASIC1a). Horizontal scale bar: 1 sec. (B) Average currents of the indicated clones normalized to the value at pH 5.0 and fit with the Hill equation. Hill coefficients are 4.3 (ASIC3, $pH_{0.5}$=6.7) and 3.9 (ASIC1a, $pH_{0.5}$=6.4).

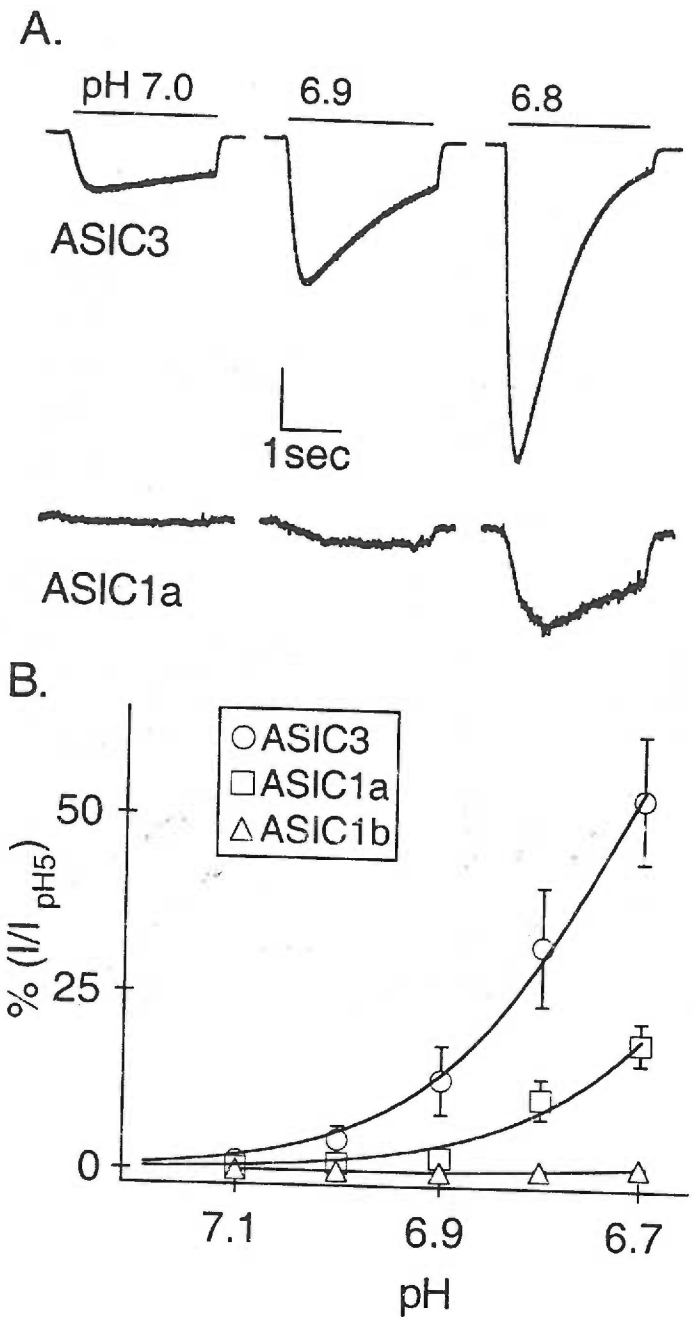
A.
pH 7.0
6.9
6.8
ASIC3
1sec
ASIC1a
B.
ASIC3
ASIC1a
ASIC1b
50
25
0
% (I/I pH5)
7.1
6.9
6.7
pH

different stimulating pH in different studies; for example, the IC_{50}'s for the cardiac afferent channel are 40 and 10 μM when measured at pH 5 and pH 6.8, respectively. Because of the wide range in the measurements of P_{Na}/P_K, we do not consider the differences in averages to be real. P_{Na}/P_K ranged from 1.99 to 6.42 for ASIC3 (n = 6) and from 3.64 to 12.04 for ASIC1a (n = 6), all measured at pH 5.

The sensitivity of ASIC3 to protons precisely mimics the cardiac afferent channel (open symbols, Fig. 8B). The other ASICs are either slightly (ASIC1a) or much (ASIC1b) less sensitive to protons (Table 1). Because the critical range for cardiac pain is pH 7.1 to 6.7[95,29], Figure 9 explores the sensitivity of the various clones in this range. ASIC3 is the most sensitive ($pH_{0.5}$=6.7). Its activation curve is best fit with a Hill coefficient of 4.3, which suggests that at least 4 protons bind to the channel in order to open it. ASIC1a has similar steepness (Hill coefficient 3.9) but with slightly lower apparent proton binding affinity ($pH_{0.5}$=6.4). ASIC1b does not respond in this physiological pH range (Fig. 9B and Table 1).

Figure 10 compares the kinetics and calcium inhibition of current from cardiac afferents to those of cloned channels. Steps to pH 6.0 were made with solutions with the indicated Ca^{2+} concentrations. The native channel and ASIC3 share essentially the same time course, whereas the other channels open and desensitize more slowly (see Table 1

Figure 10. Only ASIC3 mimics kinetics and Ca^{2+} inhibition of cardiac afferents. Representative currents evoked from a cardiac afferent (A) or from COS 7 cells expressing either ASIC3 (B), ASIC1a (C), or ASIC1b (D) by steps of pH from 8.0 to 6.0 in the indicated extracellular Ca^{2+} concentrations (mM). Cardiac and ASIC3 channels parallel each other in activation kinetics, desensitization kinetics, and Ca^{2+} inhibition. Vertical scales: 1.1 nA (A), 14 nA (B), 1.5 nA (C), and 2 nA (D). Horizontal scales: 1 sec for all traces.

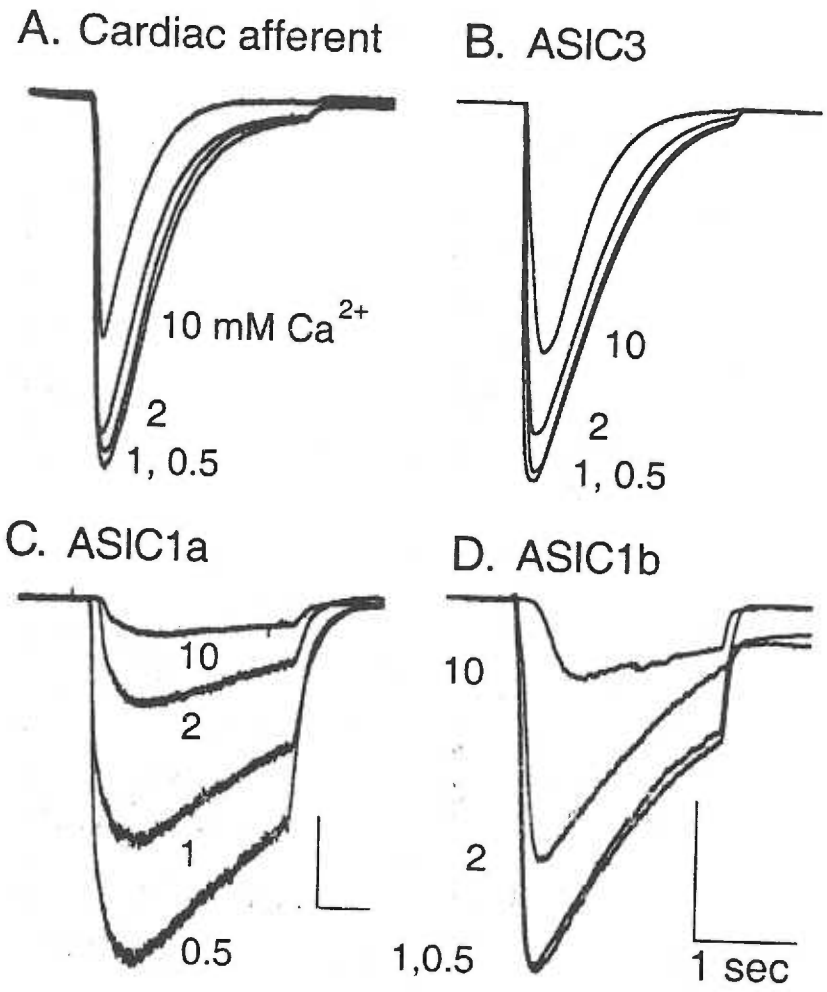
A. Cardiac afferent
B. ASIC3
10 mM Ca2+
2
1, 0.5
10
2
1, 0.5
C. ASIC1a
D. ASIC1b
10
2
1
0.5
10
2
1,0.5
1 sec

for time constants). Increasing Ca^{2+} concentration inhibits all the currents, but the native channel and ASIC3 are relatively insensitive: they are only slightly affected by 2 mM Ca^{2+} and about 40% inhibited by 10 mM at pH 6.

Recovery from desensitization also clearly distinguished ASIC3 from the other clones (Figure 11). Cells were exposed to prolonged (7-10 sec) applications of pH 6, which caused complete current desensitization (left-most traces in Figs. 11A-D), and were then returned to pH 7.4. At various times thereafter, cells received a brief (600 msec) application of pH 6 to test the fraction of channels that had recovered from desensitization. The native channel and ASIC3 both recovered very rapidly compared to the other channels. The average recovered peak current relative to the initial peak value is plotted against the time of recovery for the first 5 sec (linear scale, Fig. 11E) and 40 sec (log scale, Fig. 11F). Single exponentials fit to the data have time constants of 0.61 and 0.58 sec for the native channel and ASIC3, and 13 and 6 sec for ASIC1a and ASIC1b, respectively.

The above data rule out ASIC1a and 1b, and leave ASIC3 as a candidate for the native channel. To further test ASIC3, we made a number of other measurements, which are summarized in Table 1. All channel types share two traits: selection of Na^+ over K^+, and block by fairly high concentrations of amiloride. However, the following six properties of the native channel are shared only by ASIC3: high proton sensitivity, rapid

Figure 11. Only ASIC3 mimics recovery kinetics of cardiac afferents. Current was completely desensitized by a prolonged pulse to pH 6.0 (bar) and then the cell was returned to pH 7.4. Recovery from desensitization was tested by a 600 msec pH pulse triggered at the indicated times. (Only one pulse was given after each desensitizing prepulse, thereby avoiding accumulating desensitization; peak current occurs early in the 600 msec pulse and this time to peak was not added to the recovery time.) Currents in a cardiac afferent (A) and ASIC3 (B) recovered rapidly; currents in ASIC1a (C) and 1b (D) recovered slowly. Horizontal scales: 2 sec for desensitizing currents (left-most), 1 sec for test currents. Vertical scales: 1 nA (A), 1.25 nA (B), 0.45 nA (C), and 0.5 nA (D). Recovery of average (± SEM) currents, normalized to initial amplitude, for the first 5 sec (E) (linear) and 40 sec (F) (log scale). Solid lines are fits of single exponentials. Cardiac afferents (filled circles, τ=0.61 sec, n≥4 for each data point), ASIC3 (open circles, τ=0.58 sec, n≥5), ASIC1a (squares, τ=12.99 sec, n≥4), ASIC1b (triangles, τ=5.88 sec, n≥3).

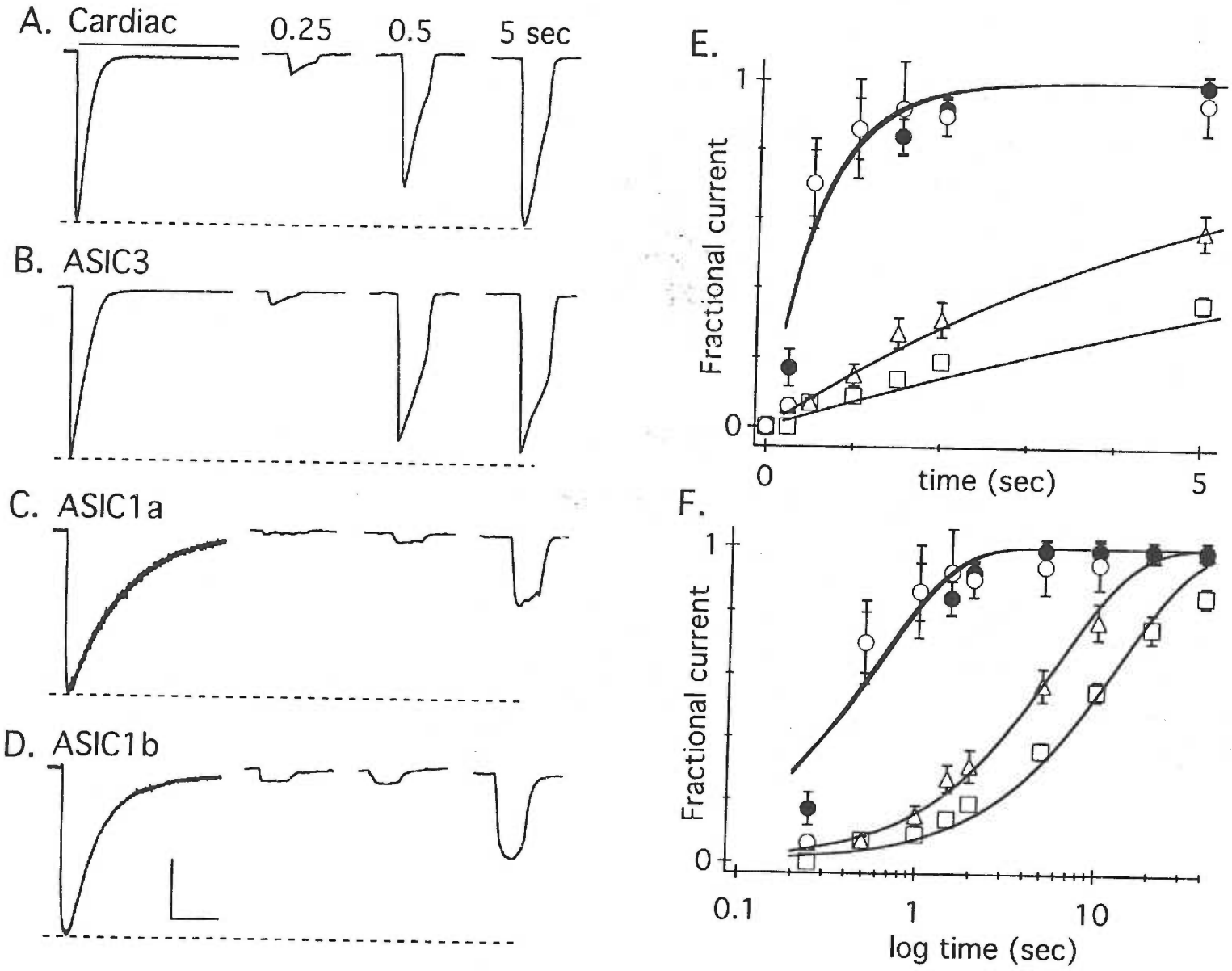
A. Cardiac
0.25
0.5
5 sec
B. ASIC3
C. ASIC1a
D. ASIC1b
E.
Fractional current
1
0
0
time (sec)
5
F.
Fractional current
1
0
0.1
1
10
log time (sec)

rates of activation, desensitization, and recovery, weak Ca^{2+} inhibition, and low but detectable Ca^{2+} permeability (see next section). Because all these functional features match in near-perfect detail, we conclude that ASIC3 is the major component of the native acid-gated channel in cardiac afferents.

Calcium Permeability of Acid-Sensing Ion Channels

Our measurements reveal some complexities of Ca^{2+} permeation and inhibition that deserve attention. Both ASIC3 and the native channel passed inward currents when 10 mM Ca^{2+} was the only external permeant ion. The amplitude of these currents increased about three-fold in 30 mM extracellular Ca^{2+} confirming that both channels can pass Ca^{2+} (Table 1). Current through ASIC1a did not increase with this solution change, but this need not imply low Ca^{2+} permeability. Indeed, Waldmann et al.[45] reported substantial Ca^{2+} permeability in ASIC1a with 1.8 mM Ca^{2+} as the current carrier. To investigate this, we measured the voltage at which current changed from inward to outward when the current carriers were 10 mM external Ca^{2+} and 15 mM internal Na^{+}. These reversal potentials (-23 ±7 mV for ASIC1a, -80 ±2 mV for ASIC3) indicate that ASIC1a is substantially more permeable to Ca^{2+} than is ASIC3 (P_{Na}:P_{Ca}=16 for ASIC1a; P_{Na}:P_{Ca}>100 for ASIC3). The native channel also has low Ca^{2+} permeability in these ionic conditions (P_{Na}:P_{Ca}>100). The inhibition, permeation, and reversal potential

measurements are consistent with the presence of an intrapore binding site in ASIC1a that is fully saturated at 10 mM Ca^{2+} and that allows Ca^{2+} to compete effectively with Na^{+} for occupancy of the pore. A relatively high Ca^{2+} permeability appears unique to ASIC1a, as there is no apparent Ca^{2+} permeation in ASIC1b[46]. We found greater Ca^{2+} inhibition than previously reported[46] for ASIC1b. Perhaps this is because our measurements were made at pH 6, whereas the published measurements were at pH 5.1. An alternative explanation is the single amino acid difference between our clone and the sequence deposited in GenBank (see methods). Because pH sensitivity and gating kinetics sufficiently distinguish either form of ASIC1b from the native channel (Table 1), we did not investigate these issues further.

An Unidentified Sustained Current

Acid-sensing ion channels select Na^{+} over other ions[97,30], but prolonged application of very low pH ($\leq$ 5.0) evokes a distinctly different current in some sensory neurons. This current is sustained, is carried equally by various monovalent cations and is not blocked by amiloride[38]. We previously described such a current in cardiac afferents with an apparent half-activation at pH 3.7[7].

Figure 12 shows that this sustained current has different properties in different cardiac afferents. In all cases, its amplitude is small compared to the transient current

Figure 12. Variable expression of a sustained, non-selective current in cardiac afferents is consistent with variable expression of ASIC2b. Peak currents are off scale to emphasize the smaller sustained component. (A) Currents, evoked by steps to pH 5 for 4 sec, from two cardiac afferents that display sustained components that differ in selectivity. Left: the sustained component is non-selective (passes Cs^+ and Na^+ equally); right: the sustained component is Na^+-selective. (B) Co-expression of ASIC3 and 2b yields a non-selective sustained component. (C) The ASIC3 homomer yields a Na^+-selective sustained component. Vertical scales: 600 pA (A, left), 150 pA (A, right), 35 pA (B), 500 pA (C). Horizontal scale: 1 sec.

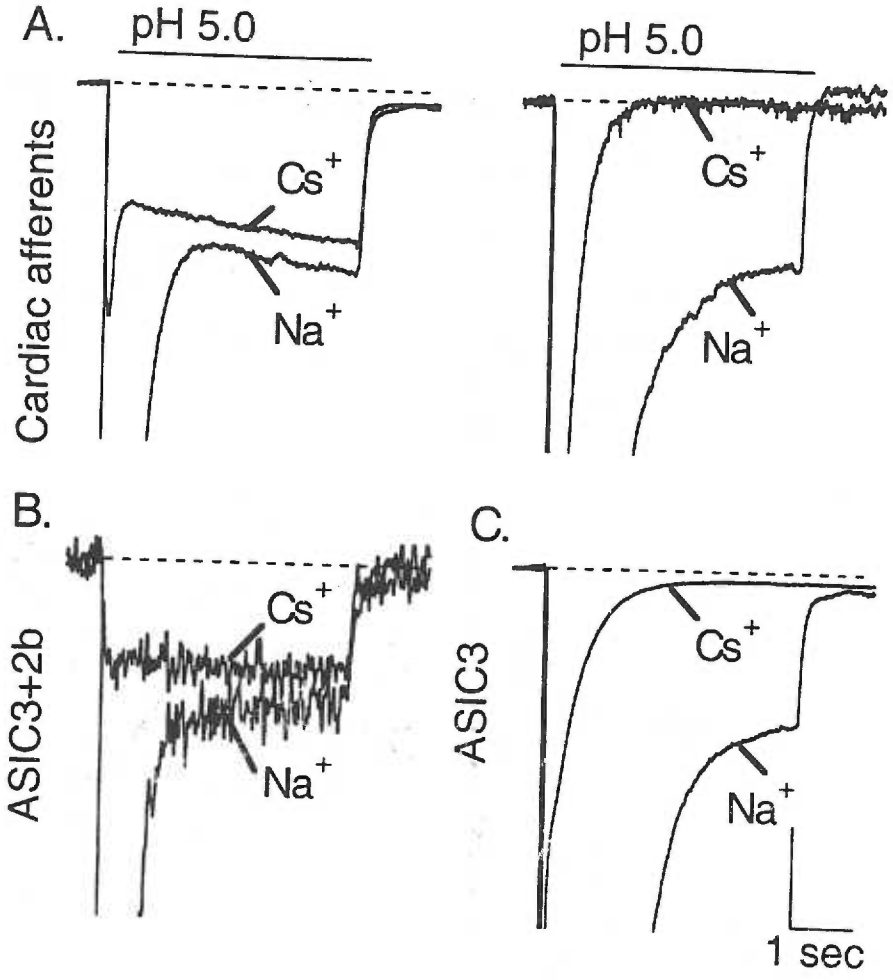
A.
pH 5.0
pH 5.0
Cardiac afferents
Cs+
Na+
Cs+
Na+
B.
C.
ASIC3+2b
Cs+
Na+
ASIC3
Cs+
Na+
1 sec

(I_{sust}/I_{trans}=0.14 ± .04 at pH 5, n=13), but its selectivity varies in different cells. In response to prolonged (4 sec) application of pH 5, the cardiac afferent on the left of Fig. 12A had a sustained current that passed Cs^+ about as well as Na^+, whereas the one on the right had a sustained current that was Na^+ selective. Nine of 13 cardiac afferents surveyed with this protocol exhibited some degree of Cs^+ permeability to the sustained current, but the Cs^+:Na^+ current ratio varied unpredictably. In all cases, the transient current (far off scale with Na^+ as the current carrier in Fig. 12) was greatly diminished when Cs^+ was the current carrier, indicating its high Na^+ selectivity.

ASIC3 homomers have a Na^+-selective sustained current[49], but, if ASIC3 is co-expressed with ASIC2b, a non-selective current appears, presumably because of ASIC3/2b heteromer formation[48]. Figs. 12B and C reproduce these observations. So, a possible explanation of the variable sustained current in Fig. 12A is that ASIC3 is highly expressed in all cardiac afferents, whereas ASIC2b is expressed in some, but not all. As discussed below, this is not the only possible mechanism.

Discussion of results:

Extracellular acid appears to be a significant part of the signal that triggers pain during cardiac ischemia[25,12] and rat cardiac sensory neurons display extremely large Na^+ currents through an acid-sensing ion channel[7]. Because the ion channels that mediate this current are

probably molecular sensors for cardiac ischemic pain, we aimed to find which, if any, of the five cloned ASICs mediates the acid sensitivity of rat cardiac sensory neurons. Our results point to ASIC3 for the following reasons: 1) the native channel and ASIC3 both open at pH 7, whereas other ASICs are less sensitive to protons (some dramatically so); 2) the native channel and ASIC3 both gate between closed, open, and desensitized states clearly faster than other ASICs; 3) the native channel and ASIC3 share aspects of permeation to and inhibition by Ca^{2+} that are unlike the other ASICs. A complete discussion of these results and related literature can be found in Chapter 6: Discussion.

Chapter 5: Results—Voltage-Dependent Block of the CNS Channel ASIC1a

Introduction: Acid-Sensing Ion Channels(ASICs) are a family of ion channels related to the mammalian epithelial sodium channels (ENaCs) and to the degenerins channels (DEG) found in nematodes[40]. Some of these cloned channels are extremely sensitive to protons, including the sensory neuron channel ASIC3 and the CNS channel ASIC1a. As shown in Chapter 4, ASIC3 acts as the primary sensor of myocardial ischemia, and is half-activated at pH 6.7[115]. ASIC1a is also very sensitive to protons; it is half-activated at pH 6.3[45]. Might ASIC1a act as a molecular ischemia sensor in the brain as ASIC3 does in the heart?

During CNS ischemia, energy depletion leads to failure of ATPase pumps and breakdown of ionic gradients. Cells become depolarized and release excitatory amino acids[51]. Coincidentally, extracellular pH falls to around pH 6.5, and even lower in some conditions[57,56]. ASIC1a passes large inward sodium currents in response to this low pH; these currents may contribute to neuronal death. The divalent ionic conditions may also contribute significantly to the degree of ASIC activation in CNS.

Data from ASIC1a suggests that the channel displays a negative-slope region[45] of its current-voltage (I-V) curve, which might be an indication of coincidence detection

ability. The NMDA-type glutamate receptor channels act as coincidence detectors of extracellular glutamate and depolarization. The negative slope region seen in the I-V curve for that channel is caused by voltage-dependent block by the divalent cation magnesium[79,80].

I sought to determine whether ASIC1a could similarly act as a coincidence detector of acidity and depolarization, by way of voltage-dependent block by Mg^{2+} or other ions. I observed a negative slope region in the I-V curve of ASIC1a that can be attributed to voltage-dependent intra-pore block by Mg^{2+} ions.

A closer look at the permeation properties of ASIC1a revealed a surprising similarity to voltage-dependent sodium channels (VDNCs). These channels and, it seems ASIC1a, are permeable to the organic cation guanidinium but not the smaller methyl-ammonium. I believe this indicates that like the VDNCs, ASIC1a has a pore that is only around 3 Å wide and is lined with oxygen atoms that form hydrogen bonds with the amino group of some permeant ions.

Amiloride is among the only drugs that block ASICs, and does so with low affinity, in the micromolar range. The molecule consists of a charged guanidine moiety attached to a larger, bulky structure. Voltage-dependent Na^+ channels (VDNCs) are blocked by tetrodotoxin, a toxin that also contains a charged guanidine moiety. Permeability studies of VDNCs revealed that the channels can pass the guanidinium ion

but not the seemingly smaller methyl-ammonium ion[81]. This is presumably made possible by hydrogen binding of the guanidinium ion within the channel pore, which compresses the size of the molecule to fit through the pore. The methyl-ammonium ion is not capable of such hydrogen binding. I examined permeation and block of ASIC1a by guanidinium and the guanidinium-containing toxins amiloride and tetrodotoxin to determine whether the pores of ASIC1a and VDNCs might be analogous.

Voltage-Dependent Magnesium Block

To determine whether Mg^{2+} ions caused voltage-dependent block of ASIC1a, I measured currents in whole-cell voltage clamp during voltage ramps in various concentrations of external Mg^{2+}. The current-voltage (I-V) plots of ASIC1a indicated voltage-dependent block by Mg^{2+} (Figure 13). While current is inwardly rectifying in the absence of Mg^{2+} ions, 10 mM Mg^{2+} results in an N-shaped I-V plot (Figure 13A). The negative slope region of the curve (between –70 and –140 mV) indicates that Mg^{2+} block is stronger at more negative voltages, up to – 140 mV. Negative to –140 mV, the force of voltage is presumably so strong that Mg^{2+} ions are driven through the pore.

Similarly, current steps measured at various voltages illustrate that block by Mg^{2+} is stronger at more negative voltages (Fig. 13B). Current amplitudes were measured in the presence and absence of external Mg^{2+}; the ratio of these current amplitudes was then

Figure 13. Magnesium ions block ASIC1a at an inta-pore site. In A, a current-voltage curve displays acid-evoked currents measured during ramps from 20 mV to –180 mV in the presence and absence of 10 mM Mg^+. Without Mg^+, the current is inwardly rectifying, whereas 10 Mg^+ blocks current significantly at voltages below –70 mV. Negative to –140 mV, magnesium ions are presumably forced through the pore by extreme voltage. This is evident in the outset, right, demonstrating the N-shape of the curve due to block and to the blow-through effect. B, a representative cell in which currents evoked by pH 6.0 were recorded in the presence and absence of 10 mM extracellular Mg^+. Magnesium had no effect on currents at –80 mV, little effect at –100 mV, but strongly blocked at –140 mV. In C, currents measured as in B were used to calculate the voltage-dependent $K_{1/2}$,(E), which is plotted vs. voltage. The fit of the data indicates that the $K_{1/2}$(0mV) = 51 mM and delta = 0.21; n = 3-7.

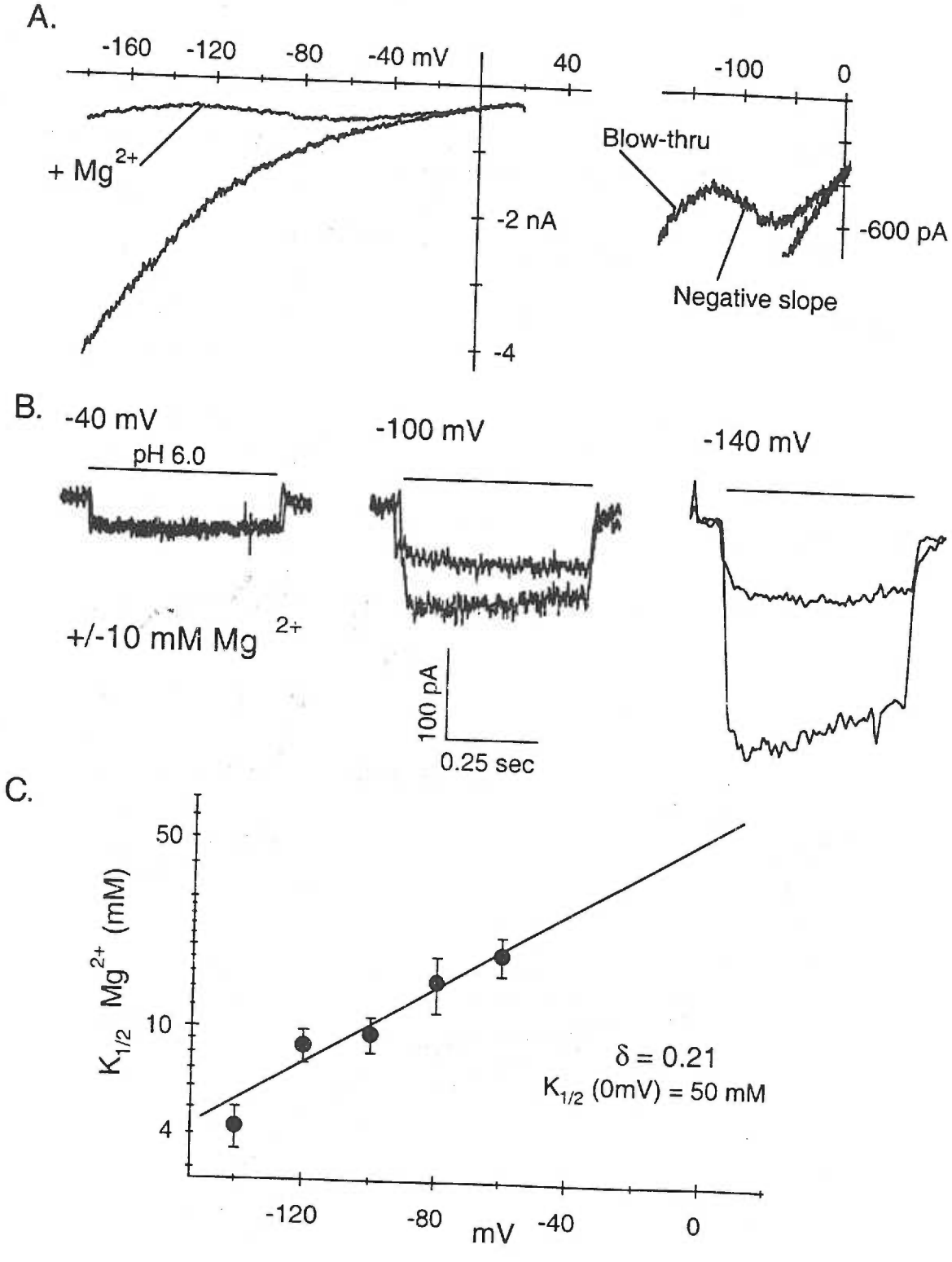
A.
-160
-120
-80
-40 mV
40
+ Mg2+
-2 nA
-4
-100
0
Blow-thru
-600 pA
Negative slope
B.
-40 mV
pH 6.0
+/-10 mM Mg 2+
-100 mV
100 pA
0.25 sec
-140 mV
C.
50
10
4
K1/2 Mg2+ (mM)
δ = 0.21
K1/2 (0mV) = 50 mM
-120
-80
mV
-40
0

used to calculate the apparent $K_{1/2}$ value of block by Mg^{2+} at each voltage, according to the analysis method used in Woodhull[82]. These values are plotted against membrane potential in Fig. 13C to reveal that the apparent half-block by Mg^{2+} occurs at 50 mM at 0 mV.

The same plot (Fig. 13C) indicates that the block by Mg^{2+} ions has a delta value of 0.21. This delta value suggests that the Mg^{2+} blocking site lies about one fifth of the way into the electrical field across the membrane. While no currents were recorded at voltages positive to –60 mV, the line representing the fit of the data is extended to 0 mV.

The method of analysis of data that provided evidence of voltage-dependent block was taken largely from Woodhull and Hille's description of proton block of sodium channels[82]. Because block is voltage dependent, K_d varied with membrane potential; the K_d at a particular voltage (E) is described by the term K(E). To find delta, the equilibrium constant K_d must first be determined at a potential of 0 mV. The K_d value at 0 mV represents the true binding affinity of the blocking ion at its site when voltage has no influence on binding, and is determined by the on- and off-rate constants of the ion at the binding site. Because depolarization relieved the block, the K_d at 0 mV was significantly higher (i.e. lower affinity) than at resting potentials, as expected. I measured the amplitude of currents recorded in two different Mg^{2+} concentrations (0 and 10 mM) at

various voltages. The K(E) values were then calculated from the ratios of these current amplitudes according to the equation:

$I_{10\,Mg}/I_{0\,Mg} = \{[0] + K(E)\} / \{[10] + K(E)\}$

The natural log of calculated K(E) values were then plotted against voltage. The slope of this line was then used to calculate the value of delta (δ), or degree of voltage dependence:

$K(E) = K(0) \exp [(z\delta F E)/R T]$

(where z, F, E, R and T have their usual meanings.) Thus, delta was determined from K(E) values (see Methods). The assumptions of this model are the following: 1) there is only one blocking site at which the blocking ion may act; 2) the blocker has access to this site only from the extracellular side of the membrane; and 3) the blocker occupies the site at an electrochemical equilibrium.

I also tested whether Ca^{2+} ions could cause voltage-dependent block of ASIC1a. I found that Ca^{2+} affected the current amplitude in a voltage-independent inhibition in a way that varied greatly with Ca^{2+} concentration. The shape of the current-voltage plot, however, did not display a negative slope region even when Ca^{2+} was at 10 mM. This is an indication that Ca^{2+} inhibition was not due to voltage-dependent block, as was seen with Mg^{2+} (data not shown).

ASIC1a Is Permeable to Guanidine

Figure 14 reveals an unexpected interaction between guanidine and the ASIC1a pore lining. Current traces depicted in Figure 14A were recorded with either sodium, guanidinium or methyl-ammonium as the external current carrier. On the left, it is evident that the current carried by sodium is far larger than those carried by the organic cations (note different scale). The outset on the right shows these smaller currents expanded; the current carried by guanidinium is larger than that by methyl-ammonium. To quantify the permeability of these two ions, I measured the reversal potential of currents recorded in solutions with each of the three cations as the current carrier: sodium, guanidinium or methyl-ammonium. The shifts in reversal potential when guanidine replaced sodium reveals that $P_{Guan^+}/P_{Na} = 0.27 \pm 0.02$ (n=5). The permeability ratio for methyl-amine shows that the ion is far less permeant: $P_{Me\text{-}Am}/P_{Na} = 0.06 \pm 0.004$ (n=5). Thus, it appears that ASIC1a is fairly permeant to guanidinium, while the methyl-ammonium ion permeability is minimal.

Judging from the chemical structure of the molecules (Fig. 14A, far right), one might guess that the methyl-ammonium ion is smaller, but the guanidinium ion is able to form hydrogen bonds whereas methyl-ammonium is not. Guanidinium is therefore distinct from methyl-amine in its ability to compress and fit through the channel pore, making it effectively smaller than methyl-amine. These results are similar to those found

Figure 14. Guanidine forms hydrogen bonds with the ASIC1a pore. A, Guanidinium permeates ASIC1a while the smaller methyl-ammonium ion does not. Acid-sensing currents were elicited by pH 6 with either in a solution of 130 mM Na^+, guanidinium$^+$, or methylammonium$^+$ as the external current carrier. The dashed lines indicate the small area (on left) that is expanded (right) to visualize the small currents carried by guanidinium and methyl-ammonium. B, Amiloride and TTX block ASIC1a currents elicited by pH 6.0 at –70 mV in the presence or absence of 10 μM amiloride (top) or TTX (bottom). The structure of each of the compounds is shown on the far right alongside its name. C, Amiloride block, but not TTX block, is voltage-dependent. Currents were evoked by pH 6 during a ramped voltage change from +20 to –160 mV with 10 μM amiloride, 10 μM TTX, or neither, and shown on an I-V plot. Each set of traces is from a representative cell.

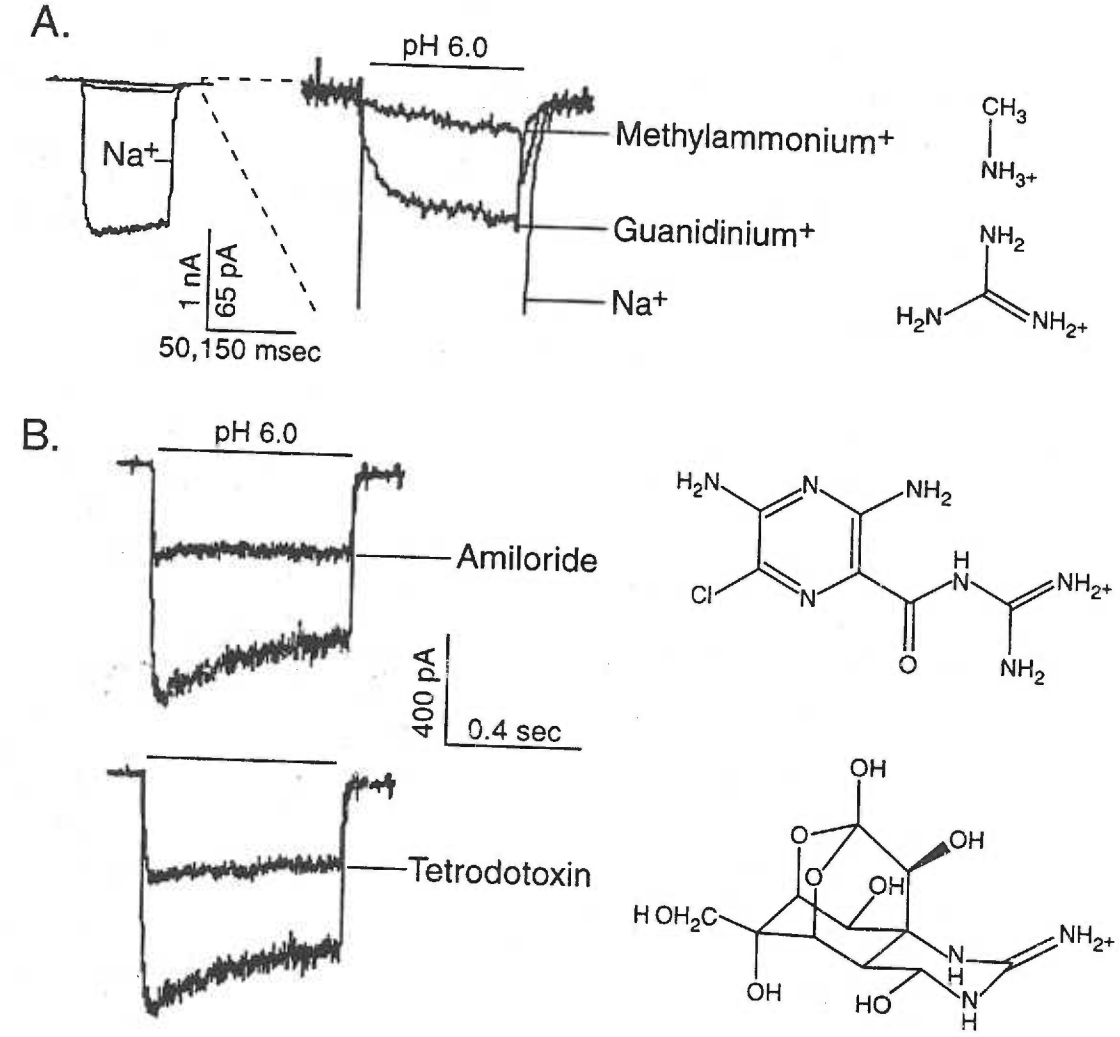
A.
pH 6.0
Na+
Methylammonium+
Guanidinium+
Na+
1 nA
65 pA
50,150 msec
B.
pH 6.0
Amiloride
400 pA
0.4 sec
Tetrodotoxin
C.
-150
-100
-50 mV
amiloride
TTX
control
-1 nA

by Hille. His postulation, in light of these results, was that the guanidinium ion must form hydrogen bonds with oxygens that line the sodium channel pore, causing the ion to compress enough in size to fit through the permeation pathway of the sodium channel pore. Methyl-ammonium, with its methyl group in place of guanidinium's amino group, cannot form hydrogen bonds and therefore cannot compress in size to fit through the pore.

ASIC1a Is Blocked By Guanidine Toxins

Once I determined that guanidinium can pass through the ASIC1a pore, I more closely examined the blocking effects of guanidinium-containing drugs. Amiloride contains a guanidine moiety and blocks all ASICs with relatively low affinity (10-100 μM). Another guanidine toxin, which blocks voltage-dependent sodium channels (VDNCs), is tetrodotoxin (TTX). (Chemical structures are shown in Figure 14B, far right.)

In Figure 14B, traces from a representative cell illustrate that both of these compounds block ASIC1a to a similar extent at –70 mV. The average current remaining in 10 μM TTX compared to control was $I_{TTX}/I_{Control} = 0.37 \pm 0.03$ (n = 12); with 10 μM amiloride it was $I_{amil}/I_{Control} = 0.4 \pm .03$ (n=11). The two compounds differed, however, in the voltage dependence of block. The shape of the I-V plot in Fig. 14C is U-shaped, suggestive of voltage dependent block by amiloride. Block by TTX in contrast appears

not to be voltage-dependent, as there is uniform inhibition of current by TTX over the entire voltage range.

In Figure 15, the voltage-dependent block by amiloride is examined in more detail. The I-V curve in Figure 15A, constructed from acid-evoked current during a voltage ramp, shows that block is stronger at more negative voltages. Unlike Mg^{2+} ions, however, amiloride is too large to be forced through the pore, so the block only continues to increase as the voltage goes more negative, resulting in a U-shaped I-V curve (Fig. 15A, right) rather than the N-shaped curve seen with magnesium (Figure 13, right). Current traces shown in Fig. 15B from a representative cell demonstrate that voltage steps likewise elicit stronger block at more negative voltages. The ratio of these current amplitudes were used to calculate the apparent $K_{1/2}$ of amiloride block and are plotted in Fig. 15C. The fit of this data indicates a $K_{1/2}$ of 41 μM at 0 mV and a delta of 0.51(see the previous section for analysis of data). This suggests that amiloride blocks ASIC1a at a site approximately half-way into the electrical field.

If amiloride and Mg^{2+} do indeed both bind at intra-pore blocking sites, as the data suggests, they should compete with one another for access to their sites. Figure 16 shows that Mg^{2+} and amiloride do compete for inhibition of ASIC1a. The two sets of current traces in Fig. 16A, from a representative cell recorded at –70 mV, show that 10 μM amiloride blocks ASIC1a current less strongly in the presence of 10 mM Mg^{2+}. (Note the

Figure 15. Amiloride blocks ASIC1a at an intra-pore site. A, a representative current-voltage plot constructed from the current measured during ramps from +20 to –180 mV in the presence and absence of 10 μM amiloride. Block is voltage-dependent, with block increasing negative to –100 mV. Unlike Mg^+ ions, amiloride cannot permeate through the pore, so there is no blow-through effect (outset, right). B, a representative cell from which currents were measured at –60, –100, and –140 mV in the presence and absence of 10 μM amiloride. C, currents measured as in B were used to calculate apparent $K_{1/2}$ and plotted vs. voltage. The fit of the data indicates that the apparent $K_{1/2}$(0 mV) is 41 μM, and delta = 0.51; n = 3-4.

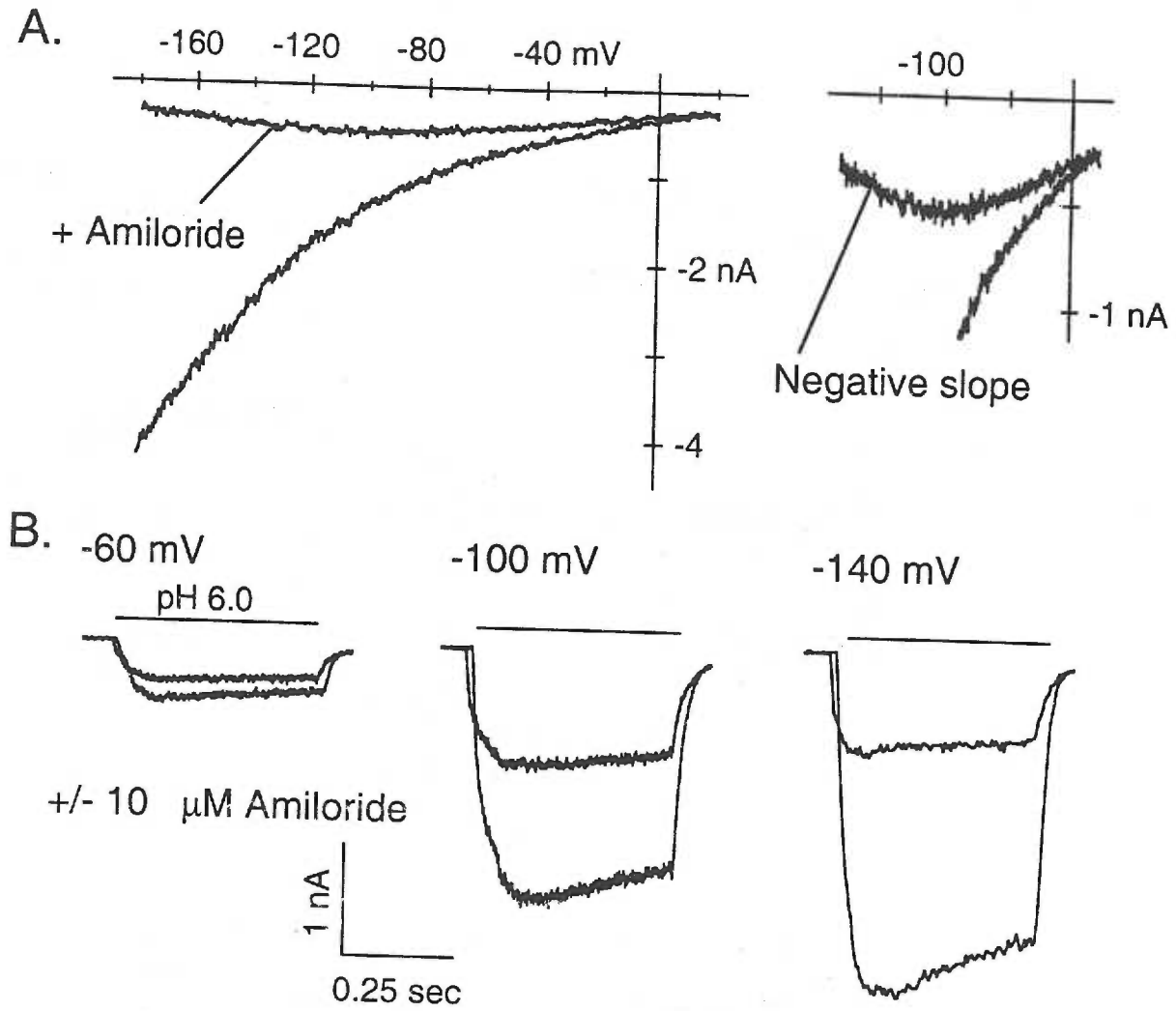
A.
-160
-120
-80
-40 mV
+ Amiloride
-2 nA
-4
-100
-1 nA
Negative slope
B.
-60 mV
pH 6.0
-100 mV
-140 mV
+/- 10 μM Amiloride
1 nA
0.25 sec
C.
50
10
3
K1/2 Amiloride (μM)
-120
-80
-40
0
mV
δ = 0.51
K1/2 (0 mV) = 41 μM

change in scale; currents were smaller in the presence of Mg^{2+} independent of amiloride.) Similarly, Fig. 16B shows that the dose-response curve for amiloride (open circles) is right-shifted in the presence of 10 mM Mg^{2+} (closed circles) with a change in half-block by amiloride from $K_{1/2}$ = 8.7 μM to $K_{1/2}$ =19 μM (n = 3-11).

Discussion of results:

The ASIC1a channel may act as a sensor of CNS ischemia. Voltage-dependent block by Mg^{2+} ions may allow ASIC1a to act as a coincidence detector, and certainly has far-reaching effects on channel behavior as divalent concentrations fluctuate. The block by Mg^{2+} may arise from the ion's high energy of dehydration. The results of this work have also revealed that the pore of ASIC1a is analogous to that of voltage-dependent sodium channels (VDNCs) and that ASIC1a is sensitive to block by the guanidinium-containing drugs amiloride and—like VDNCs—tetrodotoxin (TTX). A complete discussion of these conclusions and the associated literature can be found in Chapter 6: Discussion.

Figure 16. Mg^{+} and amiloride compete for inhibition of ASIC1a. A, traces from a representative cell show that amiloride inhibition of ASIC1a (left) is blunted by 10 mM extermal Mg^{2+} (right). B, Dose response curve for amiloride inhibition of ASIC1a with and without Mg^{2+}. Currents were measured at –70 mV in the presence and absence of 10 mM $MgCl_2$ and 0 to 200 μM amiloride. Normalized currents measured in amiloride are plotted vs amiloride concentration; n = 3-11. $K_{1/2}$ of amiloride was 8.7 μM; with 10 mM Mg^{2+}, $K_{1/2}$ was 19 μM.

A.

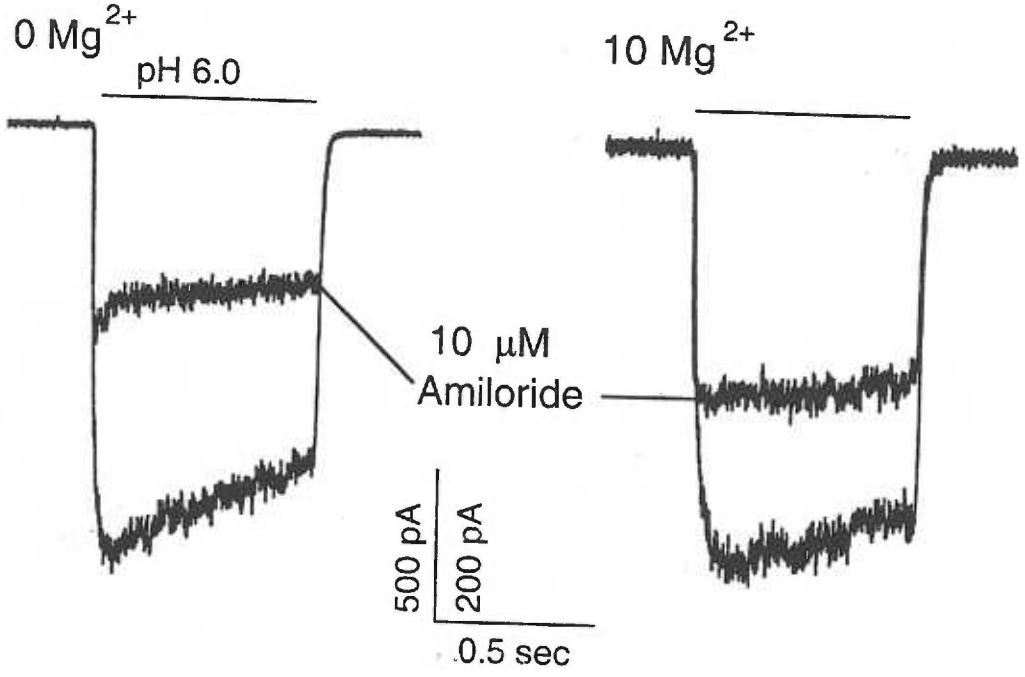
0 Mg 2+
pH 6.0
10 Mg 2+
10 μM
Amiloride
500 pA
200 pA
0.5 sec

B.

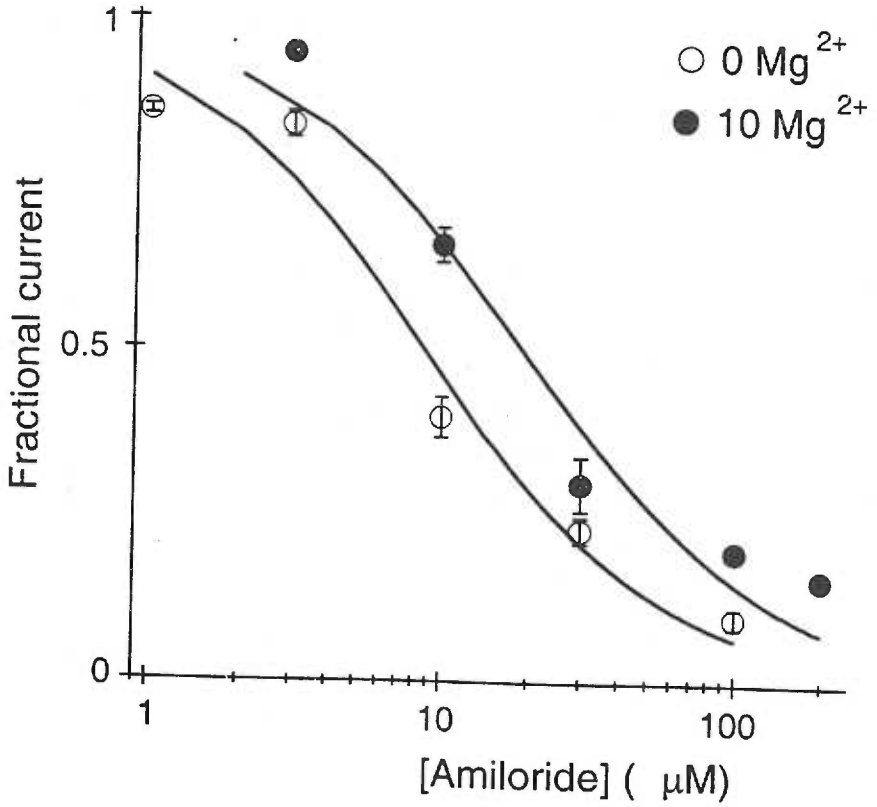
1
0.5
0
Fractional current
1
10
100
[Amiloride] (μM)
0 Mg 2+
10 Mg 2+

Chapter 6: Discussion

Part One—Summary of Results

There are four key findings described in Results: Chapter 3. 1) We describe a method to distinguish cardiac sensory neurons from neurons of other sensory modalities in primary dissociated tissue culture; 2) Compared to other sensory neurons, cardiac DRG neurons have extremely large currents evoked when pH drops to 7.0 or below; 3) Cardiac nodose neurons have smaller acid-evoked currents, but larger ATP-evoked currents, than cardiac DRG neurons; 4) Other than its large amplitude, the acid-evoked current in cardiac sensory neurons has no biophysical or pharmacological properties that are not predicted by previous studies of acid-evoked currents in sensory neurons. The large amplitude indicates the importance of acid in mediating pain due to cardiac ischemia, but certainly does not imply that other potential mediators are unimportant.

In Results: Chapter 4, I aimed to find the molecular identity of the acid-sensing channel described in the cardiac sensory neurons. I examined the five cloned ASIC channels to determine which, if any, matched the properties of the current seen in rat cardiac sensory neurons. Our results point to ASIC3 for the following reasons: 1) the native channel and ASIC3 both open at pH 7, whereas other ASICs are less sensitive to protons (some dramatically so); 2) the native channel and ASIC3 both gate between

closed, open, and desensitized states clearly faster than other ASICs; 3) the native channel and ASIC3 share aspects of permeation to and inhibition by Ca^{2+} that are unlike the other ASICs.

The work presented in Chapter 5: Results has provided new insights to the biophysical properties of the cloned ASIC1a channel, a possible ischemia sensor in the CNS. The key findings are the following: 1) ASIC1a is sensitive to voltage-dependent block by Mg^{2+} ions at an intra-pore site; 2) The pore of ASIC1a is analogous to that of voltage-dependent sodium channels (VDNCs) in its permeability to organic cations; 3) ASIC1a is sensitive to block by the guanidinium-containing drugs amiloride and—like VDNCs—tetrodotoxin (TTX).

Part Two—Discussion of Literature and Implications

1-Acid-Evoked Currents of Cardiac Sensory Neurons

In this study, we developed a new method to label the sensory neurons that innervate the myocardium of rat, tested those cardiac sensory neurons' electrophysiological response to various chemical mediators of pain, and characterized the large acid-evoked currents that were present in the overwhelming majority of these neurons. The data collected strongly points to acid as the predominant (but not necessarily sole) mediator of cardiac ischemic pain.

Isolation of Cardiac Sensory Neurons

As described in the Methods section, considerable effort was made to validate this preparation. Each of the control injection experiments resulted in significantly fewer labeled neurons compared to the pericardial space injections; this lends support to our assertion that we have specifically labeled and isolated cardiac sensory neurons. Finally, the different responses between the labeled and unlabeled DRG neurons in our whole-cell patch clamp experiments provide further evidence that we have isolated a distinct sub-group of sensory neurons from the DRG population at large.

While neuroanatomy was not the primary focus of this study, some anatomical information can be gleaned from our data. The number of labeled neurons we obtained was consistent with previous neuro-anatomical studies in the rat in which fluorescent tracers were injected into the pericardial space[85,116]. In contrast to the large number of labeled neurons following pericardial space injections, we found relatively few labeled neurons after intramural injections. This may reflect either less tissue exposure to dye compared to the pericardial space injection, or a true paucity of nerve terminals within the rat intramural myocardium. The endocardial layers were not labeled in our study. Interestingly, in a dog preparation myocardial ischemia caused cardiac sympathetic afferent firing only if the ischemia was transmural and involved the superficial epicardial layers[88].

Chemical Activation of Cardiac Sensory Neurons

Several insights arise by comparing responses to different agonists in the different cell populations we isolated. Most importantly, modest decreases in extracellular pH (i.e. to pH 7.0 or below) evoke exceptionally large currents in almost all epicardial cardiac DRG neurons. In contrast, and as reported previously[38,31], only about 50% of unlabeled DRG neurons respond to acid; those that did respond had much smaller average currents than cardiac DRG neurons[117].

Cardiac afferents with cell bodies in the DRG differed from those in the nodose ganglia. Cardiac nodose neurons had significantly smaller acid-evoked currents and larger ATP-evoked currents than cardiac DRG neurons. This raises the possibility that the two cell populations sense different chemical signals during cardiac ischemia.

There are two classes of molecules proposed to sense changes in extracellular pH in sensory neurons: ASICs and vanilloid (capsaicin) receptors. Vanilloid receptors are activated by noxious heat and by capsaicin (the compound in pepper that tastes "hot"); also, current through vanilloid receptors is strongly increased by acidic pH[37,36]. Therefore, it is considered that vanilloid receptors, in addition to sensing heat, may mediate sensory responses to acidity caused by inflammation and ischemia. The neurons we isolated detect cardiac ischemia, yet only a small fraction exhibit capsaicin-activated current and those that do respond have small currents compared to unlabeled DRG neurons. In contrast, almost all exhibit grossly large currents through ASICs. These results argue that ASICs are more important than vanilloid receptors for sensing myocardial ischemia.

5HT-evoked currents were substantial in cardiac afferents, but still smaller than the acid- or ATP-evoked currents. Various cells that contribute to the immune response to tissue damage release 5HT, so these currents may provide a means of communication between immune cells and cardiac sensory neurons.

Of the chemicals tested, protons, ATP, 5HT, and capsaicin activate ion channels (ASICs[40], P2X receptors[105,104], 5HT3 receptors[100], and vanilloid receptors[36] respectively) that are presumed to serve as sensory transducers in sensory neurons. No current was ever evoked by ACh, but currents were occasionally seen in response to BK or adenosine. We do not infer anything from the relatively rare and small currents evoked by these compounds because they do not directly gate ion channels; in fact, adenosine inhibits a Ca^{2+}-activated K^+ channel[103]. The current we saw presumably arose from modulation of a channel by an intracellular signaling cascade; the importance of this may be understated by simply comparing the amplitude to those of channels directly gated by protons, ATP, or 5HT.

Physiologic and Pathophysiologic Significance

Cardiac sensory neurons respond to lowered pH (in the range produced by myocardial ischemia) with consistent and robust depolarizing currents; this suggests that acid is a potential mediator of myocardial ischemic sensation.

In humans, the only conscious sensation from the heart is pain or angina, which most commonly occurs during myocardial ischemia. However, objective measurements of myocardial ischemia often do not correlate with the presence or severity of chest pain. In fact, ambulatory electrocardiographic monitoring in patients with myocardial ischemia

has revealed that the majority of ischemic episodes are not reported as painful[118]. Attempts to model ischemic cardiac pain in animals have produced variable results. The pseudo-affective measures of pain in these behavioral studies correlate poorly with sensory neuronal activation[91,111,14]. Thus, it is reasonable to conclude that activation of cardiac sensory neurons with acid does not equate with nociception. For example, in patients with "silent" ischemia (defined as objective myocardial ischemia that is painless) there is evidence of sensory activation to the level of the thalamus, whereas patients with typical angina have additional activation of the cerebral cortex[119]. Thus, the conscious perception of chest pain most certainly involves complex central processing and integration at multiple levels, and activation of cardiac sensory neurons is probably necessary but not sufficient to produce pain. Regardless, ischemia- or acid-induced activation of cardiac sensory neurons, whether painful or not, may be an important initiator of cardiovascular reflexes in pathologic cardiac conditions.

A broad range of cardiovascular disease processes, including myocardial ischemia[120], congestive heart failure[121], and arrhythmia, is precipitated or worsened by perturbations in the autonomic nervous system. Much of the current pharmacological therapies are directed towards blocking the compensatory, but often deleterious, neuro-hormonal systems that are activated in these diseases. In human skeletal muscle, ischemia-induced acidic pH is coupled with sympathetic efferent nerve discharge[122].

Also, abdominal visceral ischemia leads to profound cardiovascular reflex changes, the degree of which appears related to the level of the resulting acidosis[110]. A similar acid-evoked reflex loop may exist in the heart and contribute to the detrimental effect of sympathetic activation in myocardial ischemic conditions. Specific blockade of acid-evoked activation of cardiac sensory neurons presents a potential new therapeutic management strategy in the treatment of ischemic heart disease.

2-ASIC3 Is the Primary Cardiac Acid Sensor

Extracellular acid appears to be a significant part of the signal that triggers pain during cardiac ischemia[25,12] and rat cardiac sensory neurons display extremely large Na^+ currents through an acid-sensing ion channel[7]. Because the ion channels that mediate this current are probably molecular sensors for cardiac ischemic pain, we aimed to find which, if any, of the five cloned ASICs mediates the acid sensitivity of rat cardiac sensory neurons. The following is a discussion of the distinguishing characteristics of the ASIC3 channel, the primary acid-sensing molecule in cardiac sensory neurons.

High proton sensitivity is perhaps ASIC3's most critical feature. During coronary artery blockade, extracellular pH drops to neutral in a few minutes, but is unlikely to drop below about pH 6.7[25,95,29]. Such moderate pH changes readily open ASIC3 channels, which have a very steep activation curve consistent with a requirement that 4 protons

bind to open the channel. This makes the channel 4-fold more sensitive than a pH electrode to protons over the range of pH that changes during cardiac ischemia. Perhaps coincidentally, most evidence indicates that channels in this family are tetramers[41-43], although other evidence argues for different numbers of subunits[44].

ASIC3 mRNA is abundant in rat sensory ganglia and scarce elsewhere[46,49]. Moreover, I show in Fig. 8 that low threshold mechanosensors—cells uninvolved with detecting ischemia—have no functional ASIC3 channels, whereas cells specialized to sense cardiac ischemia are enriched in them. Such specificity in expression suggests that ASIC3 would be a useful pharmaceutical target for selectively suppressing angina, and maybe other forms of ischemic pain. The human homolog (84% sequence identity) of ASIC3 has been cloned and displays high proton sensitivity[123], but there is no information yet about its expression pattern in humans.

One property of the response of cardiac afferents to pH—a small, non-selective, amiloride-insensitive conductance seen at pH 5 in some, but not all, cardiac afferents—is not mimicked when ASIC3 is expressed alone. It is mimicked upon co-expression of ASIC3 and 2b, as previously reported by Lingueglia et al.[48], and the two subunits co-immunoprecipitate when co-transfected. We cannot, however, conclude that cardiac afferents express ASIC heteromers because other channel types could generate such currents. For example, vanilloid receptors generate sustained, non-selective currents at

such extreme pH[37] and are present at low levels in cardiac afferents[7]. Also, the extreme acidity required to evoke the sustained current might modify other ion channels to generate such small non-selective currents. We are pessimistic that a molecular identity can be provided to this current that varies in expression and has no kinetics, no selectivity and no pharmacology. Moreover, because the sustained current occurs only at extremely low pH, its relevance to cardiac ischemia is questionable.

Roles For Other Channels

There are several reasons to hesitate to conclude that ASIC3 is the sole sensor for cardiac ischemic pain. First, acidity is only one of a number of signals that lead to cardiac pain, and acidity can activate molecules besides ion channels (see below). Second, we previously reported that a few cardiac afferents exhibit a less-sensitive acid-evoked current with smaller amplitude and slower kinetics than the large, transient current that we studied here[7]. Thus, several channels may sense acid in rat cardiac afferents, ASIC3 being the most abundant. It is also possible that ASIC3 forms heteromers with other ASIC subtypes if these heteromers have the same properties as the ASIC3 homomer. A final issue concerns an inherent limit in our study: we can only compare the native channel to cloned channels. Could the native channel be an uncloned ASIC rather than ASIC3? We consider this unlikely because each of the known channels has a distinct

fingerprint of functional properties that is unmatched by the others. The variability of these properties among the known channels argues against an unknown channel with the precise properties of ASIC3, and thus, the precise properties of the native channel.

Search For the Mediator of Ischemic Pain

Although our efforts have focused on acid as a mediator of ischemic pain, there are other important candidates that should not be ignored. Adenosine is released from cells whenever there is a decline in intracellular ATP. There is conflicting literature about adenosine action on cardiac afferents, with some groups supporting a role in cardiac pain[16,124,125] and others not[18,17]. Bradykinin increases firing of cardiac afferents *in vivo*[17,13] by acting at B_2 receptors[126]. It is cleaved from kininogens by the enzyme kallikrein, which can be triggered by a drop in pH. Thus, kallikrein is an acid sensor that generates a pain signal, bradykinin, that appears more slowly than ASIC3 current but might persist longer (tissue half-life of 15 seconds[127]). Among other suggested mediators of cardiac pain are serotonin, ATP[86], histamine, and oxygen radicals. It may be possible to test in intact animals the relative importance of ASICs in cardiac pain by using amiloride; however, the concentrations necessary to block ASICs are very high, roughly 100-fold more than used to block ENaCs.

3-Voltage-Dependent Block Of the CNS Channel ASIC1a

The ASIC1a channel may act as a sensor of CNS ischemia. As opposed to the case in the periphery, central ischemia does not result in a sensation, but rather massive neuronal death that may be mediated in part by an ASIC channel. Voltage-dependent block by Mg^{2+} ions may give it the ability to act as a coincidence detector. The mechanism of block may arise from the high energy of dehydration for Mg^{2+}. The results of this work have also revealed that the pore of ASIC1a is analogous to that of voltage-dependent sodium channels (VDNCs) and that ASIC1a is sensitive to block by the guanidinium-containing drugs amiloride and—like VDNCs—tetrodotoxin (TTX).

Magnesium Blocks ASIC1a At An Intra-Pore Site

I observed a negative slope region of the current-voltage (I-V) curve of ASIC1a that was dependent on the presence of extracellular Mg^{2+} ions. The characteristics of this voltage-dependent block suggest an intra-pore, low-affinity Mg^{2+} binding site. Such voltage-dependent block by Mg^{2+} ions has been well characterized in the NMDA-type glutamate receptor channel[128-132,79,80]. Voltage-dependent block has been characterized in a variety of other ion channels as well, notably block of Na^+ channels by extracellular protons[82] and block of Ca^{2+} channels by various divalent cations[133].

The method of analysis of data that provided evidence of voltage-dependent block was taken largely from Woodhull and Hille's description of proton block of sodium channels[82]. Because block is voltage dependent, K_d varied with membrane potential; the K_d at a particular voltage (E) is described by the term K(E). The K_d value at 0 mV, K(0), represents the true binding affinity of the blocking ion at its site when voltage has no influence on binding, and is determined by the on- and off-rate constants of the ion at the binding site. Because depolarization relieved the block, the K_d at 0 mV was significantly higher (i.e. lower affinity) than at resting potentials, as expected.

As for the affinity of the site, there is another property seen in ASIC1a that the Woodhull equations do not account for: permeation of Mg^{2+}. As with the NMDA channel[128,132], ASIC1a appears to pass Mg^{2+} ions at extremely hyper-polarized potentials. This is evident from the N-shape of the I-V curve recorded in the presence of Mg^{2+}. Thus, Mg^{2+} ions have another pathway to leave their binding site (through the channel pore), at least at very negative potentials.

Voltage-dependent block indicates that the blocking ion binds, or interacts, with the channel pore somewhere within the electrical field across the membrane. It is this interaction within the electrical field that makes the block voltage-dependent. The distance within the electrical field can be roughly quantified by calculation of the term "delta" (δ). It would be unwise, however, to ascribe too much information to this number

for several reasons. First, there are several factors that can influence the term δ aside from just the distance of the blocking ion's interaction within the field, including surface charge near the channel mouth and ion-ion interactions[131]. Second, the permeation by Mg^{2+} at hyper-polarized potentials may attenuate the delta value. As voltage becomes more negative, the probability decreases that Mg^{2+} will unbind from its site and return to the extracellular medium; at the same time probability increases that Mg^{2+} will leave its site to go through the channel. The calculation of the delta value was made from K(E) values positive to this region where Mg^{2+} appears to permeate (i.e. positive to –140 mV), so that it should be minimally affected by permeation of Mg^{2+}.

Delta (δ) only describes the blocking ion's assumed position within the electrical field, and not the distance across the membrane or the channel. The electrical field across the membrane is not necessarily uniform, and may drop significantly over a small area. The delta value of 0.21 for Mg^{2+} block of ASIC1a suggests that the blocking ion interacts with the channel to cause block about one fifth of the way across the electrical field, but it is impossible to know exactly where within the channel or the membrane this occurs. The delta value for the NMDA-type glutamate receptor is estimated between 0.8 and 1, which suggests that Mg^{2+} ions block that channel at a site deep within the channel[128,131]. The ASIC1a channel pore seems not to be analogous to the NMDA channel in terms of the position of Mg^{2+} block in the channel, but for the reasons discussed above it is difficult to

interpret this delta value with any degree of certainty. The mechanism of voltage-dependent block, perhaps entirely independent of the location of block, may well be the same between ASIC1a and the NMDA channel.

Another indication that Mg^{2+} block occurs at an intra-pore site is the competition by amiloride for block. The dose-response curve for amiloride block of ASIC1a shifted to the right when 10 mM Mg^{2+} was added to the external media. This suggests that amiloride and Mg^{2+} compete for access to the same area of the channel pore in order to block (but do not necessarily share the same blocking site or mechanism.)

High Energy of Dehydration May Account for Mg^{2+} Block

The mechanism of voltage-dependent block is probably explained by one of the following two possibilities: 1) Mg^{2+} blocks at a constriction site within the pore where it becomes trapped due to its high energy of dehydration, or 2) Mg^{2+} is a permeant ion which, after losing its waters of hydration, binds tightly within the permeation pathway.

First, and seemingly more likely, that Mg^{2+} ions block ASIC1a at a site of constriction, or selectivity filter within the pore. In this scenario, as in the NMDA channel, ions that block the channel fall into one group whereas ions that permeate the channel fall into another[128,131,132,134]. The feature that distinguishes these groups is their energy of dehydration. Ions that do not easily shed their waters are voltage-dependent

blockers: Mg^{2+}, Co^{2+}, Ni^{2+}, and Mn^{2+}; on the contrary, ions that shed their waters easily do not block as well but are better permeators; these include Ca^{2+}, Ba^{2+}, Sr^{2+} and Cd^{2+}. These permeant ions are thought to cause a diminution of current by passing through the permeation pathway more slowly than the more permeant monovalent cations.

The second possibility is that the energy of dehydration is inconsequential to block, and each ion blocks by binding with varying affinity at an intra-pore site in the permeation pathway. This is the case for voltage-dependent Ca^{2+} channels, where block by divalent ions is not determined by their energy of dehydration[133], and seems to be entirely different from block of NMDA channels.

To determine which of the two above blocking mechanisms was at work in ASIC1a, I examined whether other divalent cations could block ASIC1a as well as Mg^{2+}. As mentioned in Results, ASIC1a currents were larger in a lowered concentration of external Ca^{2+}, but the effect did not appear to be voltage-dependent block judging from the shape of the I-V plot. Instead, it is believed that Ca^{2+} ions interact more directly with the gating mechanism of ASICs to affect the currents. (This insight comes from work done in the lab by David Immke.) A similar effect was seen with Ba^{2+} and Cs^{+} ions: currents were smaller in amplitude when the divalent concentration was increased, but the I-V plot appeared to remain linear. Perhaps unexpectedly, currents recorded in the presence of the other slowly-dehydrating ions, Ni^{2+} and Co^{2+}, were also of extremely

small amplitude compared with currents recorded in Mg^{2+}. It seems that all divalent ions tested--except for Mg^{2+}—affect ASIC1a in a way that is neither voltage-dependent, nor does it distinguish between ions with vastly different energies of dehydration. These characteristics point to an effect on the gating mechanism; alternatively the effect could arise from permeation effects by the various ions (as in Lansman et al.[133]). If the Mg^{2+}-like divalent ions do act as voltage-dependent blockers, the binding at the voltage-dependent site must be much lower affinity than at the proposed gating site because voltage-dependent block was not evident from the I-V plots for Ni^{2+} and Co^{2+} in the concentration range observed for Mg^{2+}. Thus, I cannot definitively say whether energy of dehydration determines whether an ion will block or not, but my experiments did not rule it out. My data that defines the delta value of block by Mg^{2+} as 0.21 could represent a site one fifth of the way through the field where ions must either shed their waters of hydration and permeate, or get stuck and block current.

The ASIC1a Pore Is Analogous To Voltage-Gated Sodium Channels

Voltage-gated sodium channels have been well characterized by Hille in terms of their permeation to organic cations[135]. Of the many ions Hille tested, the most striking data came from his examination of methyl-amine and guanidine permeation. If size alone were the determinant of ion permeability, the smaller methyl-ammonium ion should pass

more easily than the larger guanidinium ion, but in fact methyl-amine permeation was very low. The characteristic that distinguishes these ions is a methyl group vs. an amino group—and the ability of those groups to form hydrogen bonds. Hille concluded that the sodium channel pore is approximately 3 Å wide and is lined with oxygen atoms, which form hydrogen bonds with the amino group of some permeant ions. Ions that have either a methyl group (such as methyl-amine) or an amino group (such as guanidine) are both wider than the proposed 3 Å width of the channel, but "nevertheless, cations containing amino groups can slide through the channel by making hydrogen bonds to the oxygens," while methyl groups, which are unable to form hydrogen bonds, can not[135].

I determined that the ASIC1a channel pore is analogous to VDNCs in its unique permeability to the guanidinium ion but not to the methyl-ammonium ion. The values of the permeability ratios for guanidine and methyl-amine are strikingly similar to those reported in VDNCs[135]. The small current I recorded with methyl-amine may in fact be partly carried by the external Ca^{2+} that was present, as Ca^{2+} is slightly permeant (P_{Na}:P_{Ca}=16). Alternatively, the slightly higher permeation of methyl-amine through ASIC1a (than through VDNCs) might reflect that the pore of ASIC1a is slightly larger than that of VDNCs, allowing some methyl-amine to pass through even though it cannot form hydrogen bonds. Thus, it seems that the ASIC1a pore is analogous (but not identical) to the pore of VDNCs in terms of size and selectivity, and that it too is lined

with oxygen atoms that form hydrogen bonds with the amino group of the permeant guanidinium ion.

ASIC1a Is Blocked By Guanidinium-Containing Drugs

After determining that the guanidinium ion can interact with the ASIC1a pore, I wanted to more closely examine block by guanidine-containing drugs. Amiloride blocks all ASIC channels with low affinity (10 – 100 μM, see Table 1), roughly one hundred times lower affinity than block of the epithelial channels (ENaCs). Could the low-affinity block of ASICs arise from a simple hydrogen-bond interaction between the guanidine group and the ASIC pore?

A cartoon model is presented as a possible representation of block of ASIC1a channels by guanidine-containing drugs amiloride and TTX (Figure 17). Block by amiloride appears to involve an intra-pore interaction, as evidenced by voltage-dependence of the block. Again, the negative-slope region of the I-V curve of currents measured in the presence of amiloride determines that amiloride must enter the electrical field across the membrane at its blocking site. I quantified the voltage-dependence of block by again measuring currents with and without amiloride at various voltages. The plot of this data reveals a $K_{1/2}$ value of 41 μM at 0 mV, with a higher affinity at more negative voltages. The same plot reveals a delta value of 0.51, suggesting that the

amiloride ion blocks at a site approximately half way across the electrical field. Again, this value does not reveal where exactly within the membrane or the channel the ion is blocking; it only gives a hint about how much of the electrical field is felt by the blocking ion. Regardless of where in the channel it occurs, the guanidine group may be drawn into the pore (and perhaps form hydrogen bonds), but the larger part of the amiloride molecule then becomes wedged into the channel pore like a champagne cork in a bottle.

Such is Hille's interpretation of block of VDNCs by tetrodotoxin (TTX)[136]. This toxin contains a guanidine group and blocks the ASIC1a channel with relatively low affinity. Perhaps the guanidine group of TTX is drawn into the ASIC pore just as it is to the VDNC pore, and indeed perhaps forms interactions with the pore lining and becomes stuck in the mouth of the pore to block the channel. Unlike amiloride, however, TTX block is not voltage-dependent. TTX, therefore, must become stuck somewhere outside the electrical field across the membrane, and seems not to reach as far into the pore as amiloride or Mg^{2+} ions do.

The interaction of a toxin's guanidine group inside the ASIC pore is not meant to explain the high-affinity (nanomolar) block by amiloride at ENaC channels, or by TTX at most sodium channels. Rather, I propose that the guanidine interaction may describe the low-affinity (micromolar) interaction of amiloride at ASIC channels, and perhaps of TTX at the so-called TTX-resistant sodium channels, which are in fact blocked by TTX, but

with much lower affinity than most sodium channels are. As postulated by Hille, higher affinity associations may arise from the interaction between another part of the toxin molecule and the outer mouth of the channel, without affecting the guanidine interaction with the selectivity filter, or constriction[136]. Thus, the presence of a guanidine group on a drug might provide the foundation for an ASIC-blocking drug. From this beginning, other parts of the molecule might form a high-affinity interaction with some other part of the channel outside the pore. In this manner, it may be possible to develop drugs that block each specific ASIC channel with high affinity and specificity.

Part Three—Future Directions

The following ideas for future experiments are discussed in the form of three Aims. In Aims One and Two, I propose a further investigation of the role of ASICs in CNS ischemia. First, the properties of acid-evoked currents of cloned ASICs and native CNS neurons are compared in conditions that mimic central ischemia toward identification and characterization of the acid-sensor of CNS ischemia (perhaps a cloned ASIC). The second Aim describes experiments to examine the role of ASICs in cultured hippocampal slices, a preparation that better retains the physiological properties of the CNS, under ischemic conditions. This is the same approach that has led to the elucidation of the role of glutamate receptors in CNS ischemia. Finally, Aim Three will outline possible directions for structure-function studies of the ASIC1a pore in order to connect the channel behavior revealed in the present study to a structural feature that acts as a selectivity filter.

Aim One: ASIC1a Currents During Ischemic Conditions

Is a cloned ASIC an ischemia sensor in the CNS? Again, in the CNS, the term sensor refers not to a physical or physiological sensation of ischemia, but a detector of ischemia that may in fact add to a neuron's vulnerablility to death during CNS ischemia. The next test of ASIC physiology in the brain will be to test acid-evoked currents in

cultured hippocampal neurons and in cells expressing cloned ASIC channels in the ionic and acidotic conditions that occur during cerebral ischemia.

Strategy and Experimental design: Acid-evoked currents of hippocampal neurons of rats and cloned ASIC channels expressed in a heterologous system would be examined and compared using whole-cell electrophysiology. Because physiology is the main interest in these experiments, the extracellular conditions would mimic those of cerebral ischemia, including pH, divalent concentrations, and voltage. Extracellular divalents, Ca^{2+} in particular, fall to extremely low concentrations during CNS ischemia[137]. ASIC currents have a larger amplitude when Ca^{2+} concentration is lowered; thus at the pH relevant to ischemia (6.5), ASICs could become maximally activated as Ca^{2+} levels drop.

Rat hippocampal neurons would be acutely dissociated for electrophysiology studies. Neurons should be cultured from adult rats because some studies have shown that the neonatal rat brain is extremely resistant to damage during cerebral ischemia, and to acidosis in particular, even in rat neurons as old as 7 days[74,53]. This may be explained by age-dependent gene expression, perhaps of acid-sensing ion channel genes. ASIC1a channels would be transiently transfected in COS7 cells as in the present study.

Possible problems: Central neurons are heterogeneous in their sensitivity to protons[138-140], possibly because of differential expression of ASIC subunits. Perhaps

only a small percentage of neurons will express ASIC1a, the channel most sensitive to acid among those expressed in CNS. This heterogeneity may require study of a large number of neurons to get an accurate picture of ischemia-sensing molecules in the CNS. Another concern with neurons is a greater chance for interference by voltage-activated currents than in COS7 cells. These should be minimized by desensitization since the acid application will be delivered several seconds after the voltage change has been made. To combat any remaining steady-state potassium currents, internal K^+ ions could be replaced with Cs^+, and TEA could be added to the external solution without affecting ASICs.

Aim Two: Role of ASIC1a in Neuronal Ischemic Death

The experiments in this outline seek to extend the findings of Aim One to a more physiological setting: the hippocampal slice culture. Measurements of necrotic cell death would be made after exposure to ischemic conditions with various manipulations of acid-sensitive responses.

Strategy and Experimental Design: The goal is to use the electrophysiological properties of individual neurons (from Aim One) and the assessment of cellular survival (in this Aim) to glean a better understanding of CNS ischemia. The hippocampal slice is a more physiological setting than dissociated neurons because the cellular architecture of the CNS environment is preserved. Neurons in a slice preparation are more sensitive to

acidosis and ischemic conditions, perhaps due to excitatory signals from other neurons in conjunction with acidosis[74]. As in the studies of glutamate receptors, specific channel antagonists could be used to assess what ion channels mediate the neurotoxic affects of acidosis in CNS ischemia[74]. Neuronal death would be compared between cultures exposed to ischemic conditions, with and without blockers of ASICs. Amiloride, or more specific ASIC blockers if available, could be used to block ASIC channels during the exposure to ischemic conditions. Neuronal death would be determined with propidium iodide staining. To make the experiment more physiologically relevant, the perfusion medium will mimic ischemic conditions as closely as possible, including pH, divalent concentrations, hypoglycemia, and hypoxia. Lactic acid will be used to acidify the environment, rather than a solution simply titrated with HCl. Acid-evoked currents, neuronal firing[25] and neuronal and glial death[53,141] are all increased with lactic acid compared with HCl. These effects may be explained the chelating property of lactate ions, which effectively lowers free extracellular Ca^{2+} to potentiate ASIC activation (David Immke, personal communication).

Possible problems: Amiloride blocks acid-sensing ion channels with low affinity, in the micromolar range. At the concentration needed to block ASICs (around 100 μM), the drug may affect other ion channels of the CNS, particularly voltage-dependent sodium channels (since the pores of VDNCs and ASICs are analogous in their sensitivity

to guanidine-containing drugs, as shown in the present study). The ideal situation would be if a particular ASIC were identified (in Aim One) as the primary ischemia sensor in CNS, and a more specific toxin could be used to block that channel. It seems that this may now be possible with the news of a tarantula toxin that blocks ASIC1a currents specifically[142].

Aim Three: Structure of the ASIC1a Selectivity Filter

In the third Aim, the focus is shifted from the physiological function of ASICs in CNS to a more biophysical study of the structure-function relationships of ASICs, and experiments are discussed in more broad terms than in the previous Aims. Studies to determine the details of the structural character of various ASICs are currently under way in a number of laboratories. An understanding of ASIC1a's pore behavior seen in the current study is likely to arise from such a structural exploration.

Strategy and Experimental Design: The most parsimonious interpretation of the results presented in the current study lies in the pore structure of ASIC1a. First, the channel seems to have a pore width of about 3 Å, and is lined with oxygen molecules that form hydrogen bonds with some permeant ions. It seems that a comparison between ASIC1a and voltage-dependent sodium channels is in order with respect to coding sequence and structural features of the pores. Secondly, the voltage-dependent block by

Mg^{2+} ions and guanidinium toxins points to a constriction site somewhere within the pore and the electrical field. Mutational analysis of the ASIC1a channel is kept relatively simple by a short (~500 AA) sequence. Finally, there is much to be learned about the ASIC channels' processes of gating, permeation, block, and the roles in each of these for divalent cations. A better understanding of these features is likely to include data from structure-function studies. Block by the newly reported toxin that specifically blocks ASIC1a could be examined in more detail using structure-function studies[142]. New evidence from the same lab points to potentiation by Zn^{2+} ions of ASIC1a currents in DRG and CNS neurons[143]; an understanding of this effect will likewise arise from structure-function studies.

Chapter 7: Summary and Conclusions

The work presented here examines a role for acid-sensing ion channels (ASICs) as molecular sensors of ischemia in the heart and brain. I have shown that sensory neurons that innervate the heart respond to the pH of muscle ischemia with large, inward depolarizing currents, and that these currents are primarily carried by the channel ASIC3, a molecular ischemia sensor in sensory neurons that innervate the heart. ASIC1a is expressed in CNS neurons and may act as a molecular ischemia sensor and may contribute to neuronal ischemic death in the brain. I have found channel properties of ASIC1a that are analogous to both NMDA-type glutamate receptors (voltage-dependent block by Mg^{2+}), and to voltage-gated sodium channels (selectivity properties of the pore).

The first hurdle that I accomplished was to find a way to distinguish cardiac sensory neurons from neurons of other sensory modalities in primary dissociated tissue culture. This was achieved surgically by placing a fluorescent dye in the pericardial space of rats so that it would be taken up at the terminals of sensory nerve endings that innervate the myocardium. This preparation allowed me to perform experiments on labeled, identified, dissociated cardiac sensory neurons in culture using electrophysiology.

These electrophysiology studies have led me to the conclusion that protons are the primary chemical mediator of ischemic pain through these cardiac sensory neurons. Protons are by no means the only mediator of ischemic pain in the heart, but on the fast time scale of ion channel currents, protons gave the largest and most prevalent signal compared to other candidates. I have outlined in detail the biophysical properties of the ion channels that carry these large, inward depolarizing currents. Further, the ischemia-sensing molecule seems to be concentrated in those cardiac sensory neurons specialized for sensing ischemia (compared to other sensory neurons in the DRG). The very high expression of these currents in ischemia-sensing neurons suggests an important role of acid in mediating cardiac pain.

Next, I aimed to find the molecular identity of the acid-sensing channel described in the cardiac sensory neurons. I examined the five cloned ASIC channels to determine which, if any, matched the properties of the current seen in rat cardiac sensory neurons. There is no pharmacological agent that distinguishes the different ASICs. Therefore, I measured 8 different functional properties of the native cardiac afferent channel and compared these to each cloned ASIC, using a heterologous system to study each channel in COS7 cells. These studies created, in effect, a fingerprint or profile of each of the cloned ASICs, which I then compared to the fingerprint of the currents carried by the native channel. The fingerprint of the cardiac sensory neuron current and that of ASIC3

matched so closely—and excluded the other ASIC subtypes—that I concluded that ASIC3 is the primary ischemia sensor in the heart. The defining properties of the two currents are the following: both channels open at pH 7, whereas other ASICs are less sensitive to protons (some dramatically so); the native channel and ASIC3 both gate between closed, open, and desensitized states clearly faster than other ASICs; and the native channel and ASIC3 share aspects of permeation to and inhibition by Ca^{2+} that are unlike the other ASICs.

In the final aim of this work, I turned my attention from the heart to ischemia in the brain. Some ASIC channels are expressed throughout the CNS, particularly in hippocampal and cortical neurons. ASIC1a is one such channel, and is so sensitive to protons ($K_{1/2}$ of pH 6.3) that it should be well activated by the pH reached during brain ischemia. I therefore focused these studies on the ASIC1a channel, again expressed in the heterologous system and using electrophysiological studies. In particular, I examined voltage-dependent block of ASIC1a, and the properties of the channel pore through studies of permeation by organic cations and block by guanidine toxins.

This data has provided new insights to the biophysical properties of the cloned ASIC1a channel, a possible ischemia sensor in the CNS. The key findings are the following: ASIC1a is sensitive to voltage-dependent block by Mg^{2+} ions at an intra-pore site; the pore of ASIC1a is analogous to that of voltage-dependent sodium channels

(VDNCs) in its permeability to organic cations; and ASIC1a is sensitive to block by the guanidinium-containing drugs amiloride and—like VDNCs—tetrodotoxin (TTX).

I observed a negative slope region in the I-V curve of ASIC1a that can be attributed to voltage-dependent intra-pore block by Mg^{2+} ions. Voltage-dependent block by Mg^{2+} ions may allow ASIC1a to act as a coincidence detector of acidity and depolarization, much in the way that the NMDA receptor is a coincidence detector of glutamate and depolarization.

A study of the permeation properties of ASIC1a revealed that the pore of the channel is analogous to voltage-dependent sodium channels (VDNCs). These channels are permeable to the organic cation guanidinium but not the smaller methyl-ammonium ion. This is explained by the ability of the amino group of guanidine to form hydrogen bonds whereas methyl groups cannot. Thus it is thought that guanidine and some other permeant ions can form hydrogen bonds with atoms that line the channel pore and compress in size in order to slide through the channel pore's permeation pathway. This seems to indicate that like the VDNCs, ASIC1a has a pore that is only around 3 Å wide and is lined with oxygen atoms that form hydrogen bonds with the amino group of some permeant ions.

This interaction of guanidine with the ASIC1a pore may form the basis for block by guanidine-containing drugs or toxins. Amiloride is among the only drugs that block

ASICs, and do so with low affinity, in the micromolar range. The molecule consists of a charged guanidine moiety attached to a larger, bulky structure. Voltage-dependent Na^+ channels (VDNCs) are blocked by tetrodotoxin, a toxin that also contains a charged guanidine moiety. My data indicates that both of these toxins block the ASIC1a channel with low affinity. Amiloride blocks at a site within the electrical field across the membrane as indicated by the voltage-dependence of block. Tetrodotoxin block, however, is voltage-independent. The low affinity interactions observed in this study indicate that guanidine is an important feature of blockers of ASIC channels.

References

1. Taylor, E. J., ed., *Dorland's Illustrated Medical Dictionary*. 27th ed. 1988, Philadelphia: W.B. Saunders Company. 857.

2. Lewis, T. Pain in muscular ischemia. *Archives of Internal Medicine* **49**:5, 713-727 (1932).

3. Keele, C. A. & Armstrong, D., *Substances producing pain and itch*. 1964, London: Edward Arnold Publishers, LTD. 326-337.

4. MacWilliam, J. A. & Webster, W. J. Some applications of physiology to medicine. *British Medical Journal* **i**, 51-53 (1923).

5. Pickering, G. W. & Wayne, E. J. Observations on angina pectoris and intermittent claudication in anemia. *Clinical Science* **1**, 305-325 (1933).

6. White, J. C. Cardiac pain: anatomic pathways and physologic mechanisms. *Circulation* **16**, 644-655 (1957).

7. Benson, C. J., Eckert, S. P. & McCleskey, E. W. Acid-evoked currents in cardiac sensory neurons: A possible mediator of myocardial ischemic sensation. *Circulation Research* **84**, 921-928 (1999).

8. Cutler, E. C. Summary of experiences up to dat in the surgical treatment of angina pectoris. *American Journal of Medical Science* **173**, 613-624 (1927).

9. Brown, A. M. Excitation of afferent cardiac sympathetic nerve fibers during myocardial ischaemia. *Journal of Physiology* **190**, 35-53 (1967).

10. Meller, S. T. & Gebhart, G. F. A critical review of the afferent pathways and the potential chemical mediators involved in cardiac pain. *Neuroscience* **48**:3, 501-524 (1992).

11. Cervero, F. Sensory innervation of the viscera: peripheral basis of visceral pain. *Physiological Reviews* **74**:1, 95-138 (1994).

12. Uchida, Y. & Murao, S. Acid-induced excitation of afferent cardiac sympathetic nerve fibers. *American Journal of Physiology* **228**:1, 27-33 (1975).

13. Baker, D. G., Coleridge, H. M., Coleridge, J. C. G. & Nerdrum, T. Search for a cardiac nociceptor: stimulation by bradykinin of sympathetic afferent nerve endings in the heart of the cat. *Journal of Physiology* **306**, 519-536 (1980).

14. Malliani, A., Schwartz, P. J. & Zanchetti, A. A sympathetic reflex elicited by experimental coronary occlusion. *American Journal of Physiology* **217**:3, 703-709 (1969).

15. Leenan, F. H. Cardiovascular consequences of sympathetic hyperactivity. *Canadian Journal of Cardiology* **15 Suppl A**, 2A-7A (1999).

16. Gnecchi-Ruscone, T., *et al.* Adenosine activates cardiac sympathetic afferent fibers and potentiates the excitation induced by coronary occlusion. *Journal of the Autonomic Nervous System* **53**, 175-184 (1995).

17. Pan, H.-L. & Longhurst, J. C. Lack of a role of adenosine in activation of ischemically sensitive cardiac sympathetic afferents. *Heart Circulation Physiology* **38**, H106-H113 (1995).

18. Abe, T., *et al.* Attenuation of ischemia-induced activation of cardiac sympathetic afferents following brief myocardial ischemia in cats. *Journal of the Autonomic Nervous System* **71**, 28-36 (1998).

19. Veelken, R., *et al.* Epicardial bradykinin B2 receptors elicit a sympathoexcitatory reflex in rats. *Hypertension* **28**:4, 615-621 (1996).

20. Rotto, D. M. & Kaufman, M. P. Effect of metabolic products of muscular contraction on discharge of group III and IV afferents. *Journal of Applied Physiology* **64**, 2306-2313 (1988).

21. Stebbins, C. L. & Longhurst, J. C. Bradykinin in reflex cardiovascular responses to static muscular contraction. *Journal of Applied Physiology* **61**:1, 271-279 (1986).

22. Lindahl, O. Pain--A general chemical explanation. *Advances in Neurology* **4**, 45-47 (1974).

23. Lehninger, *Biochemistry*. 1978. 231-233.

24. Opie, L. H., Owen, P., Thomas, M. & Samson, R. Coronary sinus lactate measurements in assessment of myocardial ischemia. *American Journal of Cardiology* **32**, 295-305 (1973).

25. Pan, H.-L., Longhurst, J. C., Eisenach, J. C. & Chen, S.-R. Role of protons in activation of cardiac sympathetic C-fibre afferents during ischaemia in cats. *Journal of Physiology* **518.3**, 857-866 (1999).

26. Thimm, F., Carvalho, M., Babka, M. & Meier zu Verl, E. Reflex increases in heart-rate induced by perfusing the hind leg of the rat with solutions containing lactica acid. *Pflugers Archives* **400**, 286-293 (1984).

27. Hong, J. L., Kwong, K. & Lee, L.-Y. Stimulation of pulmonary C fibres by lactic acid in rats: contributions of H and lactate ions. *Journal of Physiology* **500**:2, 319-329 (1997).

28. Poole-Wilson, P. A. Measurement of myocardial intracellular pH in pathological states. *Journal of Molecular and Cellular Cardiology* **10**:6, 511-526 (1978).

29. Cobbe, S. M. & Poole-Wilson, P. A. The time of onset and severity of acidosis in myocardial ischaemia. *Journal of Molecular and Cellular Cardiology* **12**, 745-760 (1980).

30. Krishtal, O. A. & Pidoplichko, V. I. A receptor for protons in the nerve cell membrane. *Neuroscience* **5**, 2325-2327 (1980).

31. Krishtal, O. A. & Pidoplichko, V. I. A receptor for protons in the membrane of sensory neurons may participate in nociception. *Neuroscience* **6**:12, 2599-2601 (1981).

32. Bevan, S., Forbes, C. A. & Winter, J. Protons and capsaicin activate the same ion channels in rat isolated dorsal root gangion neurones. *Journal of Physiology* **459**, 401P (1993).

33. Zeilhofer, H. U., Kress, M. & Swandulla, D. Fractional Ca currents through capsaicin- and proton-activated ion channels in rat dorsal roo ganglion neurones. *Journal of Physiology* **503**:1, 67-78 (1997).

34. Liu, L. & Simon, S. A. A rapid capsaicin-activated current in rat trigeminal ganglion neurons. *Neurobiology* **91**, 738-741 (1994).

35. Steen, K. H., Reeh, P. W., Anton, F. & Handwerker, H. O. Protons selectively induce lasting excitation and sensitization to mechanical stimulation of nociceptors in rat skin, in vitro. *Journal of Neuroscience* **12**, 86-95 (1992).

36. Caterina, M. J., *et al.* The capsaicin receptor: a heat-activated ion channel in the pain pathway. *Nature* **389**, 818-824 (1997).

37. Tominaga, M., *et al.* The cloned capsaicin receptor integrates multiple pain-producing stimuli. *Neuron* **21**, 531-543 (1998).

38. Bevan, S. & Yeats, J. Protons activate a cation conductance in a sub-population of rat dorsal root ganglion neurones. *Journal of Physiology* **433**, 145-161 (1991).

39. Waldmann, R., *et al.* H(+)-gated cation channels. *Annals of the New York Academy of Science* **868**, 67-76 (1999).

40. Waldmann, R. & Lazdunski, M. H-gated cation channels: neuronal acid sensors in the NaC/DEG family of ion channels. *Current Opinion in Neurobiology* **8**, 418 (1998).

41. Coscoy, S., Lingueglia, E., Lazdunski, M. & Barbry, P. The Phe-Met-Arg-Phe-amide-activated sodium channel is a tetramer. *Journal of Biological Chemistry* **273**:14, 8317-8322 (1998).

42. Firsov, D., *et al.* The heterotetrameric architecture of the epithelial sodium channel (ENaC). *EMBO. J.* **17**:2, 344-352 (1998).

43. Kosari, F., *et al.* Subunit stoichiometry of the epithelial sodium channel. *J. Biol. Chem.* **273**:22, 13469-13474 (1998).

44. Snyder, P. M., *et al.* Electrophysiological and biochemical evidence that DEG/ENaC cation channels are composed of nine subunits. *Journal of Biological Chemistry* **273**, 681-684 (1998).

45. Waldmann, R., *et al.* A proton-gated cation channel involved in acid-sensing. *Nature* **386**:6621, 173-177 (1997).

46. Chen, C.-C., England, S., Akopian, A. N. & Wood, J. N. A sensory neuron-specific, proton-gated ion channel. *Proceedings of the National Academy of Science* **95**, 10240-10245 (1998).

47. Waldmann, R., *et al.* The mammalian degenerin MDEG, an amiloride-sensitive cation channel activated by mutations causing neurodegeneration in c. elegans. *Journal of Biological Chemistry* **271**:18, 10433-10436 (1996).

48. Lingueglia, E., *et al.* A modulatory subunit of acid sensing ion channels in brain and dorsal root ganglion cells. *Journal of Biological Chemistry* **272**:47, 29778-29783 (1997).

49. Waldmann, R., *et al.* Molecular cloning of a non-inactivating proton-gated Na+ channel specific for sensory neurons. *Journal of Biological Chemistry* **272**:34, 20975-20978 (1997).

50. Dirnagl, U., Iadecola, C. & Moskowitz, M. A. Pathobiology of ischaemic stroke: an integrated view. *Trends Neurosci* **22**:9, 391-397 (1999).

51. Lee, J. M., Zipfel, G. J. & Choi, D. W. The changing landscape of ischaemic brain injury mechanisms. *Nature* **399**:6738 Suppl, A7-14 (1999).

52. Tombaugh, G. C. & Sapolsky, R. M. Mechanistic distinctions between excitotoxic and acidotic hippocampal damage in an in vitro model of ischemia. *J Cereb Blood Flow Metab* **10**:4, 527-535 (1990).

53. Goldman, S. A., *et al.* The effects of extracellular acidosis on neurons and glia in vitro. *J Cereb Blood Flow Metab* **9**:4, 471-477 (1989).

54. Kraig, R. P., Petito, C. K., Plum, F. & Pulsinelli, W. A. Hydrogen ions kill brain at concentrations reached in ischemia. *J Cereb Blood Flow Metab* **7**:4, 379-386 (1987).

55. Siesjo, B. K. Acidosis and ischemic brain damage. *Neurochem Pathol* **9**, 31-88 (1988).

56. Siesjo, B. K., *et al.* Acidosis-related brain damage. *Prog Brain Res* **96**, 23-48 (1993).

57. Sapolsky, R. M., Trafton, J. & Tombaugh, G. C. Excitotoxic neuron death, acidotic endangerment, and the paradox of acidotic protection. *Adv Neurol* **71**, 237-244; discussion 244-235 (1996).

58. Choi, D. W. Glutamate receptors and the induction of excitotoxic neuronal death. *Prog Brain Res* **100**, 47-51 (1994).

59. Choi, D. W. Cerebral hypoxia: some new approaches and unanswered questions. *J Neurosci* **10**:8, 2493-2501 (1990).

60. Choi, D. W. NMDA receptors and AMPA/kainate receptors mediate parallel injury in cerebral cortical cultures subjected to oxygen-glucose deprivation. *Prog Brain Res* **96**, 137-143 (1993).

61. Koh, J. Y. & Choi, D. W. Selective blockade of non-NMDA receptors does not block rapidly triggered glutamate-induced neuronal death. *Brain Res* **548**:1-2, 318-321 (1991).

62. Kaku, D. A., Giffard, R. G. & Choi, D. W. Neuroprotective effects of glutamate antagonists and extracellular acidity. *Science* **260**:5113, 1516-1518 (1993).

63. Koh, J. Y., Goldberg, M. P., Hartley, D. M. & Choi, D. W. Non-NMDA receptor-mediated neurotoxicity in cortical culture. *J Neurosci* **10**:2, 693-705 (1990).

64. Kaku, D. A., Goldberg, M. P. & Choi, D. W. Antagonism of non-NMDA receptors augments the neuroprotective effect of NMDA receptor blockade in cortical cultures subjected to prolonged deprivation of oxygen and glucose. *Brain Res* **554**:1-2, 344-347 (1991).

65. Gwag, B. J., *et al.* Slowly triggered excitotoxicity occurs by necrosis in cortical cultures. *Neuroscience* **77**:2, 393-401 (1997).

66. Giffard, R. G., Monyer, H. & Choi, D. W. Selective vulnerability of cultured cortical glia to injury by extracellular acidosis. *Brain Res* **530**:1, 138-141 (1990).

67. Giffard, R. G., Monyer, H., Christine, C. W. & Choi, D. W. Acidosis reduces NMDA receptor activation, glutamate neurotoxicity, and oxygen-glucose deprivation neuronal injury in cortical cultures. *Brain Res* **506**:2, 339-342 (1990).

68. Tang, C. M., Dichter, M. & Morad, M. Modulation of the N-methyl-D-aspartate channel by extracellular H+. *Proc Natl Acad Sci U S A* **87**:16, 6445-6449 (1990).

69. Traynelis, S. F. & Cull-Candy, S. G. Proton inhibition of N-methyl-D-aspartate receptors in cerebellar neurons. *Nature* **345**:6273, 347-350 (1990).

70. Banasiaka, K. J., Xiab, Y. & Haddadbc, G. G. Mechanisms underlying hypoxia-induced neuronal apoptosis. *Prog Neurobiol* **62**:3, 215-249 (2000).

71. McDonald, J. W., *et al.* Extracellular acidity potentiates AMPA receptor-mediated cortical neuronal death. *J Neurosci* **18**:16, 6290-6299 (1998).

72. Christensen, B. N. & Hida, E. Protonation of histidine groups inhibits gating of the quisqualate/kainate channel protein in isolated catfish cone horizontal cells. *Neuron* **5**:4, 471-478 (1990).

73. Shen, H., Chan, J., Kass, I. S. & Bergold, P. J. Transient acidosis induces delayed neurotoxicity in cultured hippocampal slices. *Neurosci Lett* **185**:2, 115-118 (1995).

74. Ding, D., *et al.* Acidosis induces necrosis and apoptosis of cultured hippocampal neurons. *Exp Neurol* **162**:1, 1-12 (2000).

75. Lynch, J. J., 3rd, *et al.* Sodium channel blockers reduce oxygen-glucose deprivation-induced cortical neuronal injury when combined with glutamate receptor antagonists. *J Pharmacol Exp Ther* **273**:1, 554-560 (1995).

76. Alojado, M. E., Morimoto, Y. & Kemmotsu, O. Mechanism of cellular swelling induced by extracellular lactic acidosis in neuroblastoma-glioma hybrid (NG108-15) cells. *Anesth Analg* **83**:5, 1002-1008 (1996).

77. Goldberg, M. P. & Choi, D. W. Combined oxygen and glucose deprivation in cortical cell culture: calcium-dependent and calcium-independent mechanisms of neuronal injury. *J Neurosci* **13**:8, 3510-3524 (1993).

78. Bassilana, F., *et al.* The acid-sensitive ionic channel subunit ASIC and the mammalian degenerin MDEG form a heteromultimeric H+-gated Na+ channel with novel properties. *Journal of Biological Chemistry* **272**:46, 28819-28822 (1997).

79. Mayer, M. L., Westbrook, G. L. & Guthrie, P. B. Voltage-dependent block by Mg2+ of NMDA responses in spinal cord neurones. *Nature* **309**:5965, 261-263 (1984).

80. Nowak, L., *et al.* Magnesium gates glutamate-activated channels in mouse central neurones. *Nature* **307**:5950, 462-465 (1984).

81. Hille, B., *Ionic Channels of Excitable Membranes*. Second ed. 1992, Sunderland: Sinauer Associates, Inc.

82. Woodhull, A. M. Ionic blockage of sodium channels in nerve. *J Gen Physiol* **61**:6, 687-708 (1973).

83. Nakatani, T., *et al.* Pericardium of rodents: pores connect the pericardial and pleural cavities. *Anat. Rec.* **220**:2, 132-137 (1988).

84. Eckert, S. P., Taddesse, A. & McCleskey, E. W. Isolation and culture of rat sensory neurons having distinct sensory modalities. *Journal of Neuroscience Methods* **77**, 183-190 (1997).

85. McNeill, D. L. & Burden, H. W. Convergence of sensory processes from the heart and left ulnar nerve onto a single afferent perikaryon: a neuroanatomical study in the rat employing fluorescent tracers. *Anat. Rec.* **214**:4, 441-444, 396-447 (1986).

86. Huang, M. H., *et al.* Polysensory response characteristics of dorsal root ganglion neurones that may serve sensory functions during myocardial ischaemia. *Cardiovasc. Res.* **32**:3, 503-515 (1996).

87. Minisi, A. J. & Thames, M. D. Activation of cardiac sympathetic afferents during coronary occlusion. Evidence for reflex activation of sympathetic nervous system during transmural myocardial ischemia in the dog. *Circulation* **84**:1, 357-367 (1991).

88. Armour, J. A., Huang, M. H., Pelleg, A. & Sylven, C. Responsiveness of in situ canine nodose ganglion afferent neurones to epicardial mechanical or chemical stimuli. *Cardiovasc. Res.* **28**:8, 1218-1225 (1994).

89. Thames, M. D., *et al.* Preferential distribution of inhibitory cardiac receptors with vagal afferents to the inferoposterior wall of the left ventricle activated during coronary occlusion in the dog. *Circ. Res.* **43**:4, 512-519 (1978).

90. James, T. N. A cardiogenic hypertensive chemoreflex. *Anesth. Analg.* **69**:5, 633-646 (1989).

91. Euchner-Wamser, I., Meller, S. T. & Gebhart, G. F. A model of cardiac nociception in chronically instrumented rats: behavioral and electrophysiological effects of pericardial administration of algogenic substances. *Pain* **58**:1, 117-128 (1994).

92. Sleight, P. A cardiovascular depressor reflex from the epicardium of the left ventricle in the dog. *J. Physiol.* **173**, 321-343 (1964).

93. Jacobus, W. E., Taylor, G. J. I., Hollis, D. P. & Nunnally, R. L. Phosphorus nuclear magnetic resonance of perfused working rat hearts. *Nature* **265**:5596, 756-758 (1977).

94. Hirsch, H. J., *et al.* Myocardial extracellular K+ and H+ increase and noradrenaline release as possible cause of early arrhythmias following acute coronary artery occlusion in pigs. *J. Mol. Cell Cardiol.* **12**, 579-593 (1980).

95. Cobbe, S. M., Parker, D. J. & Poole-Wilson, P. A. Tissue and coronary venous pH in ischemic canine myocardium. *Clinical cardiology* **5**, 153-156 (1982).

96. Steen, K. H., Steen, A. E. & Reeh, P. W. A dominant role of acid pH in inflammatory excitation and sensitization of nociceptors in rat skin, in vitro. *J. Neurosci.* **15**:5 Pt. 2, 3982-3989 (1995).

97. Davies, N. W., Lux, H. D. & Morad, M. Site and mechanism of activation of proton-induced sodium current in chick dorsal root ganglion neurones. *Journal of Physiology* **400**, 159-187 (1988).

98. Konnerth, A., Lux, H. D. & Morad, M. Proton-induced transformation of calcium channel in chick dorsal root ganglion cells. *Journal of Physiology* **386**, 603-633 (1987).

99. Cook, S. P., *et al.* Distinct ATP receptors on pain-sensing and stretch-sensing neurons. *Nature* **387**, 505-508 (1997).

100. Maricq, A. V., *et al.* Primary structure and functional expression of the 5HT3 receptor, a serotonin-gated ion channel. *Science* **254**:5030, 432-437 (1991).

101. Sucher, N. J., Cheng, T. P. & Lipton, S. A. Neural nicotinic acetylcholine responses in sensory neurons from postnatal rat. *Brain Research* **533**, 248-254 (1990).

102. Nicol, G. D. & Cui, M. Enhancement by prostaglandin E2 of bradykinin activation of embryonic rat sensory neurones. *J. Physiol. (Lond)* **480**:Pt. 3, 485-492 (1994).

103. Allen, T. G. & Burnstock, G. The actions of adenosine 5'-triphosphate on guinea-pig intracardiac neurones in culture. *Br. J. Pharmacol* **100**:2, 269-276 (1990).

104. Lewis, C., *et al.* Coexpression of P2X2 and P2X3 receptor subunits can account for ATP- gated currents in sensory neurons [see comments]. *Nature* **377**, 432-435 (1995).

105. Chen, C. C., *et al.* A P2X purinoceptor expressed by a subset of sensory neurons [see comments]. *Nature* **377**, 428-431 (1995).

106. Kovalchuk, Y. N., Krishtal, O. A. & Nowycky, M. C. The proton-activated inward current of rat sensory neurons includes a calcium component. *Neuroscience Letters* **115**, 237-242 (1990).

107. Tang, C. M., Presser, F. & Morad, M. Amiloride selectively blocks the low threshold (T) calcium channel. *Science* **240**:4849, 213-215 (1988).

108. Canessa, *et al.* Amiloride-sensitive epithelial Na channel is made of three homologous subunits. *Nature* **367**, 463 (1994).

109. Foreman, R. D. Mechanisms of cardiac pain. *Annual Review of Physiology* **61**, 143-167 (1999).

110. Rendig, S. V., Chahal, P. S. & Longhurst, J. C. Cardiovascular reflex responses to ischemia during occlusion of celiac and/or superior mesenteric arteries. *Am. J. Physiol.* **272**:2 Pt. 2, H791-796 (1997).

111. Malliani, A. Significance of experimental models in assessing the link between myocardial ischemia and pain. *Advances in Cardiology* **37**, 126-141 (1990).

112. Korkushko, A. & Kryshtal, O. Blocking of proton-activated sodium permeability of the membranes of trigeminal ganglion neurons in the rat by organic cations. *Neirofiziologiia* **16**, 557-561 (1984).

113. Garcia-Anoveros, J., *et al.* BNaC1 and BNaC2 constitute a new family of human neuronal sodium channels related to degenerins and epithelial sodium channels. *Proceedings of the National Academy of Science* **94**:4, 1459-1464 (1997).

114. Price, M. P., Snyder, P. M. & Welsh, M. J. Cloning and expression of a novel human brain Na+ channel. *Journal of Biological Chemistry* **271**:14, 7879-7882 (1996).

115. Sutherland, S. P., Immke, D., Stone, L. S. & McCleskey, E. W. ASIC3 matches the acid-gated current in cardiac ischemia-sensing neurons. *Abstracts Society for Neuroscience* **26 Pt. 1**, 933 (2000).

116. Alles, A. & Dom, R. M. Peripheral sensory nerve fibers that dichotomize to supply the brachium and the pericardium in the rat: a possible morphological explanation for referred cardiac pain? *Brain Res.* **342**:2, 382-385 (1985).

117. Bevan, S. & Winter, J. Nerve growth factor (NGF) differentially regulates the chemosensitivity of adult rat cultured sensory neurons. *J. Neurosci.* **15**:7 Pt 1, 4918-4926 (1995).

118. Deanfield, J. E., Shea, M. J. & Selwyn, A. P. Clinical evaluation of transient myocardial ischemia during daily life. *Am. J. Med.* **79**:3A, 18-24 (1985).

119. Rosen, S. D., *et al.* Silent ischemia as a central problem: regional brain activation compared in silent and painful myocardial ischemia [comment] [see comments]. *Ann. Intern. Med.* **124**:11, 939-949 (1996).

120. Thamer, V., *et al.* Pain and myocardial ischemia: the role of sympathetic activation. *Basic Res. Cardiol.* **85**:Suppl. 1, 253-266 (1990).

121. Francis, G. S., *et al.* The neurohumoral axis in congestive heart failure. *Ann. Intern. Med.* **101**:3, 370-377 (1984).

122. Victor, R. G., Bertocci, L. A., Pryor, S. L. & Nunnally, R. L. Sympathetic nerve discharge is coupled to muscle cell pH during exercise in humans [published erratum appears in J. Clin. Invest. 1988 Dec.;82(6):following 2181]. *J Clin Invest* **82**:4, 1301-1305 (1988).

123. de Weille, J. R., Bassilana, F., Lazdunski, M. & Waldmann, R. Identification, functional expression and chromosomal localisation of a sustained human proton-gated cation channel. *FEBS Letters* **433**, 257-260 (1998).

124. Thames, M. D., Kinugawa, T. & Dibner-Dunlap, M. E. Reflex sympathoexcitation by cardiac sympathetic afferents during myocardial ischemia: role of adenosine. *Circulation* **87**, 1698-1704 (1993).

125. Crea, F., *et al.* Role of adenosine in pathogenesis of anginal pain. *Circulation* **81**, 164-172 (1990).

126. Tjen-A-Looi, S. C., Pan, H.-L. & Longhurst, J. C. Endogenous bradykinin activates ischaemically sensitive cardiac visceral afferents through kinin B2 receptors in cats. *Journal of Physiology* **510.2**, 633-641 (1998).

127. Gilman, A., Goodman, L., Rall, T. & Murid, F., *The Pharmacological Basis of Therapeutics*. 1985, New York: New York.

128. Wollmuth, L. P., Kuner, T. & Sakmann, B. Adjacent asparagines in the NR2-subunit of the NMDA receptor channel control the voltage-dependent block by extracellular Mg2+. *J Physiol* **506**:Pt 1, 13-32. (1998).

129. Jahr, C. E. & Stevens, C. F. A quantitative description of NMDA receptor-channel kinetic behavior. *J Neurosci* **10**:6, 1830-1837. (1990).

130. Jahr, C. E. & Stevens, C. F. Voltage dependence of NMDA-activated macroscopic conductances predicted by single-channel kinetics. *J Neurosci* **10**:9, 3178-3182. (1990).

131. Ascher, P. & Nowak, L. The role of divalent cations in the N-methyl-D-aspartate responses of mouse central neurones in culture. *J Physiol* **399**, 247-266. (1988).

132. Mayer, M. L. & Westbrook, G. L. Permeation and block of N-methyl-D-aspartic acid receptor channels by divalent cations in mouse cultured central neurones. *J Physiol* **394**, 501-527. (1987).

133. Lansman, J. B., Hess, P. & Tsien, R. W. Blockade of current through single calcium channels by Cd2+, Mg2+, and Ca2+. Voltage and concentration dependence of calcium entry into the pore. *J Gen Physiol* **88**:3, 321-347. (1986).

134. Ault, B., *et al.* Selective depression of excitatory amino acid induced depolarizations by magnesium ions in isolated spinal cord preparations. *J Physiol* **307**, 413-428. (1980).

135. Hille, B. The permeability of the sodium channel to organic cations in myelinated nerve. *J Gen Physiol* **58**:6, 599-619. (1971).

136. Hille, B. The receptor for tetrodotoxin and saxitoxin. A structural hypothesis. *Biophys J* **15**:6, 615-619. (1975).

137. Kral, T., Luhmann, H. J., Mittmann, T. & Heinemann, U. Role of NMDA receptors and voltage-activated calcium channels in an in vitro model of cerebral ischemia. *Brain Res* **612**:1-2, 278-288. (1993).

138. Varming, T. Proton-gated ion channels in cultured mouse cortical neurons. *Neuropharmacology* **38**, 1875-1881 (1999).

139. Aikeke, N. & Ueno, S. Proton-induced current in neuronal cells. *Progress in Neurobiology* **43**, 75-85 (1994).

140. Ueno, S., Nakaye, T. & Akaike, N. Proton-induced sodium current in freshly dissociated hypothalamic neurones of the rat. *J Physiol (Lond)* **447**, 309-327 (1992).

141. Norenberg, M. D., Mozes, L. W., Gregorios, J. B. & Norenberg, L. O. Effects of lactic acid on astrocytes in primary culture. *J Neuropathol Exp Neurol* **46**:2, 154-166. (1987).

142. Escoubas, P., *et al.* Isolation of a tarantula toxin specific for a class of proton-gated Na+ channels. *J Biol Chem* **275**:33, 25116-25121. (2000).

143. Baron, A., *et al.* Zn2+ and H+, coactivators of acid sensing ion channels (ASIC). *J Biol Chem* **16**, 16 (2001).

Figure 17. Cartoon representation of ASIC1a pore containing guanidine, amiloride and TTX molecules. This rendition of the ASIC1a channel in cross section is hypothetical and is not based on structural data from channel studies. The pore, however, is assumed to have a constriction of around 3 Å and is lined with oxygen atoms that can form hydrogen bonds with the amino group of the guanidinium ion. The geography of the electrical field across the membrane relative to the channel is unknown, but the yellow highlighted region in the pore is meant to represent the electrical drop. The three-dimensional representations of guanidine, amiloride and TTX are based on structural studies of those molecules. The small, light blue spheres are hydrogens forming H-bonds. The depictions of amiloride and TTX represent only one of several possible conformations and many rotational positions within the mouth of the channel. With this limitation in mind, the cartoon is helpful in visually imagining how each of the molecules might interact with the ASIC1a channel.

Figure 17